EFFECT OF THERMAL PRE-TREATMENT ON THE BENEFICIATION OF NDIT ILMENITE RESOURCE, BAUCHI STATE, NIGERIA

BY

PAUL JOSEPH BARKI

DEPARTMENT OF METALLURGICAL AND MATERIALS ENGINEERING,

FACULTY OF ENGINEERING,

AHMADU BELLO UNIVERSITY,

ZARIA, NIGERIA

JANUARY, 2022

EFFECT OF THERMAL PRE-TREATMENT ON THE BENEFICIATION OF NDIT ILMENITE RESOURCE, BAUCHI STATE, NIGERIA

BY
PAUL JOSEPH BARKI
B. Eng. ABU, (2015)
P17EGML8012

A DISSERTATION SUBMITTED TO THE SCHOOL OF POSTGRADUATE STUDIES,

AHMADU BELLO UNIVERSITY, IN PARTIAL FULFILMENT OF THE REQUIREMENTS FOR THE AWARD OF

MASTER OF SCIENCE DEGREE IN

METALLURGICAL AND MATERIALS ENGINEERING

DEPARTMENT OF METALLURGICAL AND MATERIALS ENGINEERING,

FACULTY OF ENGINEERING,

AHMADU BELLO UNIVERSITY,

ZARIA, NIGERIA

JANUARY, 2022

DECLARATION

I declare that this Dissertation titled "EFFECT OF THERMAL PRE-TREATMENT ON THE BENEFICIATION OF NDIT ILMENITE RESOURCE, BAUCHI STATE, NIGERIA" was carried out by me in the Department of Metallurgical and Materials Engineering. The information derived from the literatures has been duly acknowledged in the text and a list of references provided. No part of this dissertation was previously presented for another degree or diploma elsewhere.

PAUL JOSEPH BARKI

…… ……

(Signature) (Date)

CERTIFICATION

This Dissertation titled "EFFECT OF THERMAL PRE-TREATMENT ON THE BENEFICIATION OF NDIT ILMENITE RESOURCE, BAUCHI STATE, NIGERIA" by Paul Joseph Barki, meets the regulations governing the award of Master of Science Degree of the Ahmadu Bello University, Zaria and is approved for its contribution to knowledge and literary presentation.

Dr. D. G. Thomas	…….	…….
Chairman Supervisory Committee	(Signature)	(Date)
Prof. O. Aponbiede	……	……
Member Supervisory Committee	(Signature)	(Date)
Prof. R. A. Mohammed	……	……
Head of Department	(Signature)	(Date)
Prof. Sani A. Abdullahi	……..	……
Dean, School of Postgraduate Studies	(Signature)	(Date)

DEDICATION

This work is dedicated to God Almighty who is the source of all knowledge, my parents Mr. & Mrs. Joseph Barki, my siblings and the entire Barki's family

,

ACKNOWLEDGEMENT

The journey that started some years ago has finally come to an end. It is not by my power, strength nor wisdom, but by the ever abounding grace of God who is my source of wisdom and understanding.

This work wouldn't have come to completion without the inputs, guidance and contributions of my wonderful supervisory team, Dr. Dungka George Thomas and Professor Ola Aponbiede. Your contributions are immensely appreciated and may you continue to soar higher in your endeavours.

My humble appreciation goes to the Head of Department; Prof. R. A. Mohammed for the sleepless efforts he always put to see that the department maintains its status quo. To the best Post Graduate coordinator ever; Dr U. Shehu, your efforts are highly appreciated and only God can reward you. To all my distinguished Professors, Lecturers and all other departmental staff who in one way or the other contributed to the success of this research work, i say thank you all.

Special thanks to my parents Mr. & Mrs. Joseph Barki, my siblings, the entire Barki's family for their tireless efforts, advices, prayers and financial supports towards the success of my academic pursuit. You have been instrumental to my achievements in life right from day one to this stage. I cannot thank you enough but our God who is the source of all blessings to mankind will reward you abundantly.

My appreciation goes to Engr. Eyebola W. A. Oyeladun and Mr. Takur, both from Kaduna Polytechnic for making this work a success. Special thanks to Mallam Sulieman for his effort in the course of my laboratory work. May God bless you. My colleagues, friends and well-wishers, thanks for your love and companionship. God will reward you immeasurably.

I cannot forget the companionship of Emmanuel Ogbe, Engr. Dorcas Asuku, Engr. Peter Anikoh, Basil Bassey, Raymond Ioryemen, Kamo K. Haa, Williams Bitrus and Geoffrey Iliya. May this love continue to unite us together and may the Lord reward you with your heart desires. And to all members of the Fellowship of Catholic Postgraduate Students, Our Lady Queen of Peace Parish Choir, National Association of Ngas Students, ABU Zaria Chapter and the Faculty of Education Choir for making my stay in Ahmadu Bello University less stressful. May you all experience God's grace and favour in your various endeavours.

To all whose names could not be mentioned, i am also grateful. I love you all.

ABSTRACT

The effect of thermal pre-treatments on the beneficiation of Ndit Ilmenite resource has been investigated in this work. The Ilmenite resource is located at Ndit village, in Bogoro Local Government Area, Bauchi State, Nigeria. The sample was sourced from four different points at 50m interval apart. The samples were homogenized then pulverized, sieved and analyzed for their chemical and mineralogical compositions using X-ray Fluorescence (XRF), X-ray Diffractometer (XRD), Scanning Electron Microscope/Energy Dispersive Spectroscope (SEM/EDS) and Petrological microscope respectively. The chemical analysis of the head sample revealed that the Ilmenite resource contained 41.50% TiO_2, 21.78% Fe_2O_3, 15.85% Al_2O_3, and 18.20% SiO_2 as the major minerals, 1.18% Nb_2O_5 as the minor mineral, 0.20% TaO_5, 0.65% MnO and 0.64% others as trace minerals. The mineralogical analysis of the Ndit Ilmenite sample revealed the presence of Ilmenite ($FeTiO_3$), Rutile (TiO_2) as major, Alumina, Silica and other trace associated minerals as minor in the matrix of the Ilmenite resource. The SEM analysis revealed that the minerals grains are smaller in sizes, and are separated by grain boundaries. The SEM images of the Ilmenite samples also, revealed non-interlocking of minerals grains with varying sizes. Ilmenite phase is seen as the grey portion, the white portions are the Rutile Phases and Hematite is the dark portions in the matrix of the Ndit Ilmenite sample. The liberation size and work index of the sample was found to be -355+250µm and 9.35kWh/t respectively. The thermal treatment (Calcination and Roasting) of the Ilmenite sample enhances the transformation of some proportions of Ilmenite to Rutile phase and formation of Anatase, Ilmenorutile and Magnetite phases in the matrix. The optimum thermal conditions obtained for calcination treatment is; Temperature (650^oC), Time (60 minutes) which gave 58.0%TiO_2 phase, while the optimum thermal conditions for roasting treatment is; Temperature (300^oC), Time (60 minutes) which gave 47.1%TiO_2 phase. Beneficiation of the thermally treated (Calcination and Roasting) Ilmenite sample employing Two stage (double) magnetic (high intensity) - to - gravity (air-floatation) separation method reported an upgrade in the assay of mineral of interest to 82.87% TiO_2 (49.72% Ti) with a recovery of 65.13% for calcined sample and 85.64% TiO_2 (51.38% Ti) with a 69.03% recovery for the roasted sample. The percentage of TiO_2 obtained in the concentrates surpasses and met the requirements of 48% - 51% TiO_2 as minimum rutile content for rutile ore and 50% TiO_2 content as minimum for Ilmenite ore. A process flow-sheet was also developed for the beneficiation of the Ndit Ilmenite resource using the results of the tests and analysis carried out. Therefore, the Ndit Ilmenite resource can be said to be another source of Titanium bearing mineral that can be explored, beneficiated and used in the nation's metallurgical industries.

Table of Contents

COVER PAGE……..…..i

FLY LEAF……..….ii

TITLE PAGE……..iii

DECLARATION iii

CERTIFICATION iv

DEDICATION v

ACKNOWLEDGEMENT vi

ABSTRACT vii

CHAPTER ONE 1

INTRODUCTION 1

1.1 Background 1

1.2 Statement of the Research Problem 2

1.3 Justification of the Research 2

1.4 Aim and Objectives of the Study 3

1.5 Scope of the Research 4

CHAPTER TWO 5

LITERATURE REVIEW 5

2.1 Rutile Ores 5

2.2 Titanium Ore Minerals 5

2.3 Occurrence of Titanium Ores in Nigeria 7

2.4 Processing of Titanium Bearing Minerals 9

2.4.1 Thermal Pre-Treatments Given to Rutile and Titanium Bearing Minerals Prior to Beneficiation 10

2.5 Methods of Characterizing Minerals 13

2.5.1 X-Ray Fluorescence (XRF) 13

2.5.2 Scanning Electron Microscopy (SEM/EDS) 14

2.5.3 X-Ray Diffraction 14

2.6 Comminution Process 15

2.6.1 Theory of Comminution 15

2.6.2 Grindability 15

2.7 Mineral Beneficiation Processes 16

2.7.1 Processing of Titanium-Containing Minerals 17

2.8 Beneficiation of Titanium Ore 19

2.8.1 Magnetic Separation of Rutile 20
2.8.2 Gravity Separation of Rutile 21
2.8.3 Froth Flotation of Rutile 22
2.8.4 Electrical Separation of Rutile 23
2.9 Previous Works on Titanium Ores 24
CHAPTER THREE 28
MATERIALS AND METHOD 28
3.1 Materials 28
3.2 Equipment 28
3.3 Methodology 29
3.3.1 Sample Collection 29
3.3.2 Sample Preparation 29
3.3.3 Sampling 29
3.3.4 Chemical Analysis 29
3.3.5 Mineralogical Analysis 30
3.3.5.2 Scanning Electron Microscope (SEM) Analysis 30
3.3.6 Sieve Size Analysis 31
3.3.7 Liberation Size Analysis 31
3.3.8 Work Index Determination 32
3.4 Thermal Pre-Treatment 34
3.4.1 Calcination 34
3.4.2 Roasting 34
3.5 Beneficiation 35
3.5.1 Magnetic Separation Using High Intensity Magnetic Separator (Reverse Magnetic Separation) 35
3.5.2 Gravity Separation 35
CHAPTER FOUR 36
RESULTS AND DISCUSSION 36
4.1 Coordinates of the Ilmenite Resource Site 36
4.2 Chemical Composition of the Head Sample 37
4.3 Mineralogical Analysis 38
4.3.1 XRD Analysis 38
4.3.2 Scanning Electron Microscopy 39

4.3.3 Petrographic Microscopy of Ndit Ilmenite Resource 41
4.4 Sieve Analysis and Liberation Size of the Sample 43
4.5 Work Index 44
4.5.1 Test Ore (Ndit Ilmenite) and Reference (Granite) as Feeds to the Ball Mill 44
4.5.2 Test Ore (Ndit Ilmenite) and References (Granite) Products as Discharge from the Ball Mill . 46
4.6 Calcination Thermal Pre-Treatment 50
4.7 Roasting Thermal Pre-Treatment 53
4.8 Beneficiation of Ndit Ilmenite Resource 56
4.8.1 Magnetic Concentration of the Calcined Ilmenite Sample using High Intensity Magnetic Separation Process 56
4.8.2 Gravity concentration of the calcined Ilmenite sample using air-floatation separation process 59
4.8.3 Magnetic Concentration of the Roasted Ilmenite Sample using High Intensity Magnetic Separation Process 61
4.8.4 Gravity Concentration of the Roasted Ilmenite Sample using Air-Floatation Separation Process 63
4.6.2 Comparison of the Two-Stage (Double) Magnetic-to-Gravity (Air-Floatation) Concentration Method of the Calcined and Roasted Ndit Ilmenite Resource Sample 66
4.9 The Philosophy of the Developed Flow Sheet of Ndit Ilmenite Resource 68
CHAPTER FIVE 71
CONCLUSION AND RECOMMENDATIONS 71
5.1 Conclusion 71
5.2 Recommendations 72
5.3 Contribution to Knowledge 73
References 74

List of Figures

Figure 2.1 Map showing mineral locations in Nigeria with ilmenite and rutile minerals inclusive found in States like Bauchi and Plateau……...7

Figure 2.2 Map showing the location of the Ilmenite Resource at Ndit Village, Bogoro Local Government Area of Bauchi State, Nigeria ……....8

Figure 2.3 Flotation Cell……23

Figure 4.1 XRD pattern for Ndit Ilmenite Resource……..……40

Figure 4.2 Variations of phases formed after calcination thermal pre-treatment…….....51

Figure 4.3 Variations of phases formed after roasting thermal pre-treatment……..…….…...54

Figure 4.4 Bar chart of the Calcined and Roasted Two-Stage Magnetic-to-Gravity (Air-Floatation) Concentrates Assays and Recoveries of Ndit Ilmenite……...66

Figure 4.5 Flow-sheet of Ndit Ilmenite Beneficiation Process…...…….70

List of Tables

Table 2.1 World Titanium Reserves (In Thousand Metric Tonnes)……..…….6
Table 2.2 Some Nigerian Ilmenite and Rutile Resources (in million tonnes)…….…...…….9

Table 2.3 Give the work index of some minerals ores samples…….16

Table 3.2 Calcination Parameters……..34

Table 3.3 Roasting Parameters……..35

Table 4.1 Coordinates of the Ilmenite Resource Site…….....36

Table 4.2 Chemical Composition of Ndit Ilmenite Resource as Determined using the (XRF) machine…….…….…..……...37

Table 4.3 XRD Analysis of the Ndit Rutile Head Sample……..……..49

Table 4.4 Chemical analysis of various sieve size fractions using XRF…….……..43
Table 4.5 Sieve analysis of Ndit Ilmenite sample (Test Sample) feed to ball mill..…….....45

Table 4.6 Sieve analysis of granite sample (Reference Ore) feed to ball mill…….....46

Table 4.7 Sieve analysis of Ndit Ilmenite (Product of test sample) from the ball mil….....47

Table 4.8 Sieve analysis of granite (Product of reference sample) from the ball mill….....48

Table 4.9 Result of the Ilmenite sample after calcination thermal pre-treatment…...….....50
Table 4.10 Result of the Ilmenite sample after roasting thermal pre-treatment.…….....53

Table 4.11 XRF analysis of Ndit Ilmenite resource after magnetic concentration of the calcined sample…….……...…57

Table 4.12 Metallurgical Balance Accounting for Magnetic Concentration of the Calcined Sample……....58

Table 4.13 XRF analysis of Calcined Ndit Ilmenite resource after gravity concentration of the magnetic separation concentrate……59

Table 4.14 Metallurgical Balance Accounting for Gravity Concentration of the Calcined Sample after magnetic concentration…….....60

Table 4.15 XRF analysis of Ndit Ilminite resource after magnetic concentration of the roasted sample……..…..62

Table 4.16 Metallurgical Balance Accounting for Magnetic Concentration of the Roasted Sample……....63

Table 4.17 XRF analysis of Ndit Ilmenite resource after gravity concentration of the roasted sample……....64

Table 4.18 Metallurgical Balance Accounting for Gravity Concentration of the Roasted Sample after magnetic concentration……..…65

Table 4.19 Comparison of Calcined and Roasted Two-Stage Magnetic-to-Gravity (Air-Floatation) Concentrates Assays and Recoveries of Ndit Ilmenite…….....66

List of Appendices

Appendix A list of Photographs……..…79

Appendix B Plates of Samples…….....80

Appendix C List of Phases transformed after thermal pre-treatments…….....81

Appendix D Calcination XRD Results……...……..83
Appendix E Roasting XRD Results……...….....…92
Appendix F Calcination XRF Results……...…….....101
Appendix G Roasting XRF Results……...….110
Appendix H XRF Results of Beneficiated Samples…….…….....119

List of Plates

Plate I SEM micrograph showing the morphology of Ndit Ilmenite resource at 500x……...….40
Plate II SEM micrograph showing the morphology of Ndit Ilmenite resource at 750x……40
Plate III Photomicrograph of the head sample under plane polarized light (PPL)……41
Plate IV Photomicrograph of the head sample under crossed polarized light (XPL)…….....42

List of Abbreviations

AAS Atomic Absorption Spectrometry

AusIMM Australian Institute of Mining and Metallurgy

Fr 80% passing feed of the reference ore

Ft 80% passing feed of the ore test

GDP Gross Domestic Product

GPS Global Positioning System

GVS Gravity Separator

kWh/t Kilowatt hour per tonne

MGS Magnetic Separator

MMSD Ministry of Mines and Steel Development

MO Metal Oxide

MS Metal Sulfides

POM Petrological Optical Microscope

PPl Plane Polarized Light

Pr 80% passing product of the reference ore

Pt 80% passing product of the ore test

SEM-EDS Scanning Electron Microscopy-Energy Dispersive Spectrometry

TD Decomposition Temperature

USGS United States Geological Survey

Wir Work index of the reference ore

Wit Work index of the ore test

Wr Energy input in grinding the reference ore

Wt Energy input in grinding the ore test

XPl Crossed Polarized Light

XRD X-Ray Diffraction

XRF X-Ray Fluorescence

CHAPTER ONE

INTRODUCTION

1.1 Background

Mineral exploitation has been found to be of paramount importance in the diversification of any nation's economy: This is because the mineral resources of the nation can be harnessed for technological advancement and industrialization. Nigeria is endowed with abundant mineral resources which only little out of the mineral resources have been harnessed in the past 60years. Also, the non-exploration and exploitation of these vast mineral deposits have created a shortfall in the nation's earnings and thus affect it derives for technological advancement and industrialization (Falade *et. al.,* 2012).

However, among these vast mineral deposits of the nation is Titanium ores. Rutile is a mineral composed of titanium dioxide (TiO_2) which exist in three crystallographic phases/polymorphs; rutile, anatase and brookite. Natural Rutile may contain up to 10% Iron and significant amount of Niobium and Tantalum. Titanium dioxide (TiO_2) accounts for over 95% of the world-wide use of titanium. It has among the highest refractive indices of any known mineral, also exhibits high dispersion, and these properties have led to numerous industrial applications especially in the manufacture of refractory ceramics, pigment and titanium metal and alloys. Titanium metal and alloys are commonly used in the aerospace and related industries because of their light weight, strength and corrosion resistant (Baba *et al.,* 2009). It is a naturally occurring mineral found in many places across the globe including United States, Australia, India, Brazil, Sierra Leone etc (Garside, 2021).

The advent of technology today has made it possible for titanium ore to be discovered in different locations of the country. These locations whose occurrence of the ore has been reported

Include; Kwara, Niger, Plateau, Bauchi, Taraba, Osun and Kogi States respectively (Siyanbola *et al.,* 2004).

Research has shown that every mineral is unique in its nature. Therefore, the process flow sheet for the beneficiation of an ore must be designed to suit the particular mineral. Ilmenite is usually associated with impurities which include; Iron, Niobium, Tantalum, Quartz, Zirconium, etc. which are usually impediments in the extraction of Titanium from its ore. Hence, the need to beneficiate the ore in order to remove or reduce the associated impurities before further processes.

1.2 Statement of the Research Problem

The beneficiation route of any ore deposit is designed to suit its peculiarities because of the unique geological characteristics of the associated minerals. This is applicable to Ndit Ilmenite resource because there is no data and information on its chemical, mineralogical and other important characteristics which can be used to develop a befitting beneficiation route for the resource. Hence, this research work sought to address the development of the appropriate technology for the beneficiation of Ndit Ilmenite resources to metallurgical grade.

1.3 Justification of the Research

The quest for economic and technological growth of the country has prompted the need for the diversification of the economy from crude oil to solid minerals exploitation. Therefore, Titanium ore characterization and beneficiation among others will be required as a driver to the realization of the diversification of the nation's economy because titanium metal has wide applications in aerospace industries, biomaterials etc. and titanium ores are also applicable in the production of paint, refractory ceramics etc.

Through this research, characterization and beneficiation of the Ilmenite resource was achieved.

The exploitation of the ilmenite resource for the creation of wealth for Nigeria, and generating employment, reducing poverty, improving standard of living, promoting rural economy and significant contribution to the nation's Gross Domestic Product (GDP) prompted the need for this research work.

1.4 Aim and Objectives of the Study

The aim of this research is to characterize and determine the effect of thermal pre-treatment on the beneficiation of Ndit ilmenite resource, Bauchi State, Nigeria and the objectives are as follows;

i. Determination of the chemical, mineralogical, petrological compositions of the Ilmenite using X-Ray Fluorescence (XRF), X-Ray Diffraction (XRD), and Scanning Electron Microscopy-Energy Dispersive Spectrometry (SEM-EDS) and Petrological microscope
ii. Carrying out size/mineral assay analysis and determination of the liberation size and work index of the Ilmenite resources.
iii. Carrying out Calcination and Roasting thermal pre-treatments of the Ilmenite sample.
iv. Carrying out concentration of the Ilmenite resource by a double stage magnetic and gravity separation techniques at the determined optimum thermal pre-treatments conditions in iii above.
v. To use the data and information generated in (i) to (iv) to propose a process flow-sheet for the upgrading of the Ilmenite resource.

1.5 Scope of the Research

This research work is centered on the following:

i. Sourcing the representative sample from the deposit site using the grab method and preparing the sample for further analysis,

ii. Characterization using XRF, XRD, and SEM-EDS applying the standard laboratory procedures in conformity with the global practice.

iii. Determination of the mineral assay, liberation size and work index of the Ilmenite resource.

iv. Thermal Pre-treatments of the Ilmenite sample

v. Beneficiating the Ilmenite sample using double stage magnetic to gravity separation method.

vi. Development of the flow-sheet process route of the Ilmenite resource.

CHAPTER TWO

LITERATURE REVIEW

2.1 Rutile Ores

Rutile is a titanium-bearing mineral with chemical formula TiO_2. Rutile occurs as an accessory mineral in many igneous rocks and in all grades of metamorphic rocks. Titanium is the 4th most abundant element of the earth crust with an estimated TiO_2 concentration of about 0.7wt% (Su *et al.,* 2018).

The name "rutile" is derived from the Latin "rutilus" because of the deep red colour observed in some specimens in transmitted light. Rutile can be translucent or opaque. Rutile is a reddish-brown colored substance and the chief source of titanium, with hardness of 6-6.5 (in Mohr's scale) and a specific gravity of 4.18-4.25. It is usually composed of up to 10% iron in the form of iron oxides (Ellmer *et al.,* 2018).

Naturally, rutile is usually dark-red or black, nevertheless, it can be found in other colours such as brown, yellow, green or violet depending on the content of the associated elements. Rutile ore grade gives a yellow or pale-brown streak. For production of titanium, there are diverse types of rutile with larger amounts of iron, but they are not as favorable as the high-purity rutile. Some minor ores include nigrine, ilmenorutile, seyenite, brookite, and anatase (Ellmer *et al.,* 2018). Rutile can be a major host mineral for niobium, tantalum, tungsten, uranium, zirconium, and ferric iron.

2.2 Titanium Ore Minerals

Ilmenite ($FeTiO_3$) and rutile (TiO_2) are currently the most economically important titanium-bearing ore minerals. 93% of the world's titanium resources are accounted for by the mineral ilmenite; the remaining percentage is mainly from rutile and leucoxene. Leucoxene is not a true mineral but is,

rather, a finely crystalline aggregate of rutile, anatase, or brookite with greater than 70% TiO_2 that is created by the weathering of ilmenite. A few titanium-bearing oxide minerals currently have economic value. Less common, sub-economic minerals include pseudobrookite (Fe_2TiO_5), perovskite ($CaTiO_3$), geikielite ($(Mg,Fe)TiO_3$), pyrophanite ($MnTiO_3$), and titanite or sphene ($CaTiSiO_5$) (Schulz *et al.,* 2018). Titanium-bearing minerals occur in diverse geologic settings, but many of the known deposits are currently sub economic for titanium (Schulz *et al.,* 2018).

The total world reserves of ilmenite are around 700 million tonnes while rutile reserves are far less, numbering about 46 million tonnes. According to USGS, Ilmenite accounts for about 92% of the world's consumption of titanium minerals. World resources of anatase, ilmenite and rutile total more than 2 billion tonnes. Identified reserves total 746 million tonnes (ilmenite plus rutile).

From Table 2.1, China, with 230 million tonnes accounting for 29% of the world total is now the country that is most abundant in terms of ilmenite reserves followed by Australia with 150 million tones (Garside, 2021).

Table 2.1 World Titanium Reserves (In Thousand Metric Tonnes)

COUNTRY	ILMINITE	RUTILE
United States	2,000	NA
Australia	150,000	27,000
Brazil	43,000	--
Canada	31,000	--
China	230,000	--
India	85,000	7,400
Madagascar	23,000	--
Mozambique	26,000	890
Sierra Leone	--	490
Norway	37,000	--
South Africa	35,000	6,800
Kenya	440	170
Ukraine	5,900	2,500
Vietnam	1,600	--
Other Countries	26,000	400
World Total	700,000	46,000
World Total (Ilmenite and Rutile, rounded)	746,000	

Source: Garside, M. (2021)

2.3 Occurrence of Titanium Ores in Nigeria

Tatanium ores occurrence has been reported in Kwara, Niger, Plateau, Bauchi, Taraba, Osun and Kogi States respectively by the Nigerian Geological Survey Agency. It is quite obvious that many of these occurrences are small, and not commercially verified in terms of their quantity. However, it is interesting to note that many of them have not yet been thoroughly investigated and characterized to determine their economic viability. The mineral map in Figure 2.1 shows the location of the various mineral occurrences in Nigeria particularly the Ilmenite ore, while Figure 2.2 shows the location of the Ilmenite resource at Ndit Village, Bogoro Local Government Area of Bauchi State, Nigeria.

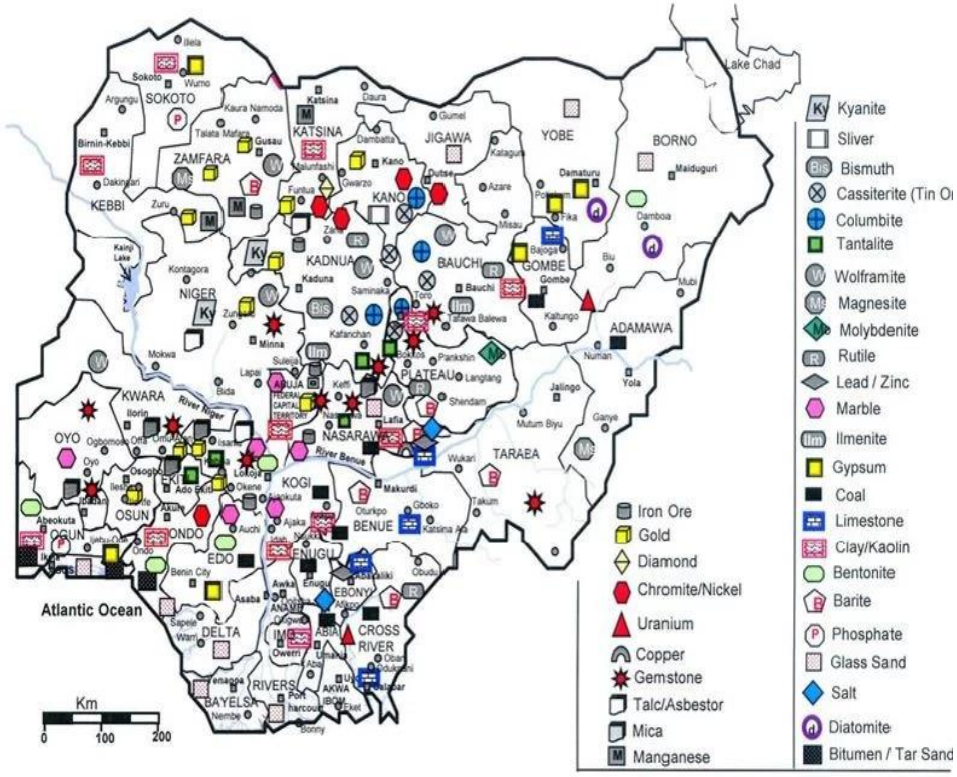


Figure 2.1 Map showing mineral locations in Nigeria with ilmenite and rutile minerals inclusive found in States like Bauchi and Plateau

Source: Report of the Vision 2020 National Technical Group on Minerals and Metals Development (Falade *et al.*, 2016)

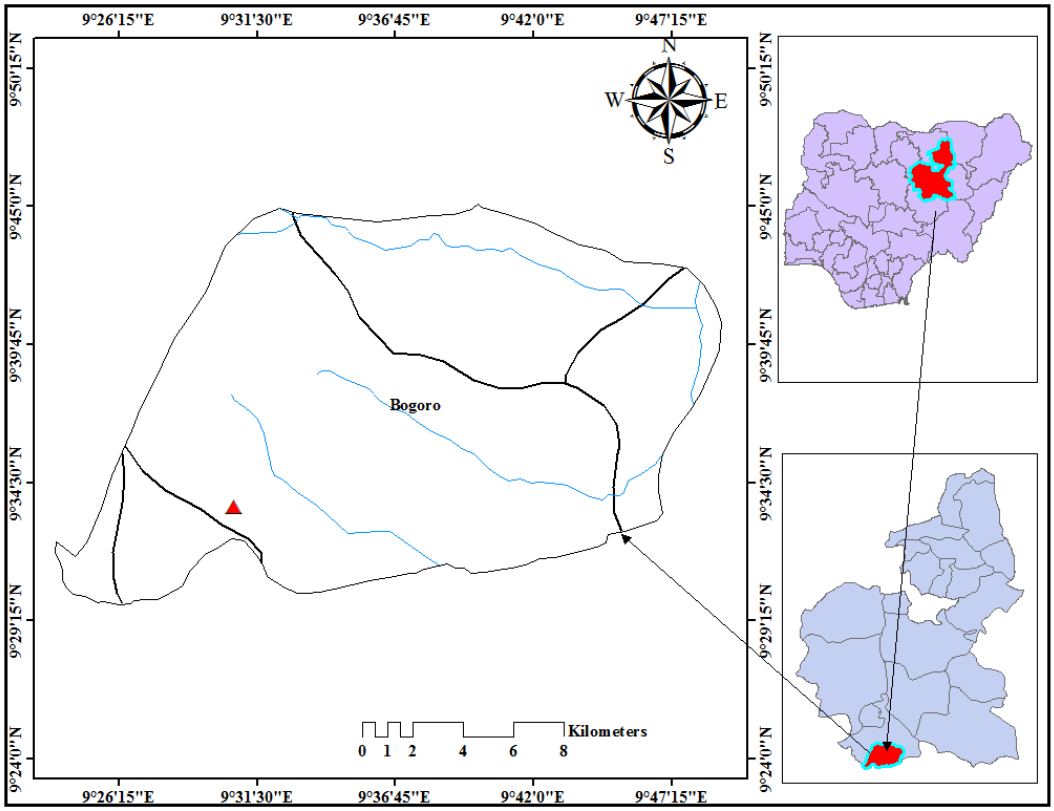


Figure 2.2 Map showing the location of the Ilmenite Resource at Ndit Village, Bogoro Local Government Area of Bauchi State, Nigeria

Table 2.2 shows the locations of some Nigerian ilmenite and rutile resources.

Table 2.2 Some Nigerian Ilmenite and Rutile Resources (in million tonnes)

S/N	Location	State	Metal Type	Estimated Reserved (Million Tonnes)
1	Tafawa Balewa, Bogoro (Ndit)	Bauchi	Ti, Si, Fe	Partially Investigated
2	Barkin Ladi	Plateau	Ti, Ta, Nb	Partially Investigated
3	Oke-Ode	Kwara	Ti, Ta, Nb	Partially Investigated
4	Ilesha	Osun	Ti, Fe, V	Partially Investigated

Source: Ministry of Mines and Steel Development (MMSD, 2012)

Ndit ilmenite resource is a newly discovered ilmenite mineral site outcrop in Bogoro Local Government Area of Bauchi State which has not been explorated and characterized for possible exploitation and beneficiation.

2.4 Processing of Titanium Bearing Minerals

Different methods of upgrading of rutile ores have been developed and more are still evolving due to the challenges of energy and complexity of the associated minerals in the ore. These processes include comminution and separation processes of magnetic separation, gravity separation, froth flotation and a combination of these techniques. The susceptibility of any rutile or titanium base ore to beneficiation by one of this technique is a major determinant into the development of process route for its concentration and also the amenability of any types of ore to beneficiation depends on the mineralogical characteristic of the ore (Wills *et al.,* 2006).

However, prior to the use of any of the separation techniques or combination of the techniques, pre-treatment process such as, calcination, roasting and sintering may be required.

2.4.1 Thermal Pre-Treatments Given to Rutile and Titanium Bearing Minerals Prior to Beneficiation

Rutile ores containing iron, silicate and sulphide minerals are usually subjected to certain thermal pre-treatments prior to beneficiation so as to induce changes in their structures. The nature and intensity of the thermal pre-treatments depend on whether the impurities are hydrated or un-hydrated and secondly whether they are chemically or physicochemical associated. The hydrated impurities are heated to about 500^0C to expel hydroxyl groups from the crystalline structure in the form of water vapour leaving behind a porous solid having a large surface area which can easily be leached with dilute acids. The un-hydrated impurities can be treated in two ways either by melting and quenching to obtain a glassy structure that can be readily crushed, ground and leached with acids or heated to a temperature below the melting point to effect a phase transformation which would result in volume change and the product would become porous which can be easily crushed and leached. In some thermal pretreatments coke breeze or fluxing agents are added to reduce or fluxed the impurities immediately after decomposition to produce two phases of metallic oxides. These two phases are usually separated using one of the concentration techniques mentioned earlier (Irannajad *et al.,* 2019).

2.4.1.1 Roasting

Roasting is a thermal process usually applied to metal sulphides or complex minerals by blowing of enriched air or oxygen to convert the sulphides to a mixture of oxide and sulphate with the production of sulfur dioxide or oxides that will result in dissociation of the mineral phases or formation of new mineral phases. The objectives in roasting can be to produce an oxide which is

subsequently acid-leached to give a solution from which the metal values can be recovered; to provide a partial desulphurization of a concentrate to facilitate the smelting operation. In some cases, to induce thermal stress that can facilitate the comminution of the mineral phases in the ore matrix.

The principal reaction in roasting is as followed:

$$MS_{(s)} + \frac{3}{2} O_{2(g)} \rightarrow MO_{(s)} + SO_{2(g)} \quad (2.1)$$

For all of the common metal sulfides (MS) the reaction is highly exothermic and proceeds spontaneously in the direction of metal oxide (MO) formation. The roasting temperatures are usually in the range of 650-1000^{0}C, the roaster gas usually contains some sulfur- trioxide due to the reaction 2.2

$$SO_2 + \frac{1}{2} O_2 \rightleftarrows SO_3 \quad (2.2)$$

Here the equilibrium shifts to the left as the temperature is raised, so that at 1000^{0}C the roaster gas contains but little SO_3. The formation of sulphates during roasting is favoured by the use of lower temperature, resulting in a corresponding high concentration of SO_3 in the off-gas (Friesinger, 2016).

2.4.1.2 Calcination

Calcination (also referred to as calcining) is a thermal treatment process applied to ores and solid materials in order to bring a thermal decomposition, phase transition, or removal of volatile fractions. The calcination process normally takes place at temperatures below the melting point of the product materials. Calcination is distinguished from roasting, in which more complex gas-solid reactions take place between the furnace atmosphere and the solids, however calcination takes place in the absence of air. Calcination comprises the heating of minerals to the temperature below their melting points to enhance their decomposition and elimination of volatile constituents. Calcination

differ from roasting in that in the latter there is a reaction between the solid and the surrounding hot gas; while in the former the gas serves merely as a source of heat (Biswas *et al.,* 2013).

Being an industrial process; calcination derives its name from its most common application, the decomposition of calcite to calcium oxide (lime). The product of calcination is usually referred to in general as "calcined," regardless of the actual minerals undergoing thermal treatment. Calcination is carried out in furnaces or reactors (sometimes referred to as kilns) of various designs including shaft furnaces, rotary kilns, multiple hearth furnaces and fluidized bed reactors (Thomas and Yaro, 2007).

Examples of calcination processes include the following:

i. Decomposition of hydrated minerals, as in the calcination of bauxite to remove crystalline water as water vapour;

ii. Decomposition of volatile matter contained in raw petroleum coke

iii. Heat treatment to effect phase transformations, as in conversion of ilmenite or anatase to rutile or devitrification of glass materials.

2.4.1.2.1 Calcination Reactions

Calcination reactions usually take place at or above the thermal decomposition temperatures (for decomposition and volatilization reactions to occur at the transition temperature for phase transitions to occur). This temperature is usually defined as the temperature at which the standard Gibbs free energy of reaction for a particular calcination reaction is negative. For example, in limestone calcination, a decomposition process, the chemical reaction is (Shen *et al.*, 2018)

$$CaCO_{3(s)} \rightarrow CaO_{(s)} + CO_{2(g)} \qquad (2.3)$$

The standard Gibbs free energy of reaction is approximated as G^{o}_{r} =177,100 - 158T (J/mol). The standard free energy of reaction is zero in this case when the temperature, T is equal to 848^{0}C

2.4.1.2.2 Oxidation

In some cases, calcination of a metal results in oxidation of the metal. Lead and tin when calcined gained weight, presumably as they were being oxidized (Shen *et al.*, 2018).

2.5 Methods of Characterizing Minerals

Metallurgical analysis involves the qualitative as well as the quantitative analysis of materials both raw (e.g. ores) and products (e.g. metals, alloys and slags).

Analytical methods in metallurgical analysis are classified into classical and instrumental methods. The classical method is slow and is employed for practical purposes. In the other hand, the instrumental methods are faster and quite precise.

The instrumental analytical techniques used are: X-Ray Fluorescence (XRF), X-Ray Diffraction (XRD), Scanning Electron Microscopy (SEM), Atomic Absorption Spectrometry (AAS) etc.

2.5.1 X-Ray Fluorescence (XRF)

XRF is an analytical method to determine the chemical composition of all kinds of materials. The materials can be solid, liquid, powder, filtered or other form. XRF sometimes can be used to determine the thickness and compositions of layers and coatings (Brouwer, 2006).

The method is fast, accurate, and non-destructive, and usually requires only a minimum of sample preparation. Applications are very broad and include the metal, cement, oil, polymer, plastic and food industries, along with mining, mineralogy and geology, and environmental analysis of water and waste materials (Brouwer, 2006).

2.5.2 Scanning Electron Microscopy (SEM/EDS)

SEM is an analytical technique which uses a focused beam of high-energy electrons to generate a variety of signals at the surface of solid specimens. The signals that derive from electron-sample interactions reveal information about the sample including external morphology (texture), chemical composition (using Energy Dispersive Spectrometry EDS), crystalline structure and orientation (using diffracted back-scattered electron EBSD) of the material (i.e. Sample).

SEM works at a high magnification reaches to 300,000x and even 1000000 (in some modern models) in producing images very precisely of wide range of materials. Energy Dispersive X-ray Spectroscopy (EDS) works together with SEM to provide qualitative and semi-quantitative results. Both techniques, together, have the potential to introduce fundamental information on material composition of scanned specimens, which could not be provided by the common laboratory tests (Mohammed *et al.*, 2018).

2.5.3 X-Ray Diffraction

XRD is a non-destructive analytical method used for both qualitative and quantitative analysis of materials. It is used to study the structure, phase composition, and physical properties of materials. This analytical technique is primarily used for phase identification of a crystalline material, also used to measure the structural properties (strain state, grain size, epitaxial, phase composition, preferred orientation and defect structure) of these phases and to determine the thickness of the thin films and multilayer (by determining the lattice mismatch between film and the substrate and to inferring stress and strain), and atomic arrangement in amorphous materials including polymers and at interface (Masok *et al.*, 2015).

XRD uses X-rays of a known wavelength that are passed through a sample for identification of the crystal structure. X-rays interact with electrons in the material and are scattered giving diffraction pattern. The position of diffraction peaks by lattice of the crystal, give a unique pattern at different angles and of different intensity (Warui, 2015).

2.6 Comminution Process

Comminution is a process whereby ores are progressively reduced to particle size which enables liberation of valuable minerals from the gangue and can be separated by various methods available for processing of ores (Wills *et al.,* 2006). Crushing and grinding are the two primary comminution processes.

2.6.1 Theory of Comminution

Comminution theory is concerned with the relationship between energy input and the particle size produced from a given feed size. The problem that is associated to comminution is the energy expended in machine operation, hence only a small fraction of the total energy is available for breaking the material (Wills *et al.,* 2006).

2.6.2 Grindability

Grindability refers to the ease with which materials can be comminuted, and data from grindability tests are used to evaluate crushing and grinding efficiency (Wills *et al.,* 2006). The most widely used parameter to measure the grindability of an ore is the Bond work index.

Table 2.3 Give the work index of some minerals ores samples

Material	Work Index	Material	Work Index
Barite	4.28 - 6.24	Fluorspar	2.98 - 9.76
Bauxite	2.38 - 9.45	Granite	2.68 - 15.13
Coal	1.63 - 11.37	Graphite	1.75 - 45.03
Dolomite	2.82 - 11.27	Limestone	2.69 - 11.61
Emery	3.48 - 58.18	Quartzite	2.71 - 12.18
Columbite	3.94 - 10.81	Titanium ore	4.23 - 11.88
Tantalite	3.6 - 11.90	Silica sand	2.65 - 16.46

Source: Ministry of Mines and Steel Development (MMSD, 2012)

2.7 Mineral Beneficiation Processes

Beneficiation of any type of ore for its mineral or metal values and also for the design of the appropriate flow-sheet(s) for the beneficiation of the ore comprises the use of unit processes of mineral beneficiation. The separation unit processes of mineral beneficiation are broadly classified into:

(a). Physical separation: Gravity, Magnetic, Froth flotation, Electrostatic or High tension and Sorting.

(b). Chemical separation: Leaching, Precipitation, Solvent separation and Electrowinning.

(c). Biological separation: Bacterial leaching.

(d). Pyrometallurgical separation: Thermal pretreatments include the followings: Roasting, Calcination, Sintering, Smelting and Refining

(e). Combinations of some or all the separation unit processes

Based on the geological, chemical, mineralogical and pilot plant concentration tests conducted conceptual flow-sheet is prepared incorporating one or a combination of the above unit processes

for the beneficiation of the ore(s). The following principles explained some of these separation methods utilize in mineral processing (Thomas and Yaro, 2007).

Heat or thermal treatment of ores is carried out by heating up the ores to a certain temperature to obtain a product with specific properties which is aimed at the breaking and removal of some associated impurities prior to beneficiation. Among the thermal treatment operations include: Calcination, Roasting etc. The upgrading of valuable mineral from their naturally occurring ores is differently referred to as “mineral dressing”, “ore dressing”; and “mineral beneficiation”. Beneficiation is an important intermediate step in the transformation of natural ore to pure metal. Thus, a successful beneficiation of an ore is greatly entangled to the available information on the nature and properties of the various components making up the ore. In achieving the aforementioned steps, chemical and mineralogical characterization of the ore are usually of utmost importance.

2.7.1 Processing of Titanium-Containing Minerals

Present invention relates to the removal of iron from titanium-containing minerals with focus on the oxidation of iron particularly. A significant quantity of the world’s titanium products is obtained from synthetic rutile (TiO_2), a material which is manufactured from the mineral ilmenite via the Becher Process. The Becher process is an industrial process used to produce rutile, a form of titanium dioxide, from the ore ilmenite. It is competitive with the chloride process and the sulfate process, which achieve similar net conversions (Benson *et al.*, 2016).

With the idealized formula $FeTiO_3$, ilmenite contains 55-65% titanium dioxide, the rest being iron and other associated minerals. The Becher process, like other beneficiation processes, aims to remove iron. The Becher process exploits the conversion of the ferrous iron (FeO) to ferric iron (Fe_2O_3). This process was developed by the Western Australian Government Laboratories in 1961

and is currently used in commercial operations. The Becher process is suitable for weathered ilmenite that has low concentrations of chromium and magnesium. There are four steps involved in removing the iron portion of the ilmenite which include: Oxidation, Reduction, Aeration and Leaching.

2.7.1.1 Oxidation

Oxidation involves heating the ilmenite in a rotary kiln with air to convert iron to iron (III) oxide:

$$4\ FeTiO_3 + O_2 \rightarrow 2\ Fe_2O3{\cdot}TiO_2 + 2\ TiO_2 \qquad (2.4)$$

This step is suitable for a range of ilmenite-containing feed stocks.

2.7.1.2 Reduction

Reduction is carried out in a kiln with pseudobrookite ($Fe_2O_3.TiO_2$) and coal then heated to a temperature greater than1200 °C. The iron oxide in the mineral grains is reduced to metallic iron to produce reduced ilmenite:

$$Fe_2O_3{\cdot}TiO_{2(s)} + 3\ CO_{(g)} \rightarrow 2\ Fe(s) + TiO_{2(s)} + 3\ CO_{2(g)} \qquad (2.5)$$

The "reduced ilmenite" is separated from the char prior to the next step.

2.7.1.3 Aeration

Aeration involves the removal of the metallic iron produced in the last step by rusting it out. This conversion is achieved in large tanks that contain 1% ammonium chloride solution with air being pumped through the tank. The tank is being continuously agitated, and the iron will rust and

Precipitate in the form of a slime (Ward *et al.,* 1999).

$$4\ Fe_{(s)} + 3\ O_{2(g)} \rightarrow 2\ Fe_2O_{3(s)} \qquad (2.6)$$

The finer iron oxide is then separated from the larger particles of synthetic rutile.

2.7.1.4 Leaching (Acid)

Once the majority of the iron oxide has been removed the remainder of it is leached away using 0.5M sulfuric acid.

2.8 Beneficiation of Titanium Ore

Titanium mineral is processed by removing gangue (unwanted materials) from the ore so as to increase its economic value. This is done for low grade ores in other to increase their value for further extraction. Most mineral including titanium occurs as low grade. Commonly used methods for beneficiating titanium ores include froth flotation, gravity and magnetic separation (Warui, 2015).

Beneficiation involves comminution (crushing and grinding); washing; filtration; sorting; sizing; gravity; magnetic; flotation; and agglomeration (pelletizing, sintering, briquetting, or nodulizing). Beneficiation upgrades the metal content of ores, especially those whose percentage levels are low, for example titanium among many minerals (Warui, 2015). This removes unwanted materials that make the ore useful for extraction. Titanium ores contains iron, silica and others as gangue in high amounts. This can be separated by use of a magnet due to magnetic nature of iron rich titanium ore. The levels of the metal of interest goes up in the ore are increased significantly making it possible to extract it at a lower cost. Low grade Ti ores has so many unwanted materials which include silica and other earthly particles (Warui, 2015).

Beneficiation leads to reduction of freight and shipping cost since less material require less space and resources to be moved from one location to another. These materials are mostly non-magnetic.

Removal of these materials makes it possible for the developing countries to manage the transportation expenses.

Titanium mining has not been exploited fully since there are no local industries to absorb the mineral and the freight costs are too prohibitive for an export market.

2.8.1 Magnetic Separation of Rutile

Magnetic separation is commonly used for beneficiating iron bearing mineral. Some gangue minerals have the properties of magnetism, such as magnetite, ilmenite, biotite, chlorite, amphibole and sphene, but rutile almost has no magnetism, so magnetic separation can be used to separate rutile from the gangue minerals mentioned above (Wang *et al.*, 2013).

The high intensity magnetic separation is mainly to remove the minerals with low magnetism, like monazite and xenotime. The low intensity magnetic separation is used to remove the mineral with high magnetite, like ilmenite and titanomagnetite (Wang *et al.*, 2013). Many studies have been done on magnetic separation technologies for rutile minerals.

Ilmenite is paramagnetic with relatively low magnetic susceptibility (Warui, 2015). Magnetic susceptibility of iron rich titanium ores such as ilmenite can be increased significantly by heating it in the presence of reducing agents, such as carbon monoxide and syngas (Ciu *et al.*, 2002).

Thermal reduction of ilmenite with carbon monoxide converts FeO in ilmenite ($FeO.TiO_2$) to maghemite (γ-$Fe_2O_3.TiO_2$). Its magnetic susceptibility is high (Ciu et al., 2002). Maghemite is also formed as a result of oxidation of magnetite, with less than 2 percent TiO_2 (Warui, 2015). Maghemite loses Fe ions but retain the spinel structure. The roasted ilmenite has a higher magnetic susceptibility and thus can be separated by use of a magnet. Magnetic separation has been used in

the concentration of magnetite due to its strong magnetic susceptibility (Warui, 2015). Magnetite can be converted to maghemite (γ-Fe_2O_3) at temperatures above 600°C. The structure of this mineral contains iron which enables the concentration of titanium dioxide.

Titanium and iron formations follow a similar trend. Magnetic susceptibility of iron can be used to concentrate Ti. This suggests that Ti can be concentrated using magnetic separation (Warui, 2015).

2.8.2 Gravity Separation of Rutile

Gravity concentration methods separate minerals of different specific gravity by their relative movement in response to gravity and one or more other forces, the latter often being the resistance to motion offered by a viscous fluid, such as water or air (Wills *et al.*, 2006).

Particles settle differently depending on their densities. Particles with the highest density settle fast while those with less density follow. The sharp differences in the density of titanium and that of iron can be utilized in their separation using the gravity separation technique.

Except for magnetite, biotite, ilmenite, hematite, goethite, chlorite, amphibole and sphene, the specific gravity of the other gangue minerals is 2.1-3.1, and the specific gravity of rutile is 4.1-5.2, so gravity separation can be used to separate rutile from the above gangue minerals with lower specific gravity (Wang *et al.*, 2013).

Gravity separation process can also be used for de-sliming, and then the dosage of flotation reagents can be reduced. The main equipment of gravity separation includes shaking table, spiral chute, centrifugal concentrator and spiral concentrator. Spiral chute and shaking table are often used in the beneficiation of rutile. With the advantages of low production cost and less pollution to the

environment, gravity separation technology has been paid much attention in the beneficiation of rutile minerals (Wang *et al.,* 2013).

Given the properties of primary rutile minerals, the effect is stilled not good enough using the common equipment of gravity separation, thus the development of highly efficient gravity separation equipment, especially for fine particle rutile minerals, is an important step for the comprehensive exploitation and utilization of rutile minerals (Wang *et al.,* 2013).

2.8.3 Froth Flotation of Rutile

Flotation is a very important method in mineral processing, and it can be used to process fine particle ores. For the flotation of rutile minerals, its main principle is to use flotation reagents with active functional groups like -COOH, -AsO_3H_2, -PO_3H_2NOH, which can absorb on the surface of TiO_2 by chemical bonds, and then cause flotation as the hydrophobic hydrocarbyl (Wang *et al.,* 2013).

The development of the flotation technologies mainly depends on the development of flotation reagents, including the collectors and regulators. The main collectors in the flotation of rutile include anionic collector like arsenic acid, fatty acid, and chelating collector like styrene phosphonate, hydroximic acid. These collectors can be used alone, some can be mixed with each other, which may cause the synergistic effect and improve the effect of flotation (Wang *et al.,* 2013).

It is widely believed that the collecting ability of different reagents for rutile from best to worst is hydroxamic acid＞benzyl arsenic acid＞styrenephosphonate＞salicyl hydroxamic acid, and the selecting ability from best to worst is styrene phosphonate＞benzyl arsenic acid＞hydroxamic acid

＞salicyl hydroxamic acid. The collectors containing phosphate radicals or phosphonate radicals have a good collecting ability for the minerals containing calcium (Wang *et al.*, 2013).

Froth flotation is used to separate a large range of sulphides, carbonates and oxides prior to further refinement. The ore is crushed to fine powder, mixed with water to form slurry. Surfactant or collector chemicals are added to make the mineral hydrophilic. The slurry is then aerated in a water bath to form air bubbles as illustrated in the Figure 2.3

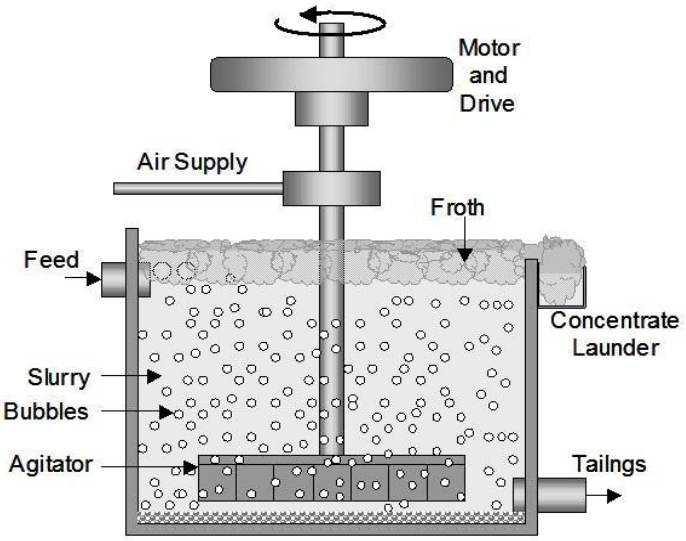


Figure 2.3 Flotation Cell: Source (Warui, 2015)

Slurry is separated into two, a hydrophilic mineral and hydrophobic gangue. The air bubble forms a stable froth with the mineral thus reducing its density hence making it possible for it to float and is skimmed off (Warui, 2015).

2.8.4 Electrical Separation of Rutile

Electrical separation utilizes the difference in electrical conductivity between the various minerals in the ore feed. Since almost all minerals show some difference in conductivity it would appear to represent the universal concentrating method (Wills *et al.*, 2006).

Rutile is a good conductor, thus electrical separation can be used to separate rutile from apatite, zircon and other minerals with low electric conductivity. High voltage double roller separator, high voltage Corona electricity separator and swing electric separator are often used in the electrical separation of rutile minerals, different electrical separators are chosen according to different contents of leucosphenite, zircon and rutile (Wang *et al.*, 2013).

2.9 Previous Works on Titanium Ores

i. Siyanbola *et al.*, (2004) worked on "Elemental Composition of rutile from south-western Nigeria using X-ray techniques". Quantitative analyses of the ore using pellets made from properly homogenized samples showed that the concentration of titanium dioxide (TiO_2), which is the dominant phase in the mineral, could be as high as 82.45 wt.%, giving Ti concentration of 49.4 wt. %. Other major elements observed in the ore include Fe (3.1 wt. %), V (1.01 wt. %), Ca (0.19 wt. %) and K (0.21 wt. %). In addition, several other elements/impurities were detected in minor and trace quantities including; Cr, Mn, Co (with concentration between 300 and 1000 ppm) and Zr, Ni, Zn, Rb, W, Pb, Sr, Y, Mo, Nb, Br, As, Cu (with concentration between 10 and 300 ppm). But do not carry out the beneficiation process of the rutile ore.

ii. Itoh *et al.*, (2006) worked on the "Feasibility Study of the New Rutile Extraction Process from Natural Ilmenite Ore Based on the Oxidation Reaction". It is found that rutile can be produced from common natural ilmenite ores not only by the reduction as the conventional titanium-rich slag process but also by an oxidation. The feasibility of the process was confirmed experimentally by oxidation of an Australian natural ilmenite ore in air followed by leaching of synthesized pseudobrookite in diluted sulfuric acid. Oxidation leads to a considerable reduction of energy consumption to extract rutile in comparison with the conventional titanium-rich slag process and

also diluted acid leaching of oxidized ore results in reduction of the amount of sulfuric acid required. The calcination thermal pret-reatment of the ilmenite ore was not investigated.

iii. Jha *et al.*, (2008) carried out the "Beneficiation of titaniferous ores by selective separation of iron oxide, impurities and rare earth oxides for the production of high-grade synthetic rutile". A new process for the production of synthetic rutile which includes high temperature alkali roasting process and the ensuing hydrometallurgical leaching steps has been developed. It was found that the various complex phases of Na–Ti–Fe–Al–Si-O formed during roasting reaction were responsible for the removal of impurities. Also, the effect of calcination on the thermal pre-treatment of the titaniferous ores was not investigated.

iv. Setyani *et al.*, (2014) worked on the "The Effect of Roasting Temperature at 400^{o}C and Sulphuric Acid Concentration on TiO_2 Extraction Process from Zircon Sand Ilmenite". In this study, the leaching process lasted in two stages. For the first leaching samples of combustion products were leached using distilled water to remove water-soluble impurities. For the second stage, the deposition obtained from stage one is leached using 8, 10, and 12 M concentrated sulphuric acid at high temperature to dissolve iron. The result showed that the sample at temperature of 400^{o}C and concentrated sulphuric acid of 12 M is whiter in colour compared to other samples. Furthermore, at temperature 400^{o}C and concentrated sulphuric acid of 12 M, the titanium dioxide produced is 32.3% and 11.5% for rutile and anatase, respectively. Here the effect of thermal pre-treatment of calcination was also not investigated.

v. Terzi *et al.*, (2015) worked on the "Investigation of Recovery Possibilities of Rutile Minerals from the Feldspar Tailings with Gravity Separation Methods". It was determined that feed sample contains TiO_2 at the rate of 1.90% and TiO_2 content is associated with the feldspar tailings to a large extent. As a result of beneficiation tests; a concentrate containing 11.26% TiO_2 with a 50.43%

rate of recovery were obtained in the shaking table tests and a concentrate containing 17.11% TiO_2 with 89.33% rate of recovery were obtained in the MGS tests by using optimum conditions. In consideration of results obtained it is presented that gravity methods are able to be used as method of a pre-beneficiation in the recovery of titanium minerals from feldspar tailings.

vi. Hiraki *et al.*, (2018) worked on the "Up-grading of natural ilmenite ore by combining oxidation and acid leaching". He showed that a fluidized bed reactor can be used to oxidize ilmenite ore to rapidly form rutile and pseudobrookite (Fe_2TiO_5) phases. Ilmenite was oxidized with 5vol% O_2 in Air at temperatures of 1173 K or 1223 K and subsequently leached using a diluted H_2SO_4 solution to dissolve the pseudobrookite phase. The effects of acid concentration, temperature, and cooling rate after oxidation were investigated. He concluded that the ilmenite was rapidly oxidized to form rutile and pseudobrookite phases at 1173K and 1223 K in a 5vol.% O_2/95 vol.% Air environment within 40 minutes . The final maximum rutile yield was 84.2mol% after leaching in (1 + 1) H_2SO_4 solution at 393 K for 12 h.

vii. Nguyen *et al.*, (2019) worked on "A review on the recovery of titanium dioxide from Ilmenite ores by direct leaching technologies". He reported that, temperature, time and acid concentration significantly affect the dissolution of titanium and impurities in ilmenite. The addition of either iron powder or chloride/sulfate salts affects significantly the leaching rate of ilmenite. He recommended either HCl leaching followed by solvent extraction or alkaline leaching followed by hydrolysis-calcination as the suitable method for the production of pure TiO_2 from ilmenite.

From all the literatures reviewed so far, none of the researchers investigated the effect of both calcination and roasting at the same time on either ilmenite or rutile ores they have worked upon. Both Calcination and Roasting thermal pre-treatments have great effect on the transformation of the structures of the ores. Literatures revealed that both calcination and roasting can be utilized in the

beneficiation of ilmenite and rutile ores. However, based on literatures reviewed on rutile and ilmenite ores, no work on the effect of thermal pre-treatment on the beneficiation of Ndit ilmenite resource has been carried out.

CHAPTER THREE

MATERIALS AND METHOD

3.1 Materials

i. Ndit Ilmenite sample

ii. Reference ore sample (Granite)

3.2 Equipment

The following equipment was used in this research.

i. Laboratory sledge hammer

ii. Pulverizing machine

iii. Ball mill

iv. Set of sieves/laboratory shaking machine

v. Electronic Weighing Scale

vi. X-Ray Fluorescence (XRF) Machine

vii. Scanning Electron Microscopy (SEM)/ Energy Dispersive Spectrometry (EDS) machine

viii. X-Ray Diffraction (XRD) machine

ix. Petrological microscope

x. Muffle furnace

xi. Global Positioning System (GPS)

xii. High Intensity Magnetic Separating Machine

xiii. Gravity Separator/Air-float Separating Machine

3.3 Methodology

3.3.1 Sample Collection

Representative sample was sourced from the ilmenite resource site in Ndit Village, Bogoro Local Government Area of Bauchi State, Nigeria. Grab sampling method was used alongside taking the GPS to determine the geographical points/coordinates at which samples were collected. Fifty kilograms (50kg) of the sample was sourced from four (4) different points at an interval of fifty meters (50m) apart in order to have a representative sample of the ilmenite resource. Table 3.1 shows the GPS coordinates of where the Rutile resource sample was sourced.

3.3.2 Sample Preparation

Sample preparation involves comminution which consists of crushing and grinding operation. The lump particles of the sample were reduced to the size that are suitable for the pulverizing machine.

3.3.3 Sampling

Coning and quartering sampling method was used to take a representative sample for sieve analysis.

3.3.4 Chemical Analysis

Chemical analysis was carried out using X-ray Fluorescence (XRF) Spectrometry (ARL QUANT`X EDXRF spectrometer) at the Umaru Musa Yar'adua University, Katsina State. This analysis was carried out to determine the elemental composition.

The Ilmenite ore sample was pulverized using jaw crushing machine, disc miller and finally cup miller to fine particle size of 100 mesh (0.15 microns). The powdered sample was placed in the sample cup filling up¾ parts of the cup with the sample. The cup was then covered with film to avoid wrinkles on it, and finally the slim ring was fixed by sliding it down and the thick ring on top of the cup. After the cups preparation, the cups were placed on the sample stage inside the

spectrometer chamber (placed with the side to be analyzed facing down toward the X-ray tube). X-rays from the X-ray tube penetrate the layers on the disk and excite the elements in the sample which emits fluorescence X-ray photons with energies that are characteristic of each element in the sample. These X-ray photons are measured by a detector, which produces a spectrum. The software automatically integrates the peaks for each element.

3.3.5 Mineralogical Analysis

Mineralogical analysis was carried using X-ray Diffraction (XRD) Panalytical Empyrean Diffractometer at the Nigerian Geological Survey Agency (NGSA) Kaduna, while Scanning Electron Microscope (SEM)/ Energy Dispersive Spectrometry (EDS) analysis was carried out using (SEM/EDS) Phenom Pro X model in the Department of Geological service, Research and development unit, National Steel Raw Materials Exploration Agency (NSRMEA) Kaduna. Through these analyses the major and minor mineral phases; size and shape of the various minerals contained in the rutile matrix were identified.

3.3.5.1 X-ray Diffraction Analysis

Powdered sample of the ilmenite was prepared and placed in a standard sample holder of the X-ray diffractometer. A collimated beam of X-rays was incident on the specimen and diffracted by the crystalline phases in the specimen. The intensity of the X-rays was as a function of the diffracted angle 2ɵ and the specimen's orientation. The peaks displayed and expressed the sample composition at the various angle of the degree theta.

3.3.5.2 Scanning Electron Microscope (SEM) Analysis

Small amount of powdered sample was placed on the sample holder and mounted inside the machine. A vacuum was built in the sample chamber, the sample was irradiated to generate

emission from which micrograph of the sample was produced. During the process the EDS was also carried out to establish the spectra of the major elements.

3.3.5.3 Petrological Analysis

Petrological analysis of the ore was carried out using the Petrological Optical Microscope (POM) with inbuilt camera at the department of Geology, Ahmadu Bello University, Zaria. Thin sections of representative sample of the pits were prepared and studied using both plane polarized and cross polarized lights. The samples were cut, ground and polished using polishing machine until a thin transparent surface is obtained. The prepared sample was mounted on glass slide glued with adhesive and heated in the oven to obtain the thin sections when removed. The thin sections were then viewed through the petrological microscope with an inbuilt camera to obtain the micrograph. The distribution of each mineral in the sample was determined using the point counting. The micrographs were used for the analysis through comparison with a mineral colour map atlas.

3.3.6 Sieve Size Analysis

Particle size analysis was carried out to establish the distribution of minerals in the various sieve fractions. Well prepared sample of 200g was poured on the set of sieves and placed on the sieve's shaking machine using the scale of root two $\sqrt{2}$ sieve arrangement as follows: +425µm, +425-355µm, -355+250µm, -250+180µm, -180+125µm, -125+90µm, -90+63µm, -63+45µm for 15 minutes. The retained sieve size fractions samples on each sieve were weighed and analyzed for their chemical contents.

3.3.7 Liberation Size Analysis

Liberation size study was carried out to establish the distribution of various minerals especially the titanium (Ti) bearing minerals in the various sieve size fractions. 200g of ground sample was subjected to sieve analysis. Nominal sieves size ranges from +425µm to -45µm with the coarsest

sieve at the top were used. A tight fitting pan was placed at the bottom sieve to receive the final undersize and a lid was placed on the top of the coarsest sieve size to prevent escape of the sample. The arranged sieves were placed on the sieve shaker which vibrates the materials vertically. This was carried out for twenty minutes after which the machine was turned off and the materials retained on each sieve size weighed and labeled appropriately. The sample in each sieve size fraction was analyzed using X-ray Fluorescence spectrometry (XRF). The sieve fraction that contains the highest percentage assay of TiO_2 content is considered as the liberation size of the ilmenite resource.

3.3.8 Work Index Determination

Modified Bond (Berry and Bruce) method which involves using test and reference ore samples was employed to determine the work index of the ore.

The sample of the reference ore was ground manually with a sledge hammer to provide required size acceptable as feed to the Denver laboratory jaw crusher. The sample was crushed and pulverized; part of the pulverized samples was weighed for sieve analysis. The modified Bond's method of determining the work index of ore involves use of reference ore of which grindability is known. The procedure is as follows:

i. 200g each of samples of the ore under test and the reference ore were crushed and pulverized in the laboratory mill machine for an hour,
ii. The samples of test and reference ores were taken and sized by sieving into a number of size fractions using the automatic sieve shaker for 15 minutes.
iii. Each size fractions of the test and the reference ores were weighed and the value noted as "feed".

iv. The "feed" test and reference ores were each gathered together and introduced into the Laboratory ball milling machine and ground for 20 minutes.

v. The test and the reference ores from the laboratory ball mill machine were sized and each sieve fraction was weighed and the value noted as the product or discharge.

vi. The results of the test were tabulated and used to calculate the work index of the test ore using the bond's equation.

The ground samples were sieved into the following sieve size fractions; +425µm, -425+355µm, -355+250µm, -250+180µm, -180+125µm, -125+90µm, -90+63µm, -63+45µm using Denver automatic sieve shaker for 15 minutes.

The selection of sieves was based on scale of root two and arranged from the coarsest on top and the finest sieve at the bottom. The sample was placed at the topmost sieve and a pan was placed at the bottom.

The work index of the ore was determined by comparing its grindability.

$$Wr = Wt \tag{3.1}$$

$$Wir = \left[\frac{10}{\sqrt{Pr}}\right] - \left[\frac{10}{\sqrt{Fr}}\right] = Wit = \left[\frac{10}{\sqrt{Pt}}\right] - \left[\frac{10}{\sqrt{Ft}}\right] \tag{3.2}$$

$$wit = wir\,\frac{\left[\frac{10}{\sqrt{Pr}}\right]-\left[\frac{10}{\sqrt{fr}}\right]}{\left[\frac{10}{\sqrt{Pt}}\right]-\left[\frac{10}{\sqrt{ft}}\right]} \tag{3.3}$$

Where Wr = Energy input in grinding the reference ore; Wt = Energy input in grinding the ore test

Wir = work index of the reference ore; Wit = work index of the test ore

Fr = 80% passing feed of the reference ore; Ft = 80% passing feed of the ore test

Pr= 80% passing product of the reference ore; Pt = 80% passing product of the ore test.

Therefore, the work index of test ore was determined using equation (3.2)

3.4 Thermal Pre-Treatment

3.4.1 Calcination

Calcination was carried out in the muffle (SX-5-12 Box-Resistance) furnace. The prepared sample of weight 250g was poured on a refractory ceramics crucible and introduced into the furnace. The furnace is then closed, switched on and the temperature and time of 650^{o}C for 60 minutes was set. The sample was heated in the absence or limited supply of air. In the attainment of the set temperature and time for the complete process to take place, the heated sample was left to furnace cool.

Table 3.1 Calcination Parameters

	Levels		
Factors	-	0	+
Time (min)	30	45	60
Temperature (^{o}C)	300	650	1000

3.4.2 Roasting

Roasting was carried out in the muffle (SX-5-12 Box-Resistance) furnace. The prepared sample of weight 250g was poured on a refractory ceramics crucible and introduced into the furnace. The furnace is then closed, switched on and the temperature and time 300^{o}C for 60 minutes was set. The sample was heated and in the attainment of the set temperature and time for the complete process to take place, the heated sample was brought out to air cool.

Table 3.2 Roasting Parameters

	Levels		
Factors	-	0	+
Time (min)	30	45	60
Temperature (^{o}C)	300	650	1000

3.5 Beneficiation

3.5.1 Magnetic Separation Using High Intensity Magnetic Separator (Reverse Magnetic Separation)

250g of prepared sample was introduced into the magnetic separator at 2.5T magnetic field. The machine separates the sample into concentrate and tailings based on magnetic susceptibility. The non-magnetic product of the machine which is the concentrate was taken for further processing on the gravity separator (Air-float) machine. This separation process was carried out at the National Metallurgical Development Centre (NMDC) Jos.

3.5.2 Gravity Separation

The non-magnetic product of the magnetic separator was introduced on the air-float machine. This was carried out to separate the constituents based on their specific gravity differences.

Both the concentrate and the tailings were collected and analyzed using the XRF to determine their chemical composition. This separation process was carried out at the National Metallurgical Development Centre (NMDC) Jos.

CHAPTER FOUR

RESULTS AND DISCUSSION

4.1 Coordinates of the Ilmenite Resource Site

Table 4.1 presents the coordinates of the Ilmenite resource site.

Table 4.1 Coordinates of the Ilmenite Resource Site

S/N	Coordinates
Pit A	Latitude 9.55938 N9^{o}33’33.75972’’
	Longitude 9.51057 E9^{o}30’38.04336’’
Pit B	Latitude 9.55712 N9^{o}32’30.72951’’
	Longitude 9.51211 E9^{o}2936.13236’’
Pit C	Latitude 9.7331 N9^{o}33;32.76132’’
	Longitude 9.54132 E9^{o}30’35.05247’’
Pit D	Latitude9.53731 N9^{o}31’33.71742’’
	Longitude 9.5029 E9^{o}28’30.14235’’

Table 4.1 shows the coordinates of the various points where the ilmenite resource was collected. The ilmenite resource was sourced from Ndit village, Bogoro Local Government Area of Bauchi State, Nigeria.

4.2 Chemical Composition of the Head Sample

Table 4.2 presents the result of the chemical analysis of Ndit Ilmenite Resource in weight percentages.

Table 4.2 Chemical Composition of Ndit Ilmenite Resource as determined using the (XRF) machine

Compounds	%
TiO_2	41.50
Fe_2O_3	21.78
SiO_2	18.20
Al_2O_3	15.85
Nb_2O_5	1.18
TaO_5	0.20
MnO	0.65
Others	0.64

From Table 4.2, the result reveals that the run-of-mine ilmenite resource contains 41.50% TiO_2, 21.78% Fe_2O_3, 15.85% Al_2O_3, and 18.20% SiO_2 as the major minerals, 1.18% Nb_2O_5 as the minor mineral, 0.20% TaO_5, 0.65% MnO and 0.64% others as trace minerals. The distribution of the various minerals in the matrix of the rutile could be attributed to the mineralization of the rutile during its geochemical formation and this trend agreed with Mallo, (2007). Despite the silica content and other associated minerals of the Ndit Ilmenite, their presents cannot stop the utilization of the Ilmenite resource. Since the silica and other associated minerals can be removed during beneficiation. Hence, the Ndit ilmenite resource can be said to be another potential source of titanium and other minerals that can be beneficiated and utilize in the nation's metallurgical industry.

4.3 Mineralogical Analysis

4.3.1 XRD Analysis

Figure 4.1 the XRD patterns and mineralogical analysis of the Ndit ilmenite resource

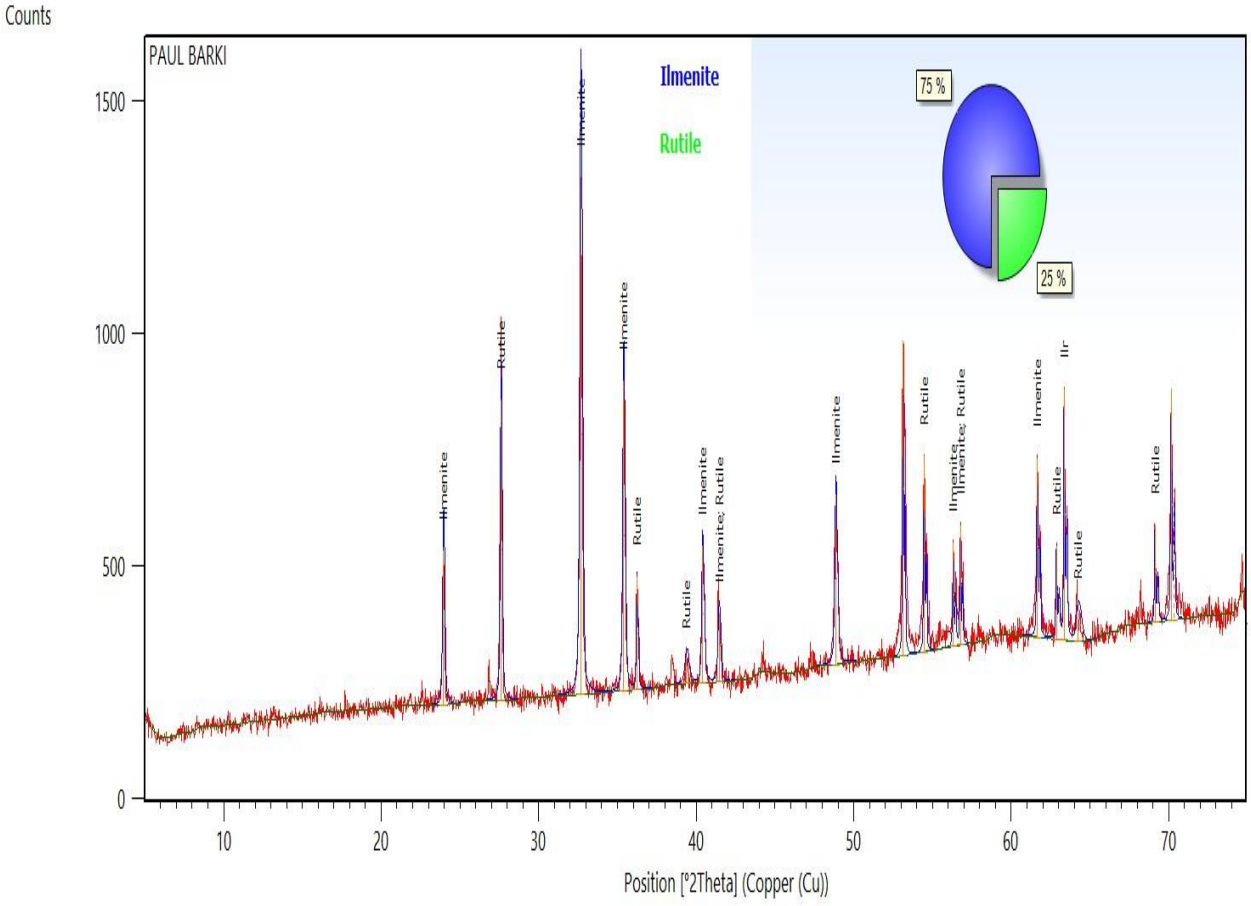


Figure 4.1 XRD pattern for Ndit Ilmenite Resource

Table 4.3 XRD Analysis of the Ndit Ilmenite Head Sample

Mineral Name	Chemical Formula	% Composition
Ilmenite	$FeTiO_3$ ($FeO.TiO_2$)	75
Rutile	TiO_2	25

Figure 4.1 shows the XRD diffractogram (spectra) pattern of the mineral phases contained in the matrix of the Ndit ilmenite while Table 4.3 presents the % proportion of the mineral phases of the Ndit ilmenite. The XRD diffractogram result in Figure 4.1 and the % proportion of the mineral phases in Table 4.3 revealed that, Ilmenite ($FeTiO_3$) or ($FeO.TiO_2$) with 75% phase proportion is the predominant and major mineral phase. While Rutile (TiO_2) with 25% phase proportion is the minor mineral phase contained in the matrix of the Ndit ilmenite. The variation in the % phase's proportion of the ilmenite resource could be attributed to the differential mineralization that probably was caused by geochemical tectonic activity/thermal fluid movement that favour more the crystallization of ilmenite to rutile phase. This trend has also, been reported in Salawu, (2015). However, the non-appearances of other minerals phases as revealed in the XRF analysis could be attributed to their low limit of detection (LOD) by the XRD. Hence, the need to correlate the XRD result with XRF, SEM/EDS and Petrological to ascertain the nature of the ilmenite resource mineral constituents since their interactions may affect their beneficiation processes.

4.3.2 Scanning Electron Microscopy

Plates I and II are the SEM micrographs of Ndit ilmenite resource showing the grains size of the mineral contained in the sample at different magnifications.

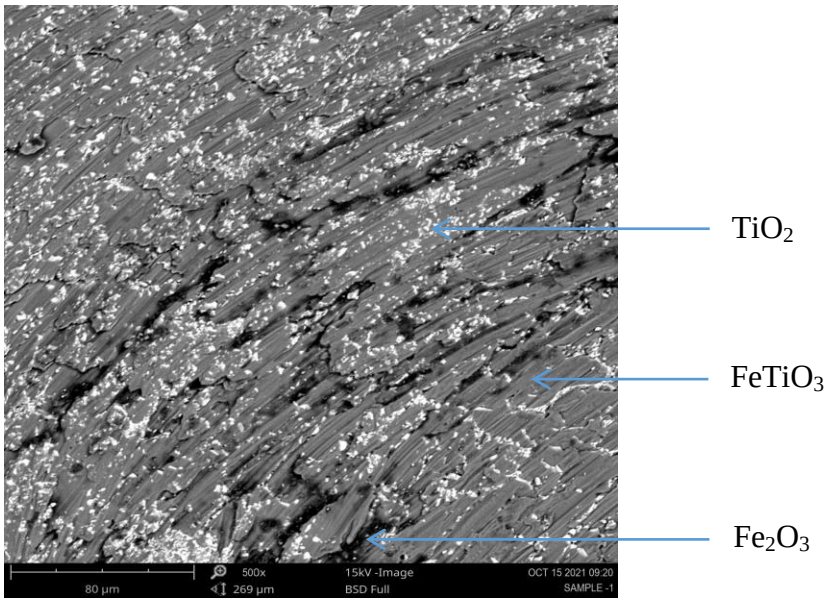


Plate I SEM micrograph showing the morphology of Ndit ilmenite resource at 500x Where grey (Ilmenite), White (Rutile) and Dark (Hematite)

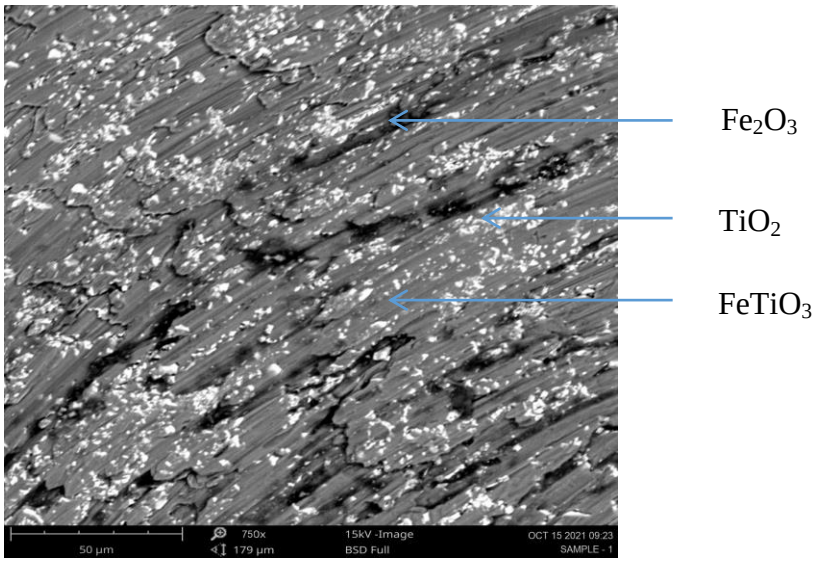


Plate II SEM micrograph showing the morphology of Ndit ilmenite resource at 750x Where grey (Ilmenite), White (Rutile) and Dark (Hematite)

From the micrographs of Plates I and II, it is observed that the minerals particle size is smaller and fine in nature and are separated by grain boundaries. The images revealed non-interlocking of minerals grains with varying sizes. This shows that the minerals can be fragmented, separated and

liberated from its gangue when comminuted. Rutile is seen as the white phases, grey represent the Ilmenite and the dark phases are Hematites. This is in line with the findings of Lv *et al.*, (2017).

4.3.3 Petrographic Microscopy of Ndit Ilmenite Resource

Plates III and IV present the photomicrographs of the Ndit Ilmenite resource under plane polarized light (PPL) and crossed polarized light (XPL) respectively.

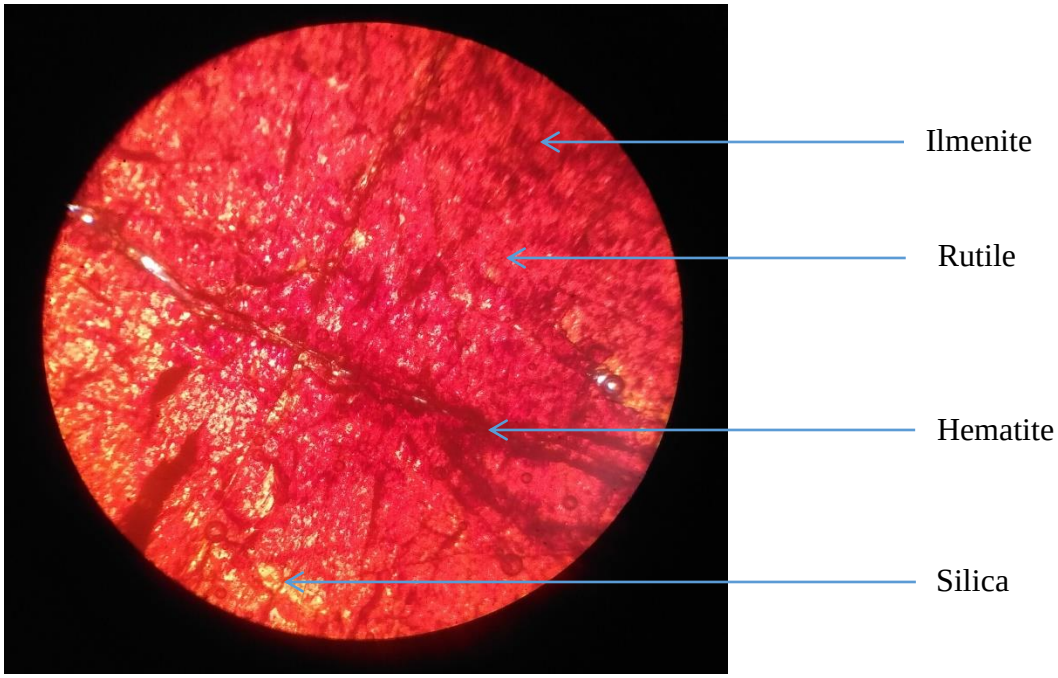


Plate III Photomicrograph of the head sample under plane polarized light (PPL)

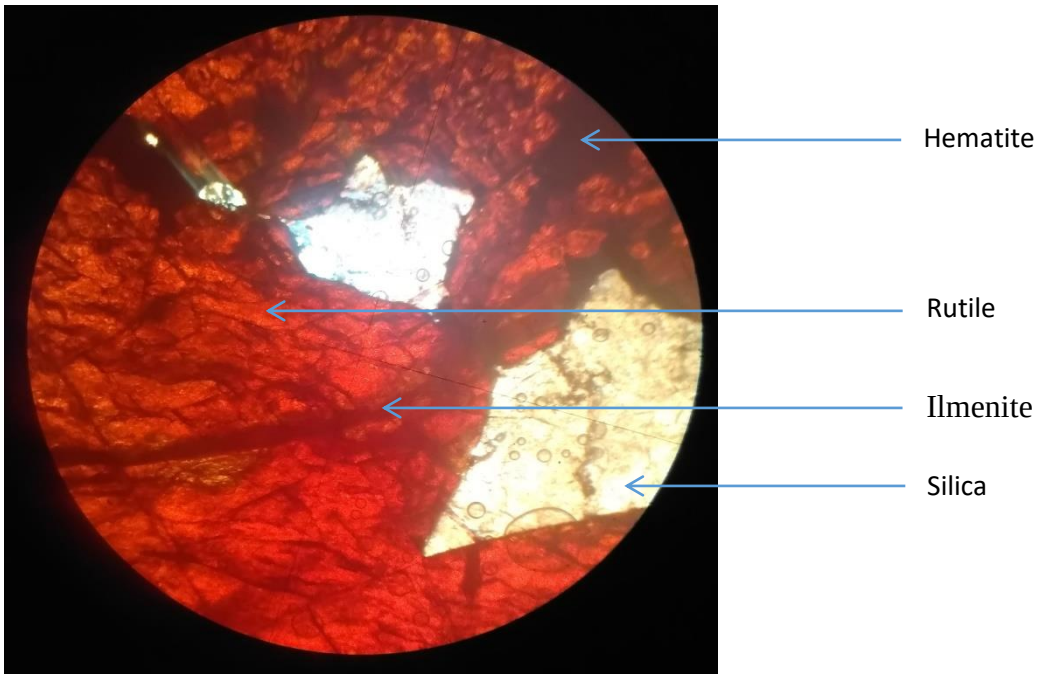


Plate IV Photomicrograph of the head sample under crossed polarized light (XPL)

From the petrological micrographs shown in Plates III and IV, the mineral phases present under both plane and crossed polarized light include Rutile (reddish-brown), Ilmenite (iron-black or brownish-black), Hematite (Opaque) and Silica (Colourless). This confirmed the result of XRD analysis that showed Ilmenite as the predominant and major mineral phase and Rutile the minor phase. However, the petrological photomicrographs further revealed that the Ndit ilmenite also contains Silica and Hematite in its matrix.

4.4 Sieve Analysis and Liberation Size of the Sample

Table 4.4 present the results of the chemical analysis of various sieve size fractions using XRF.

Table 4.4 Chemical analysis of various sieve size fractions using XRF

Element	+425	-424+355	-350+255	-250+180	-180+125	-125+90	-90+63	-63+45	-45
Al	15.29	14.76	14.93	16.59	16.41	16.18	16.36	17.18	17.94
Si	36.39	36.49	36.89	37.15	37.31	36.37	37.10	36.52	39.04
P	0.16	0.13	0.15	0.17	0.17	0.11	0.06	0.19	0.16
K	0.08	0.22	0.09	0.17	0.14	ND	ND	0.20	0.24
Ca	1.70	0.29	0.58	1.04	0.62	1.41	1.30	2.09	1.99
Ti	**42.46**	**44.63**	**44.85**	**40.42**	**41.70**	**41.92**	**41.22**	**39.16**	**35.09**
V	0.22	0.22	0.19	0.21	0.25	0.27	0.27	0.33	0.41
Mn	0.15	0.15	0.08	0.10	0.13	0.14	0.15	0.17	0.11
Fe	3.54	3.06	2.02	2.68	3.26	3.59	3.53	4.15	4.98
Nb	0.01	0.01	0.01	0.01	0.01	0.01	0.01	0.01	0.01

Table 4.4 presents the result of the chemical analysis (XRF) of the various sieve size fractions, sieve -355+250µm contained the highest percent assay of Titanium (44.85% Ti) while -45µm has the least of Titanium (35.09%Ti). -355+250µm sieve size fractions has the highest Ti assay as compared to other sieve size fractions hence, -355+250µm sieve size is the liberation size of the Ndit Rutile resource. This implies that the Ilmenite resource should be ground to -355+250µm in order to avoid over and under-grinding which will amount to energy wastage. However, exhibition of -355+250µm to have the highest proportion of Ti could be attributed to the nature of the particle size and shape factor of the rutile mineral which much are retained in sieve -355+250µm. Similar trend has also been observed and reported in Abdulkadir, (2021).

4.5 Work Index

4.5.1 Test Ore (Ndit Ilmenite) and Reference (Granite) as Feeds to the Ball Mill

Table 4.5 and 4.6 gives the sieve analysis result of the feed to ball mill of test ore (Ilmenite).

Calculation using the values in Table 4.5

If 250 μm = 77.216

Then X = 80%

Using Gaudin Schumann Expression

$\text{Size}_2 = \frac{(Percentage\ Passing\ Size2)^2}{(Percentage\ Passing\ Size1)2}$ X Size 1

Where

Size 2 =?

Size 1 = 180

Percentage passing size 2 = 80

Percentage passing size 1 = 77.97

$X\mu m = (\frac{80/100}{77.516/100})^2$ X 250 = 266.279μm at 80%

Table 4.5 Sieve Analysis of Ndit Ilmenite Sample (Test Sample) Feed to Ball Mill

Sieve Sizes (μm)	Weight Retained (g)	% Weight Retained	Nominal Apertures	Cumulative % Weight Retained	Cumulative % Weight Passing
+425	1.980	0.999	425	0.999	99.001
-425+355	5.940	2.997	355	3.996	96.004
-355+250	36.640	18.488	250	22.484	77.516
-250+180	35.380	17.852	180	40.336	59.664
-180+125	28.850	14.557	125	54.893	45.107
-125+90	23.930	12.075	90	66.968	33.032
-90+63	19.860	10.021	63	76.989	23.989
-63+45	15.840	7.993	45	84.982	15.018
-45	29.720	14.996	Pan	100	0.000
	198.180				

Table 4.6 Sieve Analysis of Granite Sample (Reference Ore) Feed to Ball Mill

Sieve Sizes (μm)	Nominal Apertures	Weight Retained (g)	% Weight Retained	Cumulative % Weight Retained	Cumulative % Weight Passing
+425	425	0.190	0.095	0.100	99.900
-425+355	355	33.120	16.570	16.665	83.335
-355+250	250	45.880	22.954	39.619	60.381
-250+180	180	22.760	11.387	51.006	48.994
-180+125	125	18.640	9.326	60.332	39.668
-125+90	90	16.760	8.385	68.717	31.283
-90+63	63	25.480	12.748	81.465	18.535
-63+45	45	15.680	7.845	89.310	10.690
-45	Pan	21.360	10.686	100	0.000
		199.870			

If 355 μm = 83.335%

Then X μm = 80%

$$X\ \mu m = \left(\frac{80/100}{83.335/100}\right)^2 X\ 355 = 327.15\ \mu m \text{ at } 80\%$$

4.5.2 Test Ore (Ndit Ilmenite) and References (Granite) Products as Discharge from the Ball Mill

Tables 4.7 and 4.8 give the sieve analysis of the product of test and reference materials from the ball mill.

Table 4.7 Sieve Analysis of Ndit Ilmenite (Product of test sample) from the Ball Mill

Sieve Sizes (µm)	Nominal Apertures	Weight Retained (g)	% Weight Retained	Cumulative % Weight Retained	Cumulative % Weight Passing
+425	425	0.970	0.493	0.493	99.507
-425+355	355	2.930	1.490	1.983	98.017
-355+250	250	12.730	6.477	8.460	91.540
-250+180	180	23.460	11.937	20.397	79.603
-180+125	125	62.560	31.833	52.230	47.77
-125+90	90	16.640	8.467	60.697	39.303
-90+63	63	21.510	10.945	71.642	28.358
-63+45	45	19.550	9.948	81.590	18.410
-45	Pan	36.170	18.405	99.995	0.005
		196.520			

If 180 µm = 79.603%

Then X µm = 80%

X µm = $(\frac{80/100}{79.603/100})^2$ X 180 = 181.799 µm at 80%

Table 4.8 Sieve Analysis of Granite (Product of reference sample) from the Ball Mill

Sieve Sizes (µm)	Nominal Apertures	Weight Retained (g)	%Weight Retained	Cumulative %Weight Retained	Cumulative % Weight Passing
+425	425	0.99	0.502	0.502	99.498
-425+355	355	3.94	1.999	2.501	97.499
-355+250	250	34.48	17.499	20.000	80.000
-250+180	180	37.43	18.997	38.997	61.003
-180+125	125	25.61	12.998	51.995	48.005
-125+90	90	16.76	8.506	60.501	39.499
-90+63	63	35.46	18.997	79.498	20.502
-63+45	45	17.73	8.998	88.496	11.504
-45	Pan	24.63	12.500	100	0.000
		197.03			

If 250 µm = 80.00%

Then X µm = 80%

Xµm= $(\frac{80/100}{80/100})^2$ X 250 = 250µm at 80%

Using Bond's equation

$$wit = wir \frac{\left[\frac{10}{\sqrt{Pr}}\right] - \left[\frac{10}{\sqrt{fr}}\right]}{\left[\frac{10}{\sqrt{Pt}}\right] - \left[\frac{10}{\sqrt{ft}}\right]}$$

Where;

Wir = work index of the reference ore; Wit = work index of test ore;

Pr = the diameter of the reference ore product, 80% of which passes through 100 µm aperture;

Pt = the diameter of the test ore product, 80% of which passes through 100 µm aperture;

Fr = the diameter of the reference ore feed, 80% of which passes through 100 μm aperture;

Ft = the diameter of the test ore feed, 80% of which passes through 100 μm aperture;

Wr = work input in kilowatt hour/short ton for reference ore and;

Wt = work input in kilowatt hour/short ton for test ore.

Pr = 250 μm Pt = 181.799 μm

Fr = 327.15 μm Ft = 266.279 μm

Wir = 15.13 (granite work index value)

Therefore:

$$\text{Wit} = 15.13\,\frac{(10\sqrt{250}-10\sqrt{327.15})}{(10\sqrt{181.799}-10\sqrt{266.279})} = 9.35\text{kWh/t}$$

The value of the work index of the ore was found to be 9.35kWh/t. This value means that approximately 9.35 kWh/t of energy is required to grind the ore from +425μm size fractions to 80% passing -355+250μm size fractions. The work index of Ndit ilmenite sample obtained compared favourably and lies within the work indexes of 4.23 - 11.88 kWh/t for Titanium mineral ores cited in Table 2.4.

4.6 Calcination Thermal Pre-Treatment

Table 4.9 presents experimental result of the ilmenite sample after calcination thermal pre-treatment.

Table 4.9 Result of the ilmenite sample after calcination thermal pre-treatment

S/N	Temperature (^{o}C)	Time (minutes)	XRD Responses		XRF Corresponding Assay content
			%Rutile Phase	%Ilmenite Phase	%Ti
1	300	30	45.00	LOD	74.212
2	300	45	40.40	12.80	74.861
3	300	60	14.60	28.40	69.778
4	650	30	31.30	42.00	67.808
5	650	45	35.90	14.10	68.838
6	650	60	58.00	18.00	65.475
7	1000	30	14.00	27.80	69.569
8	1000	45	10.00	56.00	53.554
9	1000	60	13.20	36.20	63.981

LOD: loss on detection

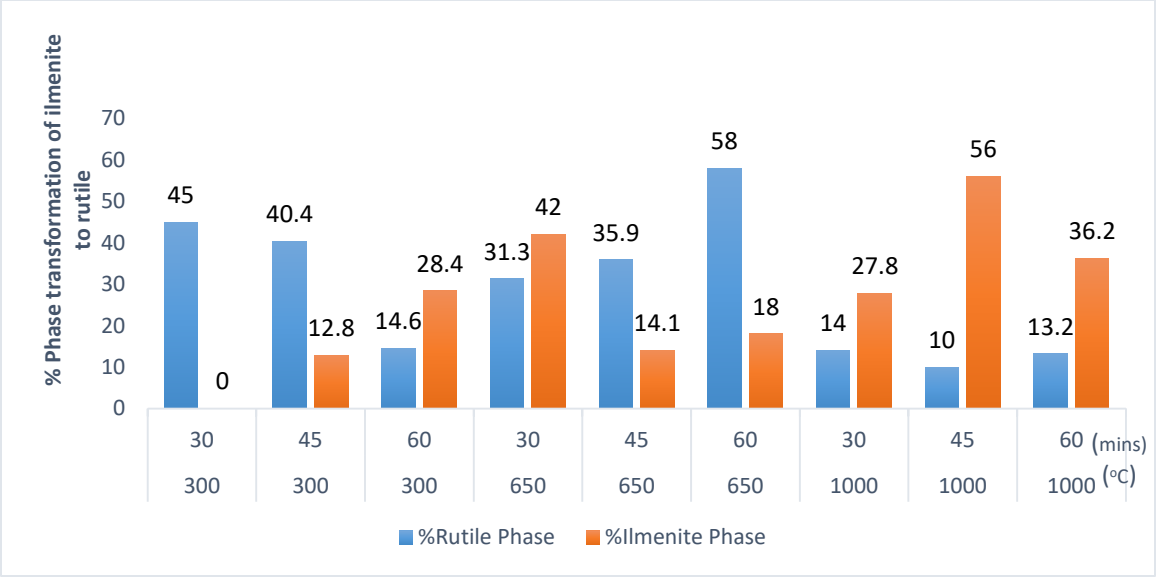


Figure 4.2 Variations of phases formed after calcination thermal pre-treatment

Table 4.9 presents the XRD results of % Ilmenite phase transformed to %Rutile phase of the calcination experimental combinations results and the corresponding XRF assay contents of % total Ti. Figure 4.2 shows the bar chart behavioral pattern XRD results of the % Rutile phase transformation from % Ilmenite phase of the calcined Ndit ilmenite. From Figure 4.2, it can be observed that, most of the transformation of Ilmenite to Rutile phase occurred at low and intermediate temperatures of 300^{o}C and 650^{o}C at short, intermediate and long thermal exposure times. The highest % Rutile phase transformation that occurred from Ilmenite was found to be 58%TiO_2 at 650^{o}C for 60 minutes thermal exposure time when compared to that of 300^{o}C (46%TiO_2) and 1000^{o}C (14%TiO_2) for 30 minutes thermal exposure times respectively. However, 4.30% Ilmenorutile and 10.00% magnetite mineral phases where observed to have been formed alongside the major Rutile phase during the calcination process. This trend could be attributed to the critical optimum phase transformation temperature of decomposition and structural rearrangement of Ilmenite to Rutile that is more attainable at 650^{o}C for 60 minutes thermal exposure time. Similar trend has also been reported in Hiraki *et al.*, (2018) and Warui, (2015)

respectively that, ilmenite transformation to pseudobrookite (Fe_2TiO_5), maghemite (γ-$Fe_2O_3.TiO_2$) and rutile (TiO_2) can occurred at the temperature of 600^oC. Also, it can be observed from Table 4.8 that, the corresponding XRF assayed values of %Ti total assumed a downward decreased pattern with some few exceptions as the temperature of calcination is increased for all thermal exposure times. The trend could be attributed to glowing (burning) transition temperature point that may have caused sublimation of some of the mineral phases of the Ndit Ilmenite. Thus, affecting the assay of Titanium content of the Ndit Ilmenite as the calcination temperature is increased. However, Thomas and Yaro, (2007) asserted that, there are instances in the literatures that explain how natural self-flux and flux-based ferrous associated minerals gradually transforms into minerals with strong magnetic properties during calcination at temperature range of 500^0C and 850 -1200^0C. This transformation and forming of new mineral phases are brought about by the interaction and rearrangement of elemental components within the matrix of the ore with respect to the kinetics of their mineral formation. Furthermore, they stated that, the transformation and formation of new minerals phases is more viable when energy providing elements (like: sulphur, phosphorus, carbon and silicon/silica) are present as one of the constituents that made up the ore matrix or mixture of the mineral concentrates. Hence, it can be observed that, one of the mentioned energy driven elements can be seen to be present in the matrix of Ndit Ilmenite as revealed in Table 4.2 and XRF analysis result of the Ilmenite in the appendix. Also, Hanaor *et. at.,* (2011) has reported that, the reaction between the solid and furnace atmosphere hot gas as the case may be in calcination can bring about decomposition, transformation and formation of mineral phases. Table 4.8 and Figure 4.2 also, present the behavioral pattern of the Ndit ilmenite at high temperature of 1000^oC for low, intermediate and long thermal exposure times. From the result in Table 4.8 and Figure 4.2 Ilmenite transformation to Rutile phase was viably insignificant when compared to that of low and

intermediate temperatures of 300^{o}C and 600^{o}C respectively. This trend could be attributed to the unstable transition Rutile-Anatase phases formed from Ilmenite at high temperature during calcination and probably also, due the exhaustion of the energy driven elements in the matrix of Ndit Ilmenite resource at high temperature. Similar trend has also been observed and reported in Hanaor *et al.*, (2011).

4.7 Roasting Thermal Pre-Treatment

Table 4.10 presents experimental result of the ilmenite sample after roasting thermal pre-treatment.

Table 4.10 Result of the ilmenite sample after roasting thermal pre-treatment

S/N	Temperature (^{o}C)	Time (minutes)	XRD		XRF
			Responses		Corresponding Assay content
			%Rutile Phase	%Ilmenite Phase	%Ti
1	300	30	7.30	13.60	69.631
2	300	45	46.00	16.00	69.744
3	300	60	47.10	8.23	70.906
4	650	30	5.00	4.90	72.135
5	650	45	10.30	3.00	72.032
6	650	60	11.90	50.40	73.511
7	1000	30	17.00	33.70	70.729
8	1000	45	30.00	20.80	65.909
9	1000	60	11.00	29.00	59.573

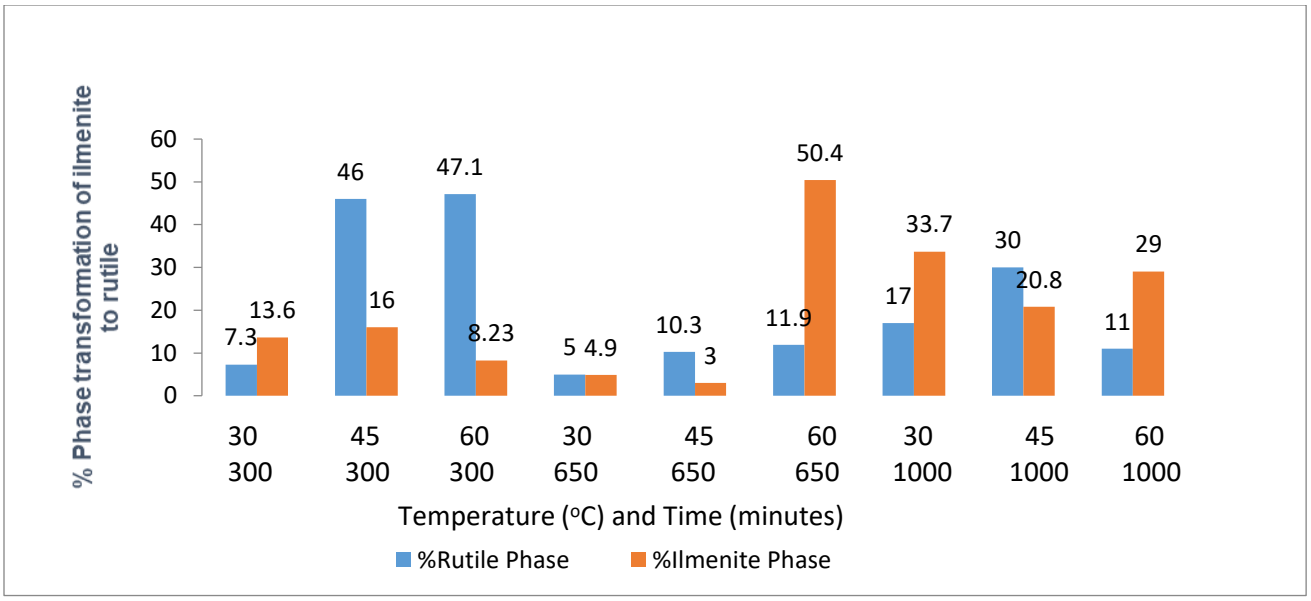


Figure 4.3 Variations of phases formed after roasting thermal pre-treatment

Table 4.10 and Figure 4.3 present the % Rutile phase proportion values of transformation from Ilmenite of the roasting thermal treatment. It can be observed that, transformation of Ilmenite to Rutile occurred due to increase in % Rutile phase proportion and relatively decrease in the % Ilmenite phase proportion in the matrix of the roasted Ndit Ilmenite. Table 4.10 and Figure 4.3, also revealed that most of the transformation of Ilmenite to Rutile phase occurred at low and high temperatures of 300^{o}C and 1000^{o}C and mostly at intermediate and long thermal exposure times of 45 and 60 minutes respectively. The highest % Rutile phase value of transformation of Ilmenite to Rutile phase was found to be 47.1%TiO_2 at 300^{o}C for 60 minutes when compared to that of 650^{o}C (11.3%TiO_2) and 1000^{o}C (11.0%TiO_2) for 60 minutes thermal exposure times respectively. However, 10.64% Ilmenorutile and 11.28% Magnetite mineral phases where also formed alongside the Rutile phase during the roasting process. The trend could be attributed to the critical optimum phase transformation temperature of decomposition and structural rearrangement of Ilmenite to Rutile that is most attainable at 300^{o}C for 60 minutes thermal exposure time. Warui, (2015) reported that Ilmenite transformation to Pseudobrookite (Fe_2TiO_5), Maghemite (γ-Fe_2O_3.TiO_2) and

Rutile (TiO_2) do occurs during roasting. Also, the formation of Pseudobrookite (Fe_2TiO_5) and Maghemite (γ-Fe_2O_3.TiO_2) mineral phases from Ilmenite during roasting tends to reduce the amount of Rutile (TiO_2) phase that will be formed in the matrix of the ore. However, the trend could be responsible for why much of the Rutile phase can't be formed from Ilmenite at intermediate temperature of 650^oC for low, intermediate and long thermal exposure times. This trend has also been observed and reported in Hanaor *et al.,* (2011). Also, Table 4.10 revealed increased in assay %Ti total content as the roasting temperature increases except for some few exceptional ones at high temperature and at intermediate and long thermal exposure times. Though increase in %Rutile phase transformed from Ilmenite seems to correlate with increase in assay %Ti total content as the thermal exposure time is increased at low temperature. However, reverse is the case at intermediate temperature where the %Rutile phase proportion decreased as the assay %Ti total content increases with increased in thermal exposure time. Thus, creating segmented patterns for the respective roasting temperatures. Hence, similar reasoning advanced above as asserted in Warui, (2015) could be responsible for the observed trend in roasting thermal treatment of the Ndit Ilmenite.

Hence, comparing the results outcome of the effect of calcination and roasting thermal pre-treatments on Ndit ilmenite, it could be said that both thermal pre-treatments have impacted on the transformation of Ilmenite to Rutile phase of the Ndit ilmenite. However, calcination gave an optimum value of 58% Rutile (TiO_2) phase transformation from Ilmenite at intermediate temperature (650^oC) for long thermal exposure time (60 minutes) with a corresponding optimum assay of 65.475%Ti total as revealed by the XRF result obtained when compared to that of roasting which gave 47.1% Rutile phase transformed with a corresponding assay of 70.806%Ti total content at 300^oC for 60 minutes. Based on the smelter requirement as asserted in the AusIMM, (2012) a

minimum of 50%Rutile phase in Ilmenite mineral ore can be accepted for processing without penalty. Therefore, the 58%Rutile phase obtained in the calcination thermal pre-treatment met and surpasses the smelter requirement for Rutile phase in Ilmenite ores/concentrates cited in AusIMM, (2012).

4.8 Beneficiation of Ndit Ilmenite Resource

The beneficiation of the thermally pre-treated ilmenite sample was carried using double stage separation technique (magnetic-to-gravity method).

4.8.1 Magnetic Concentration of the Calcined Ilmenite Sample using High Intensity Magnetic Separation Process

250g of the thermally treated (calcined) ilmenite sample was used as feed for concentration test employing the high intensity magnetic separator.

Table 4.11 presents the chemical analysis (XRF) of magnetic concentration of the calcined sample. While Table 4.12 presents the metallurgical balance accounting for magnetic concentration of the calcined sample

Table 4.11 XRF analysis of Ndit Ilmenite Resource after magnetic concentration of the calcined sample

Compound	**Magnetic Separation**	
	Non-magnetic Fractions (Concentrate)	**Magnetic Fractions (Tailings)**
SiO_2	**8.505**	**2.024**
V_2O_5	1.157	0.771
MnO	0.081	1.775
Fe_2O_3	**3.027**	**36.469**
Co_3O_4	0.054	0.151
Nb_2O_4	0.339	0.128
CuO	0.033	0.025
WO_3	0.278	0.257
SO_3	0.238	0.124
CaO	0.845	0.100
MgO	1.772	-
K_2O	0.139	0.095
BaO	0.89	0.654
Al_2O_3	**4.014**	**4.132**
Ta_2O_5	0.151	0.236
TiO_2	**78.196**	**52.096**
ZnO	0.069	0.093
Cl	0.241	0.714
ZrO_2	0.042	-
SnO_2	-	0.157

Table 4.12 Metallurgical Balance Accounting for Magnetic Concentration of the Calcined Sample

Products	**Weight (g)**	**Weight (%)**	**Assay (%Ti)**	**Unit**	**Recovery (%)**
Feed	250.000	100	36.874	3687.400	100
Concentrate	104.650	41.860	46.880	1962.396	53.21
Tailing	130.260	52.104	31.830	1658.470	46.79
Loss	15.090	6.036			

Table 4.11 revealed that the concentrate contained 78.196%TiO_2 (46.88% Ti), 3.03%Fe_2O_3, 4.014%Al_2O_3 and 8.50% SiO_2 and the tailings contained 52.10%TiO_2 (31.83%Ti), 36.47%Fe_2O_3, 4.13%Al_2O_3 and 2.02% SiO_2 respectively. The above results obtained indicated that an upgrade occurred in rutile of the calcined feed (58.00%TiO_2 phase (XRD), assaying 36.874%Ti total) to produce a calcined concentrate (78.196%TiO_2 (46.88%Ti)) with 53.21% recovery of Rutile. The content of rutile in the concentrate portion (non-magnetic fraction) could be attributed to some extend the demagnetization and transformation of Ilmenite to Rutile that favoured more the migration of Rutile to the concentrate portion of magnetic separation process while the un-demagnetized and untransformed Ilmenite to the magnetic fraction (tailing) of the magnetic separation process. The values of the test result obtained surpass that obtained and reported by Terzi *et al.*, (2015).

4.8.2 Gravity concentration of the calcined Ilmenite sample using air-floatation separation process

104.650g of the concentrate of the magnetic separation process was used to serve as feed to the air-floatation concentration process

Table 4.13 presents the chemical analysis (XRF) of the calcined Ndit ilmenite resource after gravity concentration of the magnetic separation concentrate that served as feed.

Table 4.13 XRF analysis of the Calcined Ndit Ilmenite sample after gravity concentration of the magnetic separation concentrate

Compound	**Gravity Separation**	
	Concentrate	**Tailing**
SiO_2	**2.263**	**14.747**
V_2O_5	1.001	1.111
MnO	0.082	0.079
Fe2O3	**2.918**	**3.136**
CO_3O_4	0.071	0.036
Nb_2O_4	0.440	0.238
CuO	0.025	0.040
WO_3	0.266	0.290
SO_3	0.158	0.318
CaO	0.433	1.256
MgO	3.543	-
K_2O	-	0.139
BaO	1.329	0.451
Al_2O_3	**3.921**	**4.106**
Ta_2O_5	0.141	0.161
TiO_2	**82.867**	**73.525**
ZnO	0.078	0.059
Cl	0.246	0.235
ZrO_2	0.011	0.073
SnO_2	-	-

Table 4.14 Metallurgical Balance of Gravity Concentration of the Calcined Magnetic Separation Concentrate

Products	Weight(g)	Weight (%)	Assays (%Ti)	Unit	Recovery (%)
Feed	104.650	100	46.880	4688.000	100
Concentrate	68.180	65.15	49.720	3239.258	69.09
Tailing	30.470	29.11	44.120	1284.333	30.90
Loss	6.000	5.74			

Table 4.13 presents the chemical analysis of the concentrate and the tailings produced after gravity concentration of the magnetic separation concentrate of the calcined Ndit Ilmenite sample, while Table 4.14 presents the metallurgical account balance sheet of the separation process. The chemical analysis result revealed that, the concentrate produced contained 82.87% TiO_2 (49.72% Ti), 2.92% Fe_2O_3, 3.92% Al_2O_3, and 2.26% SiO_2 while the tailing produced contained 73.525% TiO_2 (44.12% Ti), 3.14% Fe_2O_3, 4.12% Al_2O_3, 14.75% SiO_2 and a recovery 27.40% Rutile respectively. The high assay %Rutile content in the tailing produced could be attributed to the differences in sizes and shapes of the Rutile mineral grains which tends to favour the migration of some of the Rutile mineral grains of the sieve size fractions -355+250µm (been a range, about 105 various sizes and shapes are contained in it) to the tailing portion of the gravity air-floatation separation process. However, the Rutile in the tailing can be scavenged to recover more of the rutile mineral content. The result obtained shows that the Rutile content of the magnetic separation concentrate assaying 78.196%TiO_2 (46.88%Ti)) with Rutile recovery of 53.21% was upgraded to 82.87% TiO_2 (49.72% Ti) with Rutile recovery of 69.09% in the second stage using gravity air-floatation process. The result obtained compared favourably and surpasses that obtained in similar work reported by Terzi *et al.,* (2015).

4.8.3 Magnetic Concentration of the Roasted Ilmenite Sample using High Intensity Magnetic Separation Process

250g of the thermally treated (roasted) ilmenite sample was used as feed for concentration test employing the high intensity magnetic separator.

Table 4.15 presents the chemical analysis (XRF) of the Ndit Ilmenite sample after magnetic concentration of the roasted sample. Concentration was carried out at liberation size

-355+250µm roasted sample that served as feed.

Table 4.15 XRF analysis of Ndit Ilmenite sample after magnetic concentration of the roasted sample

Compound	Magnetic Separation	
	Non-Magnetic Fractions (Concentrate)	**Magnetic Fractions (Tailings)**
SiO_2	**8.467**	**2.313**
V_2O_5	0.953	0.744
MnO	0.109	1.866
Fe_2O_3	**3.886**	**36.914**
CO_3O_4	0.039	0.203
Nb_2O_4	0.255	0.043
CuO	0.064	0.021
WO_3	0.319	0.256
SO_3	0.269	0.026
CaO	0.635	0.136
MgO	1.771	-
K_2O	0.117	0.015
BaO	0.607	0.525
Al_2O_3	**3.137**	**4.273**
Ta_2O_5	0.212	0.172
TiO_2	**78.319**	**51.663**
ZnO	0.053	0.104
Cl	0.229	0.676
ZrO_2	0.553	0.049
SnO_2	0.006	-

Table 4.16 Metallurgical Balance Accounting for Magnetic Concentration of the Roasted Sample

Products	Weight(g)	Weight (%)	Assay (%Ti)	Unit	Recovery (%)
Feed	250	100	39.881	3988.100	100
Concentrate	126.083	50.433	46.990	2369.846	59.43
Tailing	114.475	45.790	30.990	1419.032	40.57
Loss	9.44	3.777			

Tables 4.15 and 4.16 present the chemical analysis of the concentrate and the tailings produced after magnetic concentration of the roasted Ndit Ilmenite sample and the metallurgical accounting balance sheet. The chemical analysis revealed that, the concentrate contained 78.32% TiO_2 (46.99% Ti), 3.89% Fe_2O_3, 3.14% Al_2O_3, and 8.47% SiO_2 while the tailing contained 51.66% TiO_2 (30.99% Ti), 36.91% Fe_2O_3, 4.27% Al_2O_3 and 2.31% SiO_2 respectively. The trend indicate that most of the Rutile migrated to the concentrate portion (non-magnetic phase) of the magnetic separation process due to their demagnetization during roasting. Also, the presence of certain % of Rutile in the tailing phase of the magnetic separation process could be attributed to the Ilmenorutile ($TiO.FeNb_2O_6$: said to possess magnetic property) formed during roasting. However, the trend shows that there is an upgrade in the mineral of interest rutile from 70.906% TiO_2 (39.881% Ti) to 78.32% TiO_2 (46.99% Ti) with 59.434% recovery of Rutile. The result obtained agreed with similar works reported by Hiraki *et al.*, (2018) and Terzi *et al.*, (2015).

4.8.4 Gravity Concentration of the Roasted Ilmenite Sample using Air-Floatation Separation Process

126.083g of the concentrate of the magnetic separation process was used to serve as feed to the air-floatation concentration process.

Table 4.17 presents the chemical analysis (XRF) of the Roasted Ndit Ilmenite sample after gravity concentration of the magnetic separation concentrate that served as feed.

Table 4.17 XRF analysis of Ndit Ilmenite sample after gravity concentration of the roasted sample

Compound	**Gravity Separation**	
	Concentrate	**Tailings**
SiO_2	**3.699**	**13.235**
V_2O_5	1.001	0.905
MnO	0.053	0.165
Fe_2O_3	**2.101**	**5.670**
CO_3O_4	0.023	0.055
Nb_2O_4	0.154	0.356
CuO	0.033	0.064
WO_3	0.298	0.340
SO_3	0.182	0.356
CaO	0.160	1.109
MgO	2.499	1.042
K2O	0.048	0.186
BaO	0.572	0.641
Al_2O_3	**2.895**	**3.379**
Ta_2O_5	0.223	0.201
TiO_2	**85.641**	**70.997**
ZnO	0.057	0.049
Cl	0.206	0.252
ZrO_2	0.153	0.953
SnO_2	-	0.006

Table 4.18 Metallurgical Balance Accounting for Gravity Concentration of the Roasted Sample after magnetic concentration

Products	Weight(g)	Weight (%)	Assay (Ti %)	Unit	Recovery (%)
Feed	126.083	100	46.990	4699.000	100
Concentrate	75.099	59.563	51.380	3060.346	65.127
Tailing	42.649	33.826	42.590	1440.649	34.87
Loss	8.335	6.611			

Tables 4.17 and 4.18 present the chemical analyses of concentrate and tailing produced after gravity concentration (Second stage after magnetic concentration) of the roasted Ilmenite sample and the metallurgical accounting balance sheet of the concentration process. The chemical analysis revealed that the concentrate contained 85.64% TiO_2 (51.38% Ti), 2.10% Fe_2O_3, 2.89% Al_2O_3, and 3.69% SiO_2 while the tailing contained 70.99% TiO_2 (42.59% Ti), 5.67% Fe_2O_3, 3.38% Al_2O_3 and 13.23% SiO_2 respectively. From the result it can be observed that most of Rutile migrated to the concentrate phase of the gravity air floatation separation process with less hematite, alumina and silica contents when compared to of the tailing. The trend could be attributed to the differences in the various minerals relative density and also, their sizes and shapes factors. The observed trend agreed with Hanaor *et. al.*, (2011) and Wills *et al.,* (2006), where they asserted that the differences in density, size and shape of mineral particles enhances their separation using gravity concentration processes. Also, the result indicated that, there is an upgrade of Rutile from 78.391% TiO_2 (46.99%Ti) of feed to 85.64% TiO_2 (51.38% Ti) of the concentrate with 65.125% recovery of the Rutile using gravity air floatation concentration process.

4.6.2 Comparison of the Two-Stage (Double) Magnetic-to-Gravity (Air-Floatation) Concentration Method of the Calcined and Roasted Ndit Ilmenite Resource Sample

Table 4.19 and Figure 4.4 presents the various % values obtained for the thermal treatments of calcination and roasting optimum conditions values obtained for the calcined and roasted concentrates using Two-Stage Magnetic-to- Gravity (air-floatation) method.

Table 4.19 Comparison of Calcined and Roasted Two-Stage Magnetic-to-Gravity (Air-Floatation) Concentrates Assays and Recoveries of Ndit Ilmenite

Thermal Treatment	Product	Assay				%Recovery
		$\%TiO_2$	$\%Fe_2O_3$	$\%Al_2O_3$	$\%SiO_2$	
Calcination	Concentrate 2	82.87	2.92	3.93	2.26	69.097
Roasting	Concentrate 2	85.64	2.10	2.89	3.69	65.127

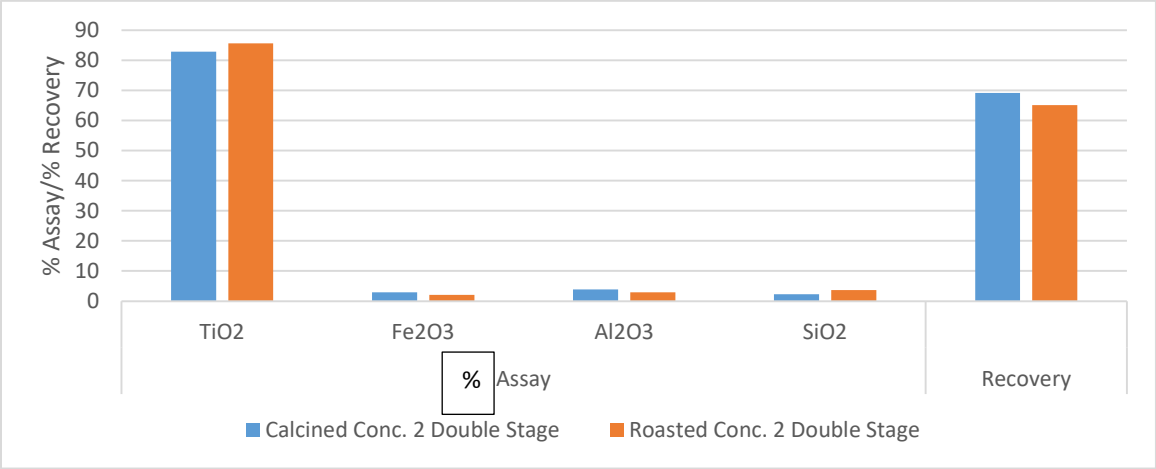


Figure 4.4: Bar chart of the Calcined and Roasted Two-Stage Magnetic-to-Gravity (Air-Floatation) Concentrates Assays and Recoveries of Ndit Ilmenite

Comparing the results obtained from the Two-Stage concentration process of the calcined and roasted Ndit Ilmenite respectively. It can be observed that the Two-Stage concentration process of the calcined Ilmenite produced a calcined concentrate assaying 82.87%TiO_2 (49.720%Ti), 2.92% Fe_2O_3, 3.92% Al_2O_3, and 2.26% SiO_2 with a Rutile recovery of 69.097%, while the roasted Ndit

Ilmenite using the same concentration process produced a roasted concentrate assaying 85.64%TiO_2 (51.380%Ti), 2.10% Fe_2O_3, 2.89% Al_2O_3, and 3.69% SiO_2 with a Rutile recovery of 65.127%. Also, considering the % contents of Rutile, Iron and Alumina with the exception of Silica it is evidently clear that more of the mentioned minerals are contained in the concentrate of the calcined Ndit Ilmenite when compared to that of roasted concentrate. The trend could be attributed to the decomposition of Ilmenite and formation of more iron mineral phases with high induced magnetic fields created by the roasting treatment when compared to the calcination process. The above trend can be justified by the results of the mineral contents of the various concentrates obtained for the magnetic separation in stage 1 for the calcined and roasted Ndit Ilmenite (see: calcined magnetic concentrate 1: 78.196%TiO_2, 3.03%Fe_2O_3, 4.01%Al_2O_3 and 8.50% SiO_2; Roasted magnetic concentrate 1: 78.32% TiO_2, 3.89% Fe_2O_3, 3.14% Al_2O_3, and 8.47% SiO_2). Also, the oxidation of the Hematite present in the Ndit Ilmenite matrix during the roasting thermal treatment process could be another added advantage. The outcome of the above results favoured more the roasting treatment process than the calcination, thus impacting differences in the density or specific gravity of the various minerals of the roasted magnetic concentrate which enhances their separation using gravity air floatation concentration process than the calcined magnetic concentrate. Though, calcination and roasting thermal treatments impacted significantly on the decomposition and transformation of Ndit Ilmenite that leads to the production of various concentrates that met the requirements of 48% - 51% TiO_2 minimum Rutile ore and 50% TiO_2 minimum for Ilmenite ore cited in AusIMM, (2012). However, based on the outcome of the results, roasting thermal treatment can be said to be the optimum process that can be used in the beneficiation process of Ndit Ilmenite.

4.9 The Philosophy of the Developed Flow Sheet of Ndit Ilmenite Resource

The philosophy for the development of the flow-sheet of Ndit Ilmenite Resource consists of the following steps; characterization, comminution, thermal treatment and concentration of the Ndit Ilmenite Resource sample.

Characterization:

The Ndit ilmenite resource's run-of-mine head sample containing (41.50%TiO_2, 21.78%Fe_2O_3, 15.85%Al_2O_3, 18.20%SiO_2) with mineral phases of Ilmenite ($FeTiO_3$), Rutile (TiO_2) as major, Hematite, Alumina, Silica and other trace associated minerals as minor are present in the matrix of the ilmenite resource as revealed by XRD/SEM/EDS.

Comminution:

The comminution process of the ilmenite consists of crushing and grinding processes. The ilmenite run-of mine head sample is crushed using Jaw crusher and the liberation size of the ilmenite resource is achieved by grounding to -355+250 (74.81%TiO_2 (44.85%Ti)) using Ball milling machine.

Thermal Pre-Treatments:

The product of the Ball milling process -355+250 (74.81%TiO_2((44.85%Ti)) is thermally treated (either by calcination at 650^oC for 60 minutes to obtain 58% Rutile phase with 65%TiO_2 total or roasting at 300^oC for 60 minutes to obtain 47.1% Rutile phase with 70.806%TiO_2 total respectively). The product of the thermally treated Ndit Ilmenite is then sent to the concentration unit.

Concentration Process:

Two-Stage (Double) Magnetic (high-intensity)-to-Gravity (air-floatation) separation process is used to produce a concentrated assaying 82.87%TiO_2 (49.720%Ti), 2.92% Fe_2O_3, 3.92% Al_2O_3, and 2.26% SiO_2 with a Rutile recovery of 69.097% for calcination thermal pre-treatment. While a concentrate assaying 85.64%TiO_2 (51.380%Ti), 2.10% Fe_2O_3, 2.89% Al_2O_3, and 3.69% SiO_2 with a Rutile recovery of 65.127% was obtained for roasting thermal pre-treatment respectively. However, the tailings of the processes can be scavenged for Rutile in order to recover more of the Rutile that is loss to the tailings before sending the tailings to the tailing dump.

Therefore, the Ndit Ilmenite resource various concentrates produced met the requirements of 48% - 51% TiO_2 minimum Rutile ore's concentrate and 50% TiO_2 minimum for Ilmenite ore's concentrate cited in AusIMM, (2012).

Figure 4.5 illustrates the proposed developed Ndit Ilmenite flow-sheet which can be used for the beneficiation of the Ndit Ilmenite resource.

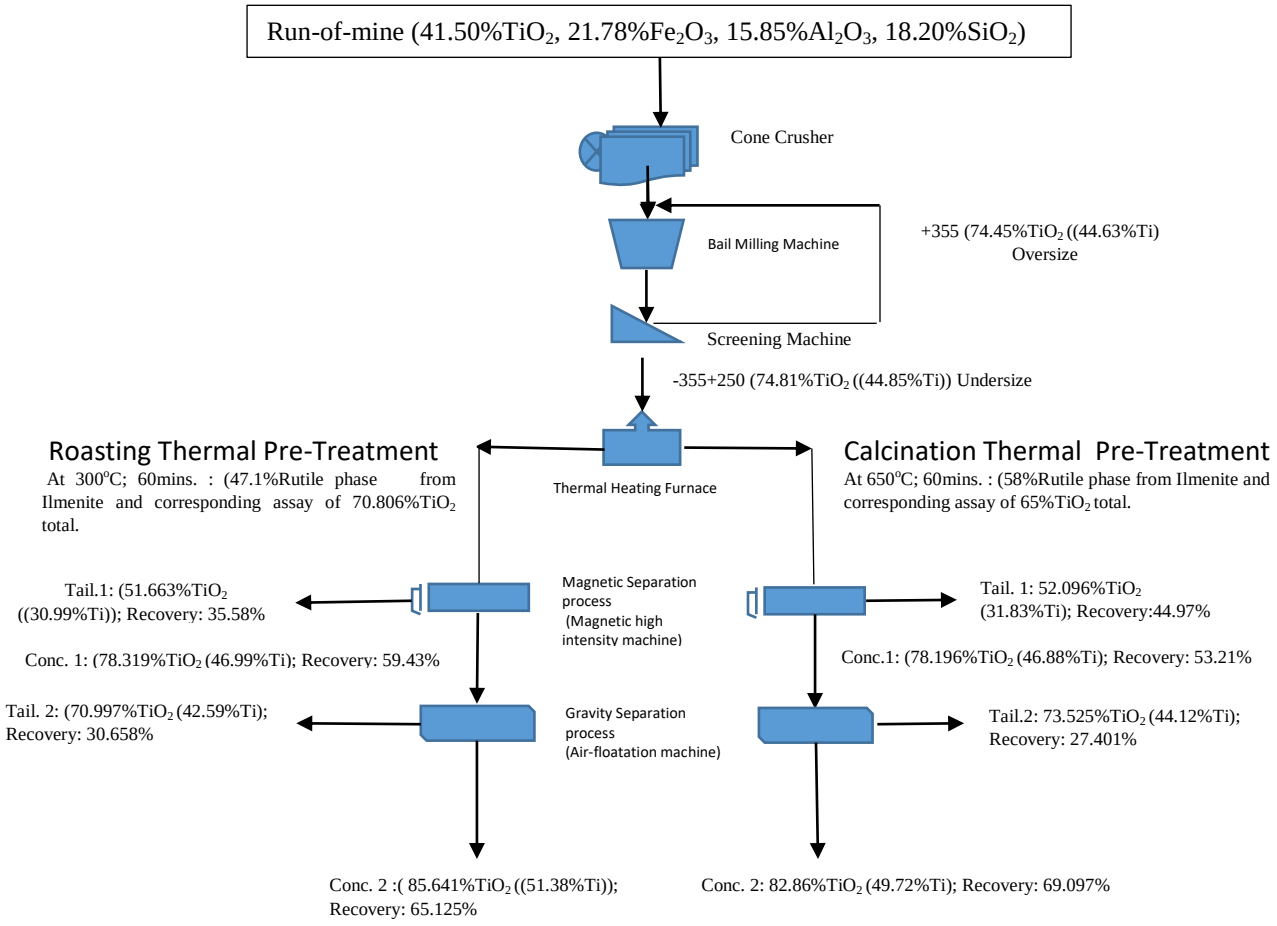


Figure 4.5 Flow-sheet of Ndit Ilmenite Beneficiation Process

CHAPTER FIVE

CONCLUSION AND RECOMMENDATIONS

5.1 Conclusion

The effect of thermal pre-treatment on the beneficiation of Ndit Ilmenite resource has been carried out in this work and the following conclusions were drawn based on the results obtained:

i. The chemical analysis of the head sample revealed that the ore contain 41.50% TiO_2, 21.78% Fe_2O_3, 15.85% Al_2O_3, and 18.20% SiO_2 as the major minerals, 1.18% Nb_2O_5 as the minor mineral, 0.20% TaO_5, 0.65% MnO and 0.64% others as trace minerals.

ii. The mineralogical analysis revealed that the Ilmenite resource comprised of mineral phases of Ilmenite ($FeTiO_3$), Rutile (TiO_2) as major titanium bearing minerals while Hematite, Alumina, Silica and others as minor and trace mineral phases present in the matrix of the Ndit Ilmenite resource. The minerals particle sizes are smaller in nature and are separated by grain boundaries, photo-images revealed non-interlocking of mineral grains with varying sizes. This shows that the minerals can be fragmented, separated and liberated from its gangue when comminuted. Rutile is seen as the white phases while the grey phases are Ilmenite and dark phases are Hematite.

iii. The liberation size of the Ndit Ilmenite resource was found to be -355+250µm, this means that the mineral of interest can be separated optimally from other associated minerals at this particle size. The work index of the Ilmenite resource was found to be 9.35kWh/t. This value means that, approximately 9.35 kW of energy is required to grind the ore from +425µm sieve size to 80% passing -355+250 µm. The result obtained lies favourably within the work indexes of 4.23 - 11.88 KWh/t for Titanium mineral ores cited in the literatures.

iv. The optimum thermal Pre-treatment conditions obtained are:- Calcination: Temperature 650^{o}C, Time 60 minutes with 58.0% Rutile phase from Ilmenite transformation with a corresponding assay of 65%Ti total. Roasting: Temperature 300^{o}C, Time 60 minutes with 47.1% Rutile phase from Ilmenite transformation with a corresponding assay of 70.806%Ti total.

v. The Two-Stage (Double) magnetic-to-gravity method produced a concentrate assaying 82.87%TiO_2 (49.720%Ti), 2.92% Fe_2O_3, 3.92% Al_2O_3 and 2.26% SiO_2 with a Rutile recovery of 69.097% for calcination thermal treatment. While a concentrate assaying 85.64%TiO_2 (51.380%Ti), 2.10% Fe_2O_3, 2.89% Al_2O_3, and 3.69% SiO_2 with a Rutile recovery of 65.127% was obtained for roasting thermal treatment respectively. However, the tailings of the processes can be scavenged for Rutile in order to recover more of the Rutile that is loss to the tailings before sending the tailings to the tailing dump.

   Therefore, the Ndit Ilmenite resource various concentrates produced met the requirements of 48% - 51% TiO_2 minimum Rutile ore's concentrate and 50% TiO_2 minimum for Ilmenite ore's concentrate cited in AusIMM, (2012).

   Therefore, the Ndit Ilmenite resource can be said to be another potential source of Rutile mineral that can be explored, beneficiated and use in the nation's metallurgical industries.

5.2 Recommendations

Based on the research carried out, the following recommendations were made:

i. Further research should be carried out to establish the estimated reserve of the Ndit Ilmenite resource

ii. Other beneficiation techniques like hydrometallurgical leaching process should be carried out to ascertain its susceptibility to alternative methods

5.3 Contribution to Knowledge

Presently, no work has been done on the effect of thermal pre-treatment on the beneficiation of Ndit ilmenite resource. This research work contributes to knowledge in the following:

i. Provide information on the chemical, mineralogical and petrological characteristics of the Ndit ilmenite resource that are found to be 41.50% TiO_2, 21.78% Fe_2O_3, 15.85% Al_2O_3, and 18.20% SiO_2 as the major minerals, 1.18% Nb_2O_5 as the minor mineral, 0.20% TaO_5, 0.65% MnO and 0.64% others as trace minerals.
ii. The liberation size (-355+250µm), work index (9.35kWh/t) and suitable concentration techniques for the beneficiation of Ndit Ilmenite resource are established.
iii. Optimum thermal treatments temperatures values of 300^oC for roasting and 650^oC for calcination at 60 minutes respectively for the transformation of Ilmenite to Rutile phase for Ndit Ilmenite resource have been established.
iv. That Two-Stage (Double) magnetic (high intensity) -to- gravity (air-floatation) method produced a concentrate assaying 82.87%TiO_2 (49.720%Ti), 2.92% Fe_2O_3, 3.92% Al_2O_3 and 2.26% SiO_2; Rutile recovery of 69.097% for calcination and another concentrate assaying 85.64%TiO_2 (51.380%Ti), 2.10% Fe_2O_3, 2.89% Al_2O_3, and 3.69% SiO_2; Rutile recovery of 65.127% for roasting thermal treatment respectively.

References

Abdulkadir, A. G. (2021). Characterization and Beneficiation of Ebiya Iron ore, Kogi State Nigeria. An MSc. Dissertation submitted to the Department of Metallurgical and Materials Engineering, Ahmadu Bello University Zaria. Unpublished.

Alabi, O. O., Yaro, A. S., Thomas, G. D., Asuke, F. and Dauda, E. T. (2015). Determination of Work Index of Gyel-Bukuru Columbite Ore in Plateau State, Nigeria. *Journal of Minerals and Materials Characterization and Engineering,* 2015, 3, 194-203

Allen, N. R. (1970). Effect of roasting temperature on the magnetism of ilmenite. *Physical Separation in Science and Engineering*, *12*.

Arachchi, N. D. H (2016). Effect of Thermal and Chemical Treatments on Photocatalytic Activity and Acid Leaching Behavior of Ilmenite. MSc. Dissertation submitted to the Department of Chemistry, University of Colombo.

Aristanti, Y., Supriyatna, Y. I., Masduki, N. P., & Soepriyanto, S. (2019, February). Effect of calcination temperature on the characteristics of TiO2 synthesized from ilmenite and its applications for photocatalysis. In *IOP Conference Series: Materials Science and Engineering* (Vol. 478, No. 1, p. 012019). IOP Publishing.

AusIMM, (2012). Smelting, Refining, Shipping and Treatment Terms Revenue Calculations and Marketing. Mineral Processing Toolbox. A publication of Australasian Institute of Mining and Metallurgy. Pp. 353.

Baba, A. A., Adekola, F. A., Toye, E. E., & Bale, R. B. (2009). Dissolution kinetics and leaching of rutile ore in hydrochloric acid. *Journal of Minerals and Materials Characterization and Engineering*, *8*(10), 787.

Baba, A. A., Swaroopa, S., Ghosh, M. K., & Adekola, F. A. (2013). Mineralogical characterization and leaching behavior of Nigerian ilmenite ore. *Transactions of Nonferrous Metals Society of China*, *23*(9), 2743-2750.

Benson, L. L., Mellor, I., & Jackson, M. (2016). Direct reduction of synthetic rutile using the FFC process to produce low-cost novel titanium alloys. *Journal of Materials Science*, *51*(9), 4250-4261.

Biswas, A. K., & Davenport, W. G. (2013). *Extractive metallurgy of copper: international series on materials science and technology* (Vol. 20). Elsevier.

Bordbar, H., Yousefi, A. A., & Abedini, H. (2017). Production of titanium tetrachloride (TiCl4) from titanium ores: A review. *Polyolefins Journal*, *4*(2), 149-173.

Brouwer, P. (2006). Theory of XRF. *Almelo, Netherlands: PANalytical BV*.

Budnuka, A. C., Clinton, A., & Agi-Ottoh, C. (2015). The effect of unplanned exploitation of environmental resources: The Nigeria's experience. *Journal of Environment Pollution and Human Health*, *3*(2), 39-45.

Carp, O., Huisman, C. L., & Reller, A. (2004). Photoinduced reactivity of titanium dioxide. *Progress in solid state chemistry*, *32*(1-2), 33-177.

Chen, L., Wen, S., Xu, G., & Xie, H. (2013). A novel process for titanium sand by magnetic separation and gravity concentration. *Mineral Processing and Extractive Metallurgy Review*, *34*(3), 139-150.

Cui, Z. L. Q. E. T. H., Liu, Q., & Etsell, T. H. (2002). Magnetic properties of ilmenite, hematite and oilsand minerals after roasting. *Minerals Engineering*, *15*(12), 1121-1129.

Ellmer, K., Mientus, R., & Seeger, S. (2018). Metallic oxides (ITO, ZnO, SnO2, TiO2). *Transparent Conductive Materials: Materials, Synthesis, Characterization, Applications*, 31-80.

Ertuğrul, İ., Öztaş, T., Özçil, A., & Öztaş, G. Z. (2016). Grey relational analysis approach in academic performance comparison of university a case study of Turkish universities.

Falade, M. O., & Adeyeye, P. (2016). A profile of Nigeria's solid minerals a detailed desk review

Friesinger, W. (2016). *A fundamental investigation of the high temperature oxidation of gold ores that contain sulfides and carbonaceous materials*. Colorado School of Mines.

Garside, M. (2021) Global Reserves of Titanium Minerals By Country 2020

Ghosh, S., Sahoo, P., & Sutradhar, G. (2013). Tribological performance optimization of Al-7.5% SiCp composites using the Taguchi method and grey relational analysis. Journal of Composites, 2013.

Grass, V. É., Sekushin, N. A., & Goldin, B. A. (2010). Thermochemical transformations of ilmenite–leucoxene concentrate. *Glass and Ceramics*, *67*(1-2), 59-62.

Hanaor, D. A., & Sorrell, C. C. (2011). Review of the anatase to rutile phase transformation. *Journal of Materials science*, *46*(4), 855-874.

Hanaor, D. A., & Sorrell, C. C. (2011). Review of the anatase to rutile phase transformation. *Journal of Materials science*, *46*(4), 855-874.

Hiraki, T., Maruyama, Y., Suzuki, Y., Itoh, S., & Nagasaka, T. (2018). Up-grading of natural ilmenite ore by combining oxidation and acid leaching. International Journal of Minerals, Metallurgy, and Materials, 25(7), 729-736.

Holmyard, E. J. (1990). *Alchemy*. Courier Corporation.

Hossein, H., Somayeh, A. and Tabatabaei, G. A. (2012). Grey Relational Analysis to Determine the Optimum Process Parameters for Open-End Spinning Yarns. *Journal of Engineered Fibers and Fabrics.* 7(2) pp 81-86

Huang, T. C., & Parrish, W. (1978). Characterization of Thin by X-Ray Fluorescence and Diffraction Analysis. *Advances in X-ray Analysis*, *22*, 43-63.

Irannajad, M., Nuri, O. S., & Mehdilo, A. (2019). Surface dissolution-assisted mineral flotation: A review. *Journal of Environmental Chemical Engineering*, *7*(3), 103050.

Itoh, S., Sato, S., Ono, J., Okada, H., & Nagasaka, T. (2006). Feasibility study of the new rutile extraction process from natural ilmenite ore based on the oxidation reaction. *Metallurgical and Materials Transactions B*, *37*(6), 979-985.

Jankovic, A., Dundar, H., & Mehta, R. (2010). Relationships between comminution energy and product size for a magnetite ore. *Journal of the Southern African Institute of Mining and Metallurgy*, *110*(3), 141-146.

Janković, B., Stopić, S., Güven, A., & Friedrich, B. (2014). Kinetic modeling of thermal decomposition of zinc ferrite from neutral leach residues based on stochastic geometric model. *Journal of magnetism and magnetic materials*, *358*, 105-118.

Jha, A., Lahiri, A., & Kumari, E. J. (2008). Beneficiation of titaniferous ores by selective separation of iron oxide, impurities and rare earth oxides for the production of high grade synthetic rutile. Mineral Processing and Extractive Metallurgy, 117(3), 157-165.

Jordens, A., Sheridan, R. S., Rowson, N. A., & Waters, K. E. (2014). Processing a rare earth mineral deposit using gravity and magnetic separation. *Minerals Engineering*, *62*, 9-18.

Lv, J. F., Zheng, Y. X., Tong, X., Zheng, Y. M., & Zhang, H. P. (2017). Mineralogy, physical characterization and magnetic separation performance of a raw ilmenite concentrate for its purification. *Russian Journal of Non-Ferrous Metals*, *58*(2), 101-108.

Mackey, T. S. (1994). Upgrading ilmenite into a high-grade synthetic rutile. *Jom*, *46*(4), 59-64.

Mallo, S. J. (2012). The Nigerian mining sector: An overview. *Cont. J. Appl. Sci*, *7*(1), 34-45.

Masok, Y. S., Yaro, S. A., Thomas, D.G. (2015). Characterization of Zurak Lead-Zink Ore Using X-Ray Fluorescence (XRF) Spectrometry and X-Ray Diffraction (XRD). *Nigerian Journal of Engineering, Faculty of Engineering, Zaria*. 22(1), 8-14

Milnes, A. R., & Fitzpatrick, R. W. (1989). Titanium and zirconium minerals. *Minerals in soil environments*, *1*, 1131-1205.

Ministry of Mines and Steel Development (2012). Road Map for the Development of Solid Minerals and Metals Sector. Stack Holders Forum, Abuja, 3, 4-9.

Mohammed, A., & Abdullah, A. (2018, November). Scanning electron microscopy (SEM): A review. In *Proceedings of the 2018 International Conference on Hydraulics and Pneumatics—HERVEX, Băile Govora, Romania* (pp. 7-9).

Musa, E. D. (2019). Characterization and Beneficiation of Gurum Cassiterite Plateau State, Nigeria. Masters Dissertation submitted to the Department of Metallurgical and Materials Engineering, Ahmadu Bello University Zaria, Nigeria: Unpublished.

Mutembei, P. K., Muriithi, N. T., & Wachira, J. M. (2014). Iron enrichment in laterites soils from selected regions in Kenya using magnetic separation.

Nguyen, T. H., & Lee, M. S. (2019). A review on the recovery of titanium dioxide from ilmenite ores by direct leaching technologies. Mineral Processing and Extractive Metallurgy Review, 40(4), 231-247.

Nguyen, T. H., & Lee, M. S. (2019). A review on the recovery of titanium dioxide from ilmenite ores by direct leaching technologies. *Mineral Processing and Extractive Metallurgy Review*, *40*(4), 231-247.

Okechukwu, I. N., Muhammed, M., Ashiru, M. A., & Dada, G. I. (2009). Strategies, prospects and constraints of solid minerals development in Nigeria. *The Nigerian Journal of Research and Production Volume*, *15*(2).

Olade, M. A. (2019). Solid mineral deposits and mining in Nigeria: A sector in transitional change. *Achievers Journal of Scientific Research*, *2*(1), 1-16.

Olanipekun, E. (1999). A kinetic study of the leaching of a Nigerian ilmenite ore by hydrochloric acid. *Hydrometallurgy*, *53*(1), 1-10.

Petersen, J. (2016). Heap leaching as a key technology for recovery of values from low-grade ores–A brief overview. *Hydrometallurgy*, *165*, 206-212.

Porikli, S., & Kurucu, Y. (2011). Determination of Chemical State and External Magnetic Field Effect on the Energy Shifts and X-Ray Intensity Ratios of Yttrium and Its Compounds. Radioisotopes-Applications in Phisical Sciences book. Nirmal Singh, Chapiter, 5, 89-114.

Schulz, K. J., DeYoung, J. H., Seal, R. R., & Bradley, D. C. (Eds.). (2018). *Critical mineral resources of the United States: economic and environmental geology and prospects for future supply*. Geological Survey.

Setyani, E., Rahman, T. P., Nugroho, D. W., Rahman, S., Irawan, F., Ikono, R., ... & Dwandaru, W. S. B. (2014). The Effect of Roasting Temperature at 400C and Sulphuric Acid Concentration on TiO2 Extraction Process from Zircon Sand Ilmenite. JFA (Jurnal Fisika dan Aplikasinya), 10(3), 109-112.

Shen, Y., Yang, Y., Yang, G., Hou, X., Ye, W., You, Z., & Xi, J. (2018). Damage characteristics and thermo-physical properties changes of limestone and sandstone during thermal treatment from− 30° C to 1000° C. *Heat and Mass Transfer*, *54*(11), 3389-3407.

Siyanbola, W. O., Fasasi, A. Y., Funtua, I. I., Afolabi, O. M., Adesiyan, T. A., & Adetunji, A. R. (2004). Elemental composition of rutile from south-western Nigeria using X-ray techniques. *Nuclear Instruments and Methods in Physics Research Section B: Beam Interactions with Materials and Atoms*, *215*(1-2), 240-245.

Su, W., Li, J., Mao, Q., Gao, J., Liu, X., Chen, F., & Ge, X. M. (2018). Rutile in HP rocks from the western Tianshan, China: Mineralogy and its economic implications. *Journal of Earth Science*, *29*(5), 1049-1059.

Terzi, M., & Kursun, I. (2015). Investigation of recovery possibilities of rutile minerals from the feldspar tailings with gravity separation methods. Russian Journal of Non-Ferrous Metals, 56(3), 235-245.

Thomas, D.G. and Yaro, S.A., (2007). The Effects of Calcination on the Beneficiation of Koton Karfe Iron Ore. *Nigerian Mining Journal, a Publication of Nigerian Society of Mining Engineers,* Vol.5, N0.1, pp 49-59

U.S. Geological Survey, Mineral Commodity Summaries, January 2020

Van Tonder, W. (2010). *South African titanium: techno-economic evaluation of the alternatives to the Kroll process* (Doctoral dissertation, Stellenbosch: University of Stellenbosch).

Wang, J., Zhao, H. B., Qin, W. Q., Qiu, G. Z., Hu, Y. H., Jiang, T., ... & Wang, Y. (2013). Review on Mineral Processing Technology of Rutile in China. *Sci. Technol. Mag. Online*.

Ward, J., Bailey, S., & Avraamides, J. (1999). The use of ethylenediammonium chloride as an aeration catalyst in the removal of metallic iron from reduced ilmenite. *Hydrometallurgy*, *53*(3), 215-232.

Warui, K. S. (2015). Beneficiation of Low grade Titanium Ores from selected sites in Meru, Murang'a and Tharaka Nithi Counties, Kenya.

Wills, B. A., & Finch, J. (2015). *Wills' mineral processing technology: an introduction to the practical aspects of ore treatment and mineral recovery*. Butterworth-Heinemann.

Wills, B.A. and Napier-Mum, T.J. (2006) Mineral Processing Technology. 7th Edition, Elsevier Science & Technology Books, Amsterdam, 109-439.

Yilleng, M. T., Gimba, C. E., Ndukwe, I. G., & Bugaje, I. M. (2015). Assessing the photo catalytic activity of rutile ore from the Middle Belt Region of Nigeria on the degradation of phenol in water. *IOSR Journal of Applied Chemistry*, *8*, 36-43.

APPENDICES

APPENDIX A

List of Photographs



X-ray Diffraction Machine



X-ray Fluorescence Machine



High Intensity Magnetic Separator (Rapid)



Murple Furnace



Sieve Shaking Machine

APPENDIX B

Plates of Samples



Crude Rutile Sample



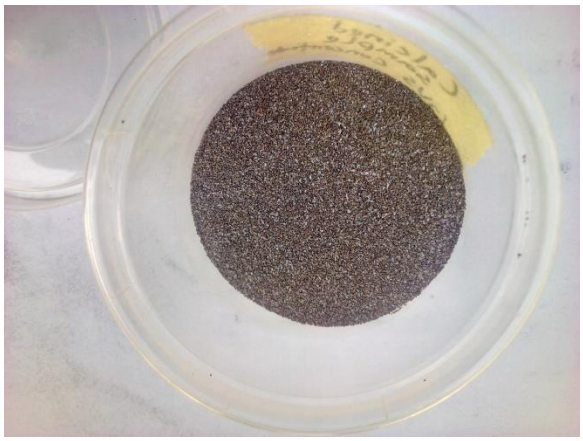
Tailings of Calcined Sample (MGS)



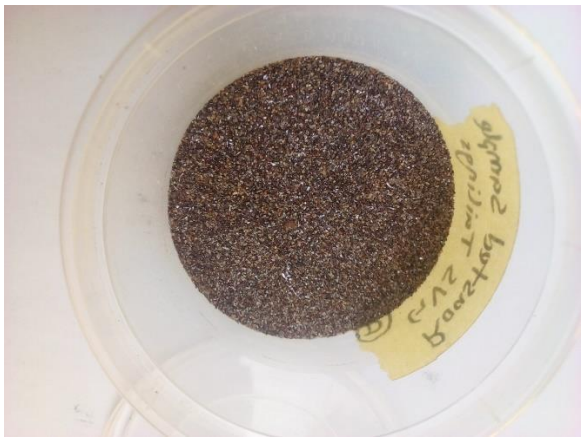
Tailings of Roasted Sample (MGS)



Tailings of Calcined Sample (GVS)



Concentrate of Calcined Sample (GVS)



Tailings of Roasted Sample (GVS)



Concentrate of Roasted Sample (GVS)

APPENDIX C

List of phases transformed after thermal pre-treatment

Appendix C-i Calcination Thermal Pre-Treatment

			Rutile Phase(s)			Ilmenite Phase	Other Phases			
S/N	**Temp(^{o}C)**	**Time(min)**	**%Rutile Phase**	**%Ilmenorutile Phase**	**%Rutile Tantalium Phase**	**% Ilmenite Phase**	**%Geothite Phase**	**% Quartz Phase**	**% Garnet Phase**	**% Magnetite Phase**
C1	300	30	45.00	16.20	-	-	14.00	7.00	14.00	-
C2	300	45	40.40	-	-	12.80	-	7.40	-	18.80
C3	300	60	14.60	31.30	-	28.40	-	14.20	-	11.47
C4	650	30	28.00	-	3.30	42.00	-	27.00	-	-
C5	650	45	35.90	15.50	-	14.10	-	19.00	-	15.7
C6	650	60	58.00	4.30	-	18.00	-	9.00	-	10.80
C7	1000	30	14.00	38.00	-	27.80	-	14.90	-	5.00
C8	1000	45	10.00	23.00	-	56.00	-	12.00	-	-
C9	1000	60	13.20	21.70	-	36.20	-	28.60	-	-

Appendix C-ii Roasting Thermal Pre-Treatment

			Rutile Phase(s)			Ilmenite Phase	Other Phase	
S/N	**Temp(^{o}C)**	**Time(min)**	**%Rutile Phase**	**% Anatase Phase**	**%Ilmenorutile Phase**	**% Ilmenite Phase**	**% Magnetite Phase**	**%Quartz Phase**
C1	300	30	-	7.30	47.00	13.60	2.20	30.0
C2	300	45	34.00	12.00	4.00	16.00	-	34.0
C3	300	60	47.10	-	10.64	8.23	11.28	22.80
C4	650	30	5.00	-	67.00	4.90	5.50	18.00
C5	650	45	10.30	-	21.50	3.00	21.80	43.00
C6	650	60	11.90	-	23.00	50.40	-	14.70
C7	1000	30	17.00	-	20.00	33.70	20.40	9.10
C8	1000	45	30.00	-	22.20	20.80	23.10	3.00
C9	1000	60	11.00	-	40.00	29.00	-	20.00

APPENDIX D

Calcination XRD Results for 300^0C, 30 minutes

Path: C:\Users\Rigaku pc\Desktop\ANALYSIS\OGA\12-07-2021\THE 18 \C1 Solution.rmrsln

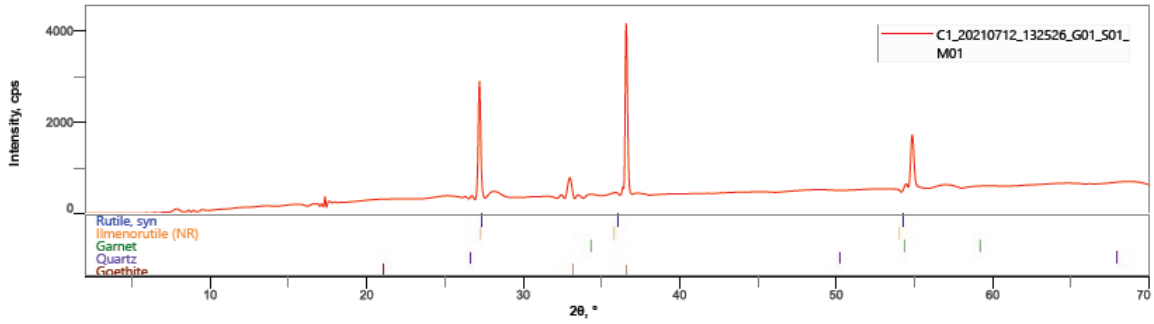
Solution

Quantitative analysis report

General information

Analysis date	2021-07-12 16:19:02	Measurement start time	2021-07-12 13:26:25
Analyst	Administrator	Operator	Administrator
Sample name	C1	Comment	
Measured data name	C:\Users\Rigaku pc\Desktop\ANALYSIS\OGA\12-07-2021\TH...	Memo	

Multiple Profile



Path: C:\Users\Rigaku pc\Desktop\ANALYSIS\OGA\12-07-2021\THE 18 \C1 Solution.rmrsln

Solution

Plot of results

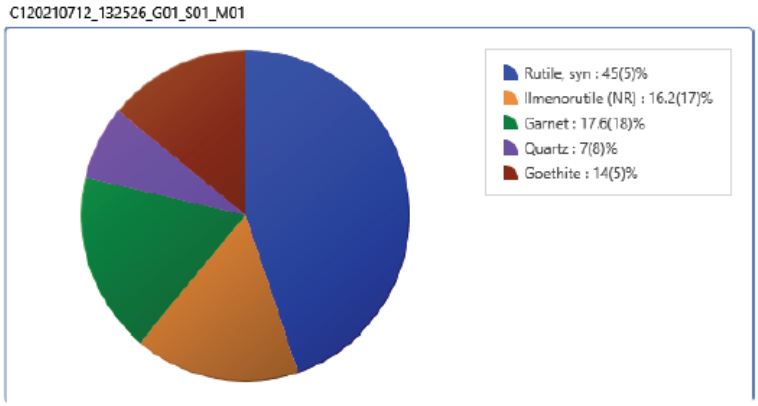


Table of results

Dataset / Weight Fraction, wt%	Value, Unit	Rutile, syn	Ilmenorutile (NR)	Garnet	Quartz	Goethite
C1_20210712_132526_G01_S01...	0	45(5)	16.2(17)	17.6(18)	7(8)	14(5)

Calcination XRD Results for 300^0C, 45 minutes

Path: C:\Users\Rigaku pc\Desktop\ANALYSIS\OGA\12-07-2021\THE 18 \C2 Solution.rmrsln

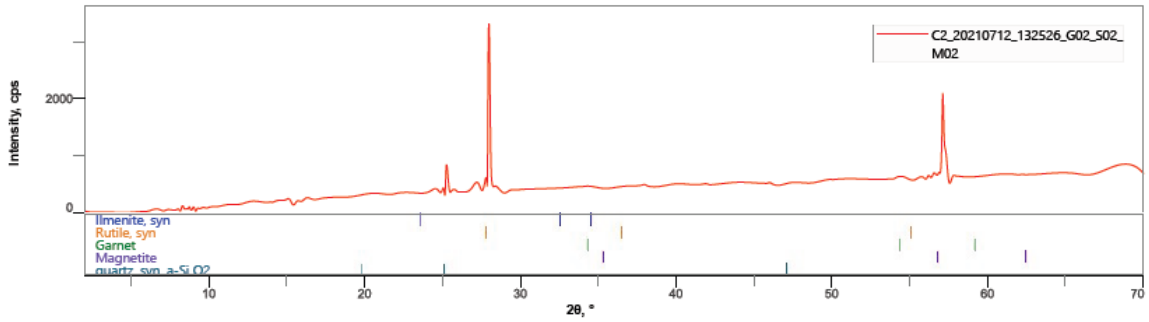
Solution

Quantitative analysis report

General information

Analysis date	2021-07-13 14:14:35	Measurement start time	2021-07-12 13:30:15
Analyst	Administrator	Operator	Administrator
Sample name	C2	Comment	
Measured data name	C:\Users\Rigaku pc\Desktop\ANALYSIS\OGA\12-07-2021\TH...	Memo	

Multiple Profile



Path: C:\Users\Rigaku pc\Desktop\ANALYSIS\OGA\12-07-2021\THE 18 \C2 Solution.rmrsln

Solution

Plot of results

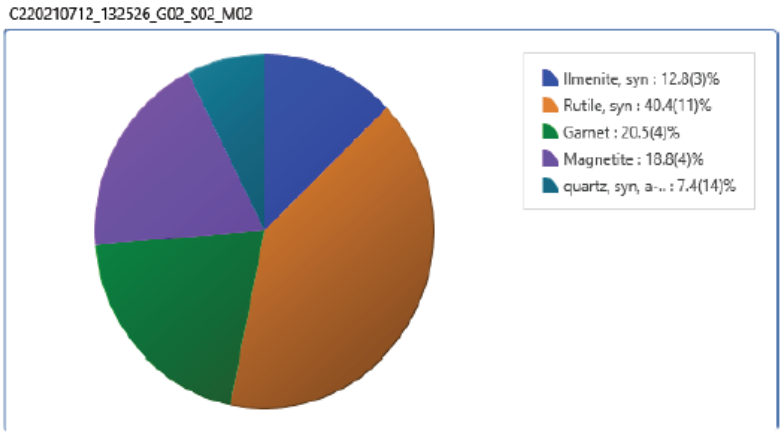


Table of results

Dataset / Weight Fraction, wt%	Value, Unit	Ilmenite, syn	Rutile, syn	Garnet	Magnetite	quartz, syn, a-Si O2
C2_20210712_132526_G02_S02...	0	12.8(3)	40.4(11)	20.5(4)	18.8(4)	7.4(14)

Calcination XRD Results for 300^0C, 60 minutes

Path: C:\Users\Rigaku pc\Desktop\ANALYSIS\OGA\12-07-2021\THE 18 \C3 Solution.rmrsln

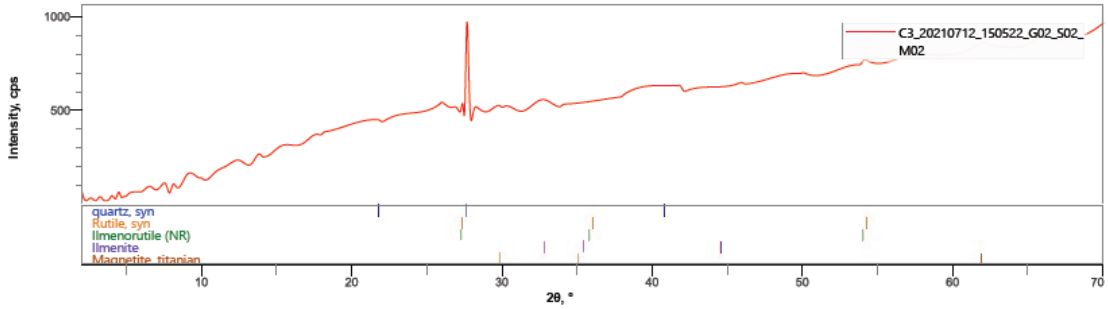
Solution

Quantitative analysis report

General information

Analysis date	2021-07-13 14:24:17	Measurement start time	2021-07-12 15:10:16
Analyst	Administrator	Operator	Administrator
Sample name	C3	Comment	
Measured data name	C:\Users\Rigaku pc\Desktop\ANALYSIS\OGA\12-07-2021\TH...	Memo	

Multiple Profile



Path: C:\Users\Rigaku pc\Desktop\ANALYSIS\OGA\12-07-2021\THE 18 \C3 Solution.rmrsln

Solution

Plot of results

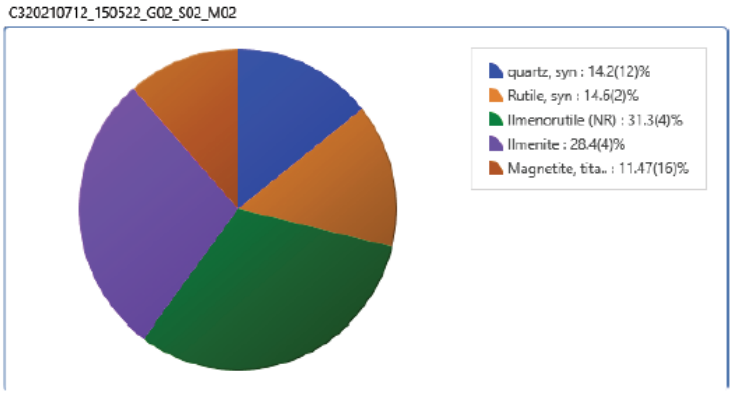


Table of results

Dataset / Weight Fraction, wt%	Value, Unit	quartz, syn	Rutile, syn	Ilmenorutile (NR)	Ilmenite	Magnetite, titanian
C3_20210712_150522_G02_S02...	0	14.2(12)	14.6(2)	31.3(4)	28.4(4)	11.47(16)

Calcination XRD Results for 650^0C, 30 minutes

Path: C:\Users\Rigaku pc\Desktop\ANALYSIS\OGA\12-07-2021\THE 18 \C4 Solution.rmrsln

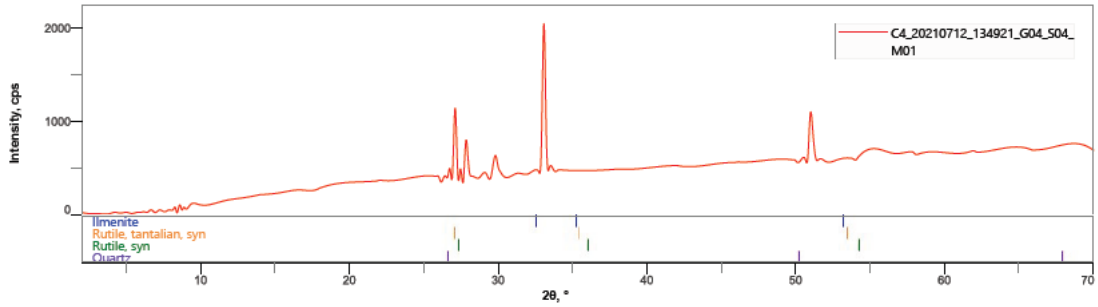
Solution

Quantitative analysis report

General information

Analysis date	2021-07-13 14:45:58	Measurement start time	2021-07-12 13:50:36
Analyst	Administrator	Operator	Administrator
Sample name	C4	Comment	
Measured data name	C:\Users\Rigaku pc\Desktop\ANALYSIS\OGA\12-07-2021\TH...	Memo	

Multiple Profile



Path: C:\Users\Rigaku pc\Desktop\ANALYSIS\OGA\12-07-2021\THE 18 \C4 Solution.rmrsln

Solution

Plot of results

C420210712_134921_G04_S04_M01

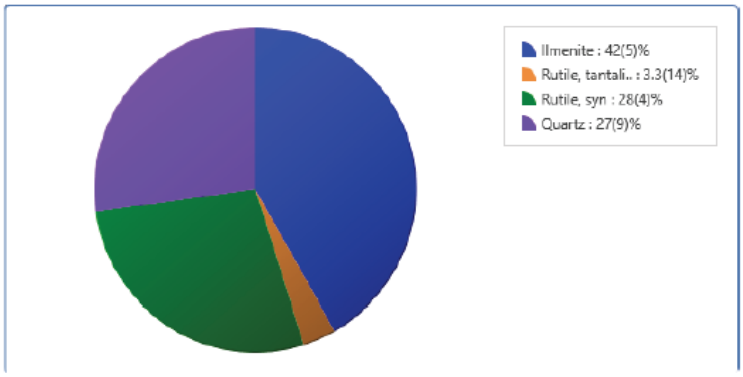


Table of results

Dataset / Weight Fraction, wt%	Value, Unit	Ilmenite	Rutile, tantalian, syn	Rutile, syn	Quartz
C4_20210712_134921_G04_S04_M01	0	42(5)	3.3(14)	28(4)	27(9)

Calcination XRD Results for 650^0C, 45 minutes

Path: C:\Users\Rigaku pc\Desktop\ANALYSIS\OGA\12-07-2021\THE 18
\C5 Solution.rmrsln

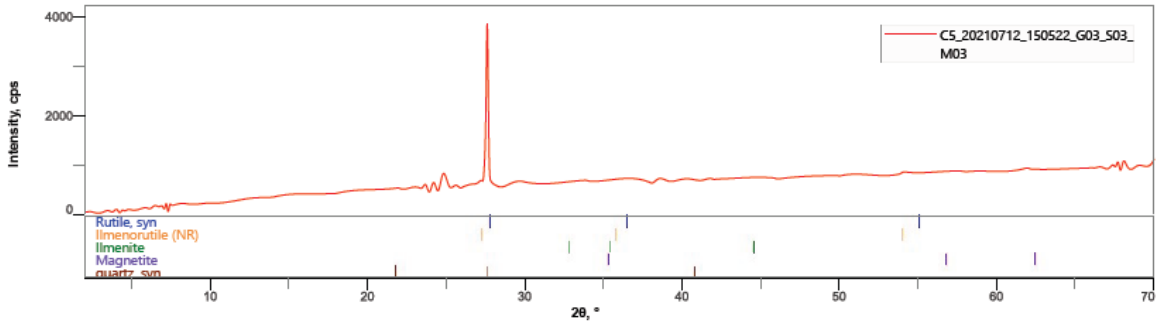
Solution

Quantitative analysis report

General information

Analysis date	2021-07-13 14:51:35	Measurement start time	2021-07-12 15:14:05
Analyst	Administrator	Operator	Administrator
Sample name	C5	Comment	
Measured data name	C:\Users\Rigaku pc\Desktop\ANALYSIS\OGA\12-07-2021\TH...	Memo	

Multiple Profile



Path: C:\Users\Rigaku pc\Desktop\ANALYSIS\OGA\12-07-2021\THE 18
\C5 Solution.rmrsln

Solution

Plot of results

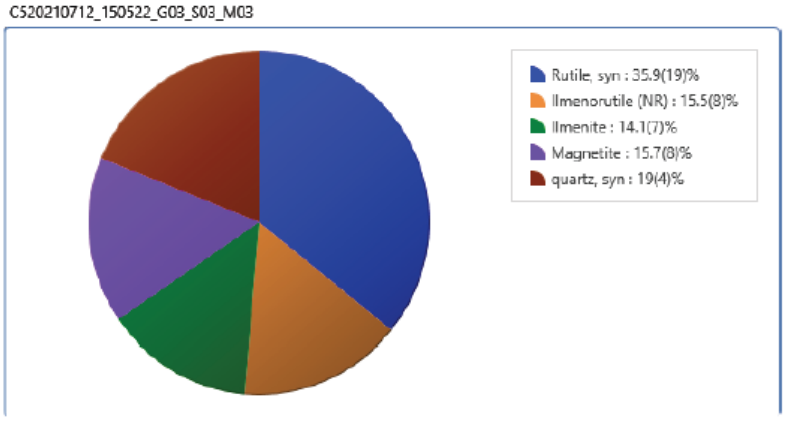


Table of results

Dataset / Weight Fraction, wt%	Value, Unit	Rutile, syn	Ilmenorutile (NR)	Ilmenite	Magnetite	quartz, syn
C5_20210712_150522_G03_S03...	0	35.9(19)	15.5(8)	14.1(7)	15.7(8)	19(4)

Calcination XRD Results for 650^0C, 60 minutes

Path: C:\Users\Rigaku pc\Desktop\ANALYSIS\OGA\12-07-2021\THE 18
\C6 Solution.rmrsln

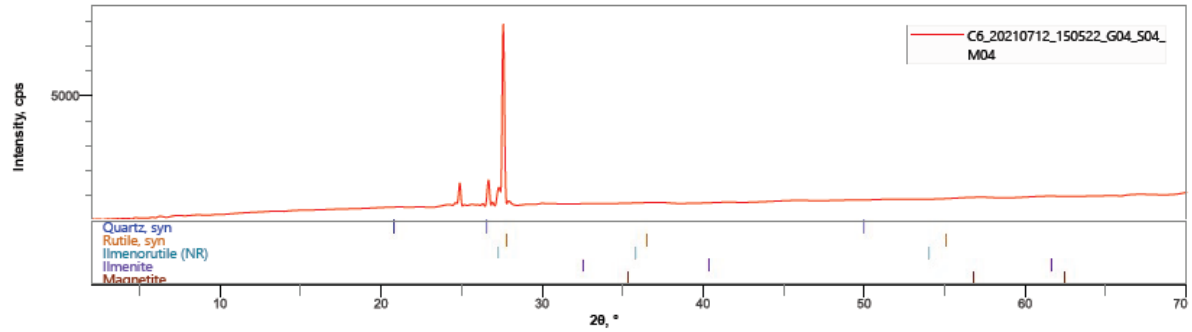
Solution

Quantitative analysis report

General information

Analysis date	2021-07-13 14:56:28	Measurement start time	2021-07-12 15:17:56
Analyst	Administrator	Operator	Administrator
Sample name	C6	Comment	
Measured data name	C:\Users\Rigaku pc\Desktop\ANALYSIS\OGA\12-07-2021\TH...	Memo	

Multiple Profile



Path: C:\Users\Rigaku pc\Desktop\ANALYSIS\OGA\12-07-2021\THE 18
\C6 Solution.rmrsln

Solution

Plot of results

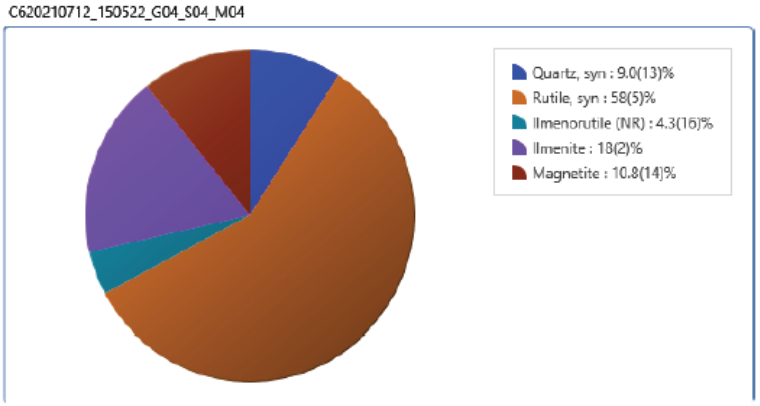


Table of results

Dataset / Weight Fraction, wt%	Value, Unit	Quartz, syn	Rutile, syn	Ilmenorutile (NR)	Ilmenite	Magnetite
C6_20210712_150522_G04_S04...	0	9.0(13)	58(5)	4.3(16)	18(2)	10.8(14)

Calcination XRD Results for 1000^0C, 30 minutes

Path: C:\Users\Rigaku pc\Desktop\ANALYSIS\OGA\12-07-2021\THE 18
\C7 Solution.rmrsln

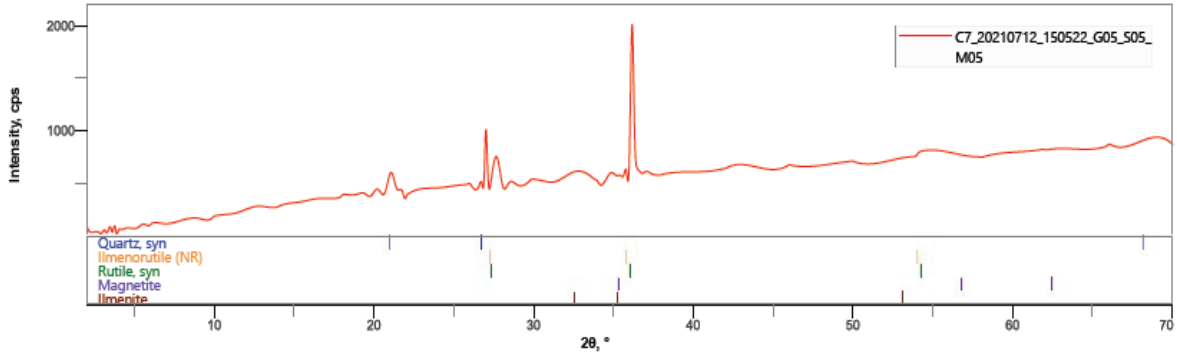
Solution

Quantitative analysis report

General information

Analysis date	2021-07-13 15:00:29	Measurement start time	2021-07-12 15:21:45
Analyst	Administrator	Operator	Administrator
Sample name	C7	Comment	
Measured data name	C:\Users\Rigaku pc\Desktop\ANALYSIS\OGA\12-07-2021\TH...	Memo	

Multiple Profile



Path: C:\Users\Rigaku pc\Desktop\ANALYSIS\OGA\12-07-2021\THE 18
\C7 Solution.rmrsln

Solution

Plot of results

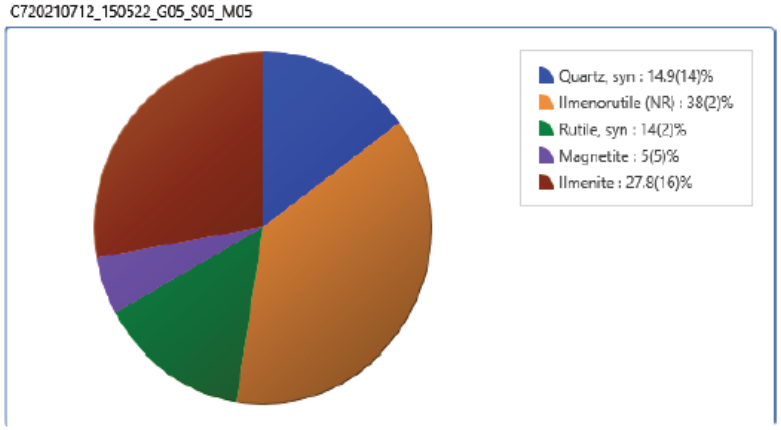


Table of results

Dataset / Weight Fraction, wt%	Value, Unit	Quartz, syn	Ilmenorutile (NR)	Rutile, syn	Magnetite	Ilmenite
C7_20210712_150522_G05_S05...	0	14.9(14)	38(2)	14(2)	5(5)	27.8(16)

Calcination XRD Results for 1000^0C, 45 minutes

Path: C:\Users\Rigaku pc\Desktop\ANALYSIS\OGA\12-07-2021\THE 18 \C8 Solution.rmrsln

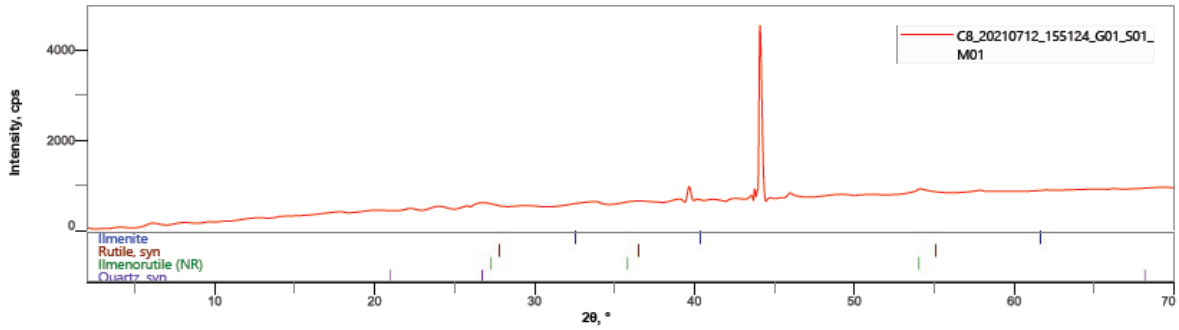
Solution

Quantitative analysis report

General information

Analysis date	2021-07-13 15:09:34	Measurement start time	2021-07-12 15:52:29
Analyst	Administrator	Operator	Administrator
Sample name	C8	Comment	
Measured data name	C:\Users\Rigaku pc\Desktop\ANALYSIS\OGA\12-07-2021\TH...	Memo	

Multiple Profile



Path: C:\Users\Rigaku pc\Desktop\ANALYSIS\OGA\12-07-2021\THE 18 \C8 Solution.rmrsln

Solution

Plot of results

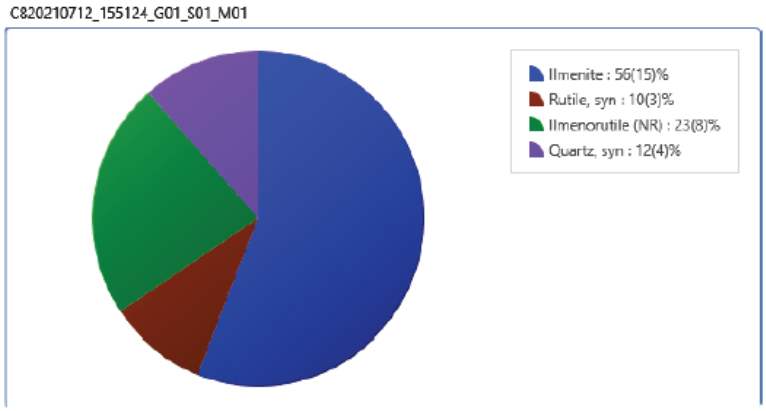


Table of results

Dataset / Weight Fraction, wt%	Value, Unit	Ilmenite	Rutile, syn	Ilmenorutile (NR)	Quartz, syn
C8_20210712_155124_G01_S01_M01	0	56(15)	10(3)	23(8)	12(4)

Calcination XRD Results for 1000^0C, 60 minutes

Path: C:\Users\Rigaku pc\Desktop\ANALYSIS\OGA\12-07-2021\THE 18 \C9 Solution.rmrsln

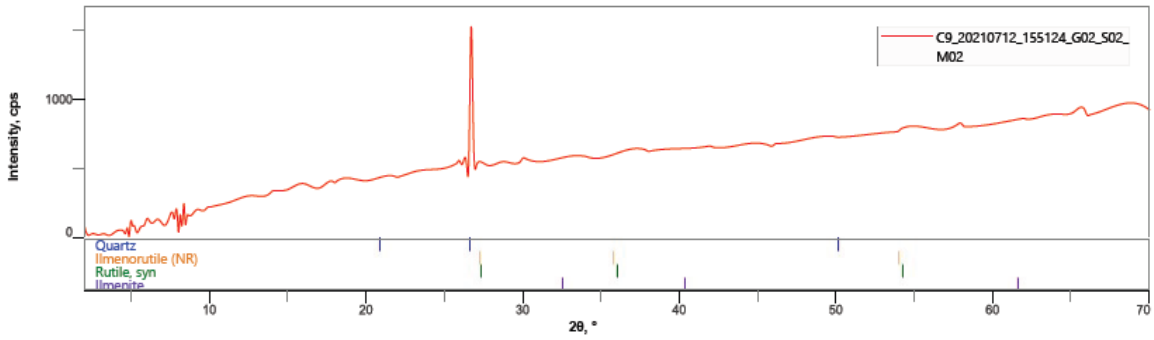
Solution

Quantitative analysis report

General information

Analysis date	2021-07-13 15:14:36	Measurement start time	2021-07-12 15:56:19
Analyst	Administrator	Operator	Administrator
Sample name	C9	Comment	
Measured data name	C:\Users\Rigaku pc\Desktop\ANALYSIS\OGA\12-07-2021\TH...	Memo	

Multiple Profile



Path: C:\Users\Rigaku pc\Desktop\ANALYSIS\OGA\12-07-2021\THE 18 \C9 Solution.rmrsln

Solution

Plot of results

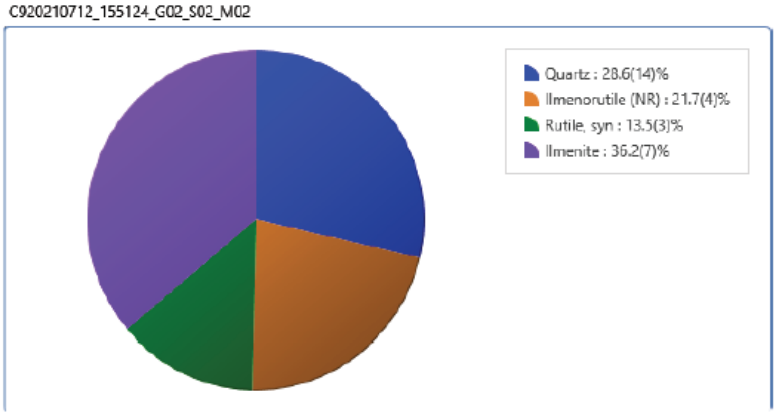


Table of results

Dataset / Weight Fraction, wt%	Value, Unit	Quartz	Ilmenorutile (NR)	Rutile, syn	Ilmenite
C9_20210712_155124_G02_S02_M02	0	28.6(14)	21.7(4)	13.5(3)	36.2(7)

APPENDIX E
Roasting XRD Results for 300^0C, 30 minutes

Path: C:\Users\Rigaku pc\Desktop\ANALYSIS\OGA\12-07-2021\THE 18 \R1 Solution.rmrsln

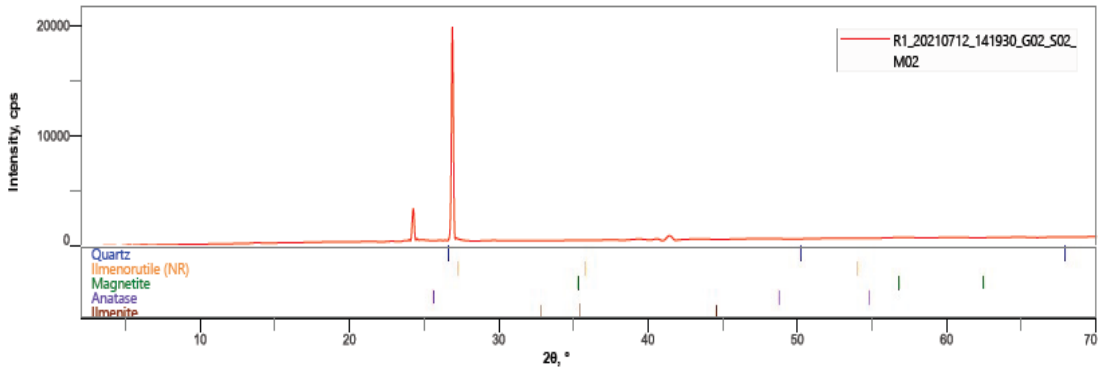
Solution

Quantitative analysis report

General information

Analysis date	2021-07-13 15:42:02	Measurement start time	2021-07-12 14:24:24
Analyst	Administrator	Operator	Administrator
Sample name	R1	Comment	
Measured data name	C:\Users\Rigaku pc\Desktop\ANALYSIS\OGA\12-07-2021\TH...	Memo	

Multiple Profile



Path: C:\Users\Rigaku pc\Desktop\ANALYSIS\OGA\12-07-2021\THE 18 \R1 Solution.rmrsln

Solution

Plot of results

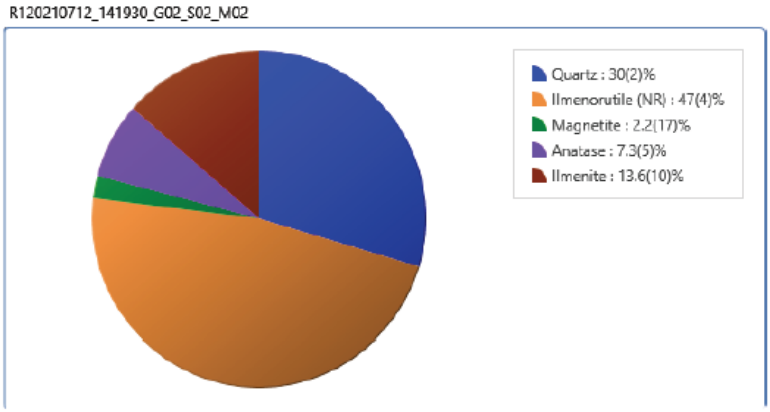


Table of results

Dataset / Weight Fraction, wt%	Value, Unit	Quartz	Ilmenorutile (NR)	Magnetite	Anatase	Ilmenite
R1_20210712_141930_G02_S02...	0	30(2)	47(4)	2.2(17)	7.3(5)	13.6(10)

Roasting XRD Results for 300^0C, 45 minutes

Path: C:\Users\Rigaku pc\Desktop\ANALYSIS\OGA\12-07-2021\THE 18 \R2 Solution.rmrsln

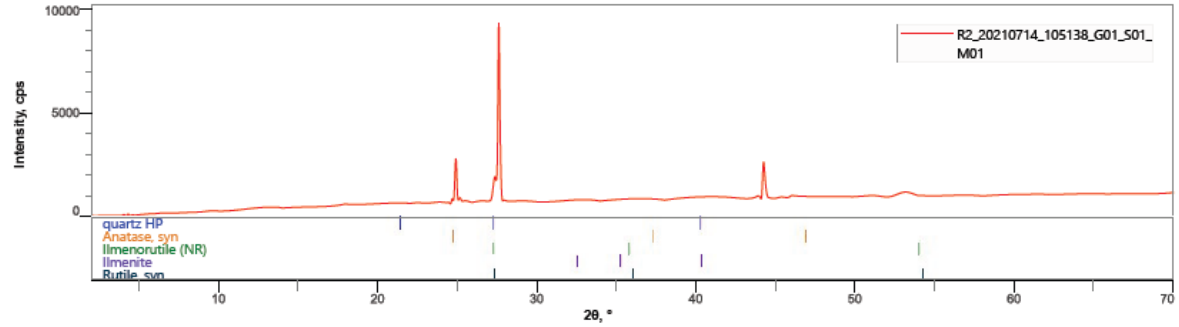
Solution

Quantitative analysis report

General information

Analysis date	2021-07-14 14:08:00	Measurement start time	2021-07-14 10:51:38
Analyst	Administrator	Operator	Administrator
Sample name	R2	Comment	
Measured data name	C:\Users\Rigaku pc\Desktop\ANALYSIS\OGA\12-07-2021\TH...	Memo	

Multiple Profile



Path: C:\Users\Rigaku pc\Desktop\ANALYSIS\OGA\12-07-2021\THE 18 \R2 Solution.rmrsln

Solution

Plot of results

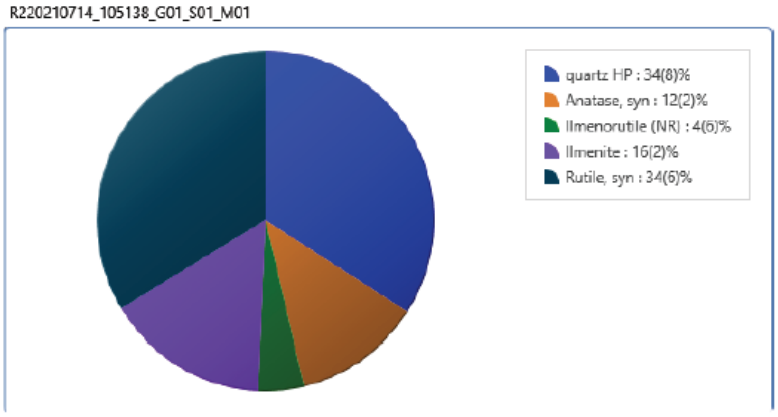


Table of results

Dataset / Weight Fraction, wt%	Value, Unit	quartz HP	Anatase, syn	Ilmenorutile (NR)	Ilmenite	Rutile, syn
R2_20210714_105138_G01_S01...	0	34(8)	12(2)	4(6)	16(2)	34(6)

Roasting XRD Results for 300^0C, 60 minutes

Path: C:\Users\Rigaku pc\Desktop\ANALYSIS\OGA\12-07-2021\THE 18
\R3 Solution.rmrsln

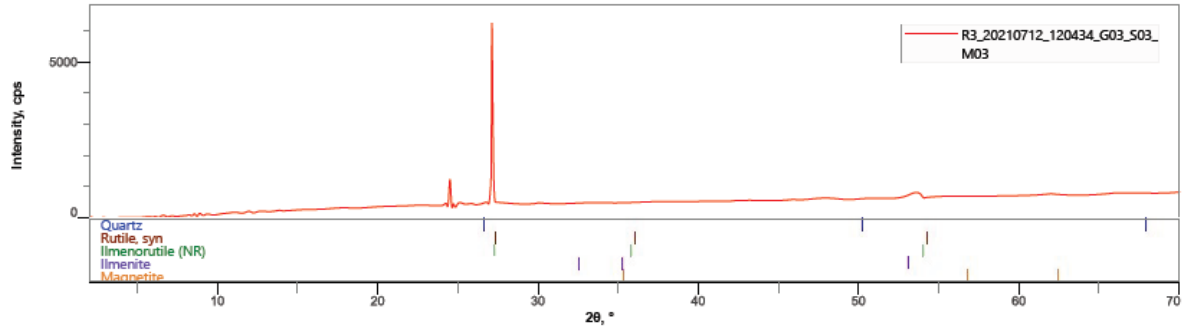
Solution

Quantitative analysis report

General information

Analysis date	2021-07-13 15:45:34	Measurement start time	2021-07-12 12:13:10
Analyst	Administrator	Operator	Administrator
Sample name	R3	Comment	
Measured data name	C:\Users\Rigaku pc\Desktop\ANALYSIS\OGA\12-07-2021\TH...	Memo	

Multiple Profile



Path: C:\Users\Rigaku pc\Desktop\ANALYSIS\OGA\12-07-2021\THE 18
\R3 Solution.rmrsln

Solution

Plot of results

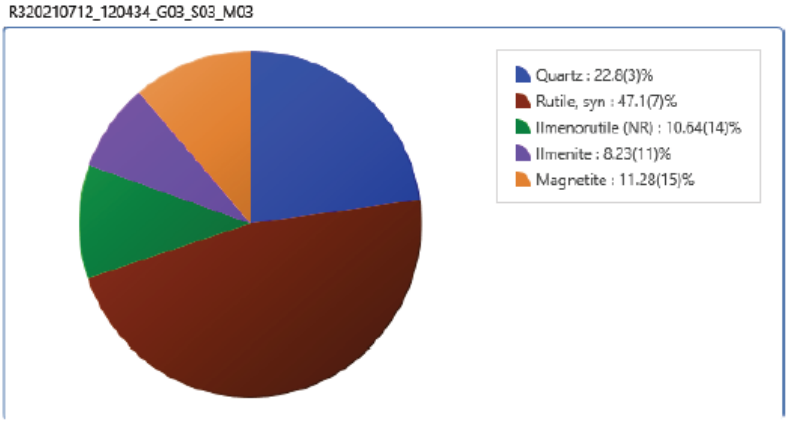


Table of results

Dataset / Weight Fraction, wt%	Value, Unit	Quartz	Rutile, syn	Ilmenorutile (NR)	Ilmenite	Magnetite
R3_20210712_120434_G03_S03...	0	22.8(3)	47.1(7)	10.64(14)	8.23(11)	11.28(15)

Roasting XRD Results for 650^0C, 30 minutes

Path: C:\Users\Rigaku pc\Desktop\ANALYSIS\OGA\12-07-2021\THE 18 \R4 Solution.rmrsln

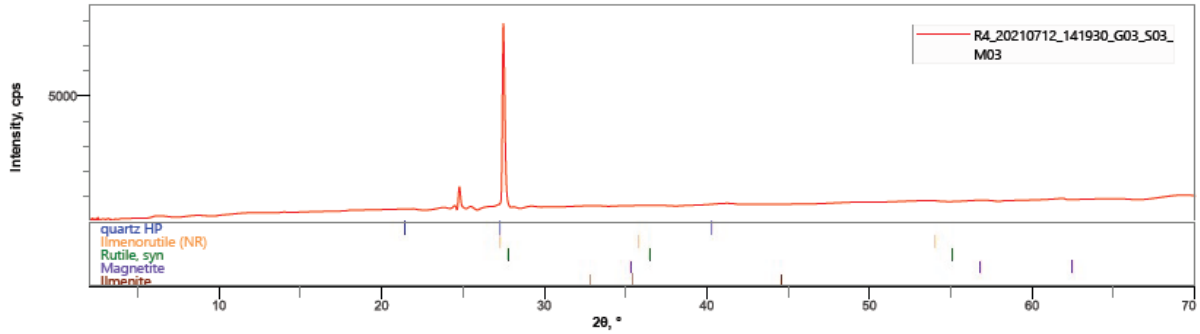
Solution

Quantitative analysis report

General information

Analysis date	2021-07-13 15:49:23	Measurement start time	2021-07-12 14:28:14
Analyst	Administrator	Operator	Administrator
Sample name	R4	Comment	
Measured data name	C:\Users\Rigaku pc\Desktop\ANALYSIS\OGA\12-07-2021\TH...	Memo	

Multiple Profile



Path: C:\Users\Rigaku pc\Desktop\ANALYSIS\OGA\12-07-2021\THE 18 \R4 Solution.rmrsln

Solution

Plot of results

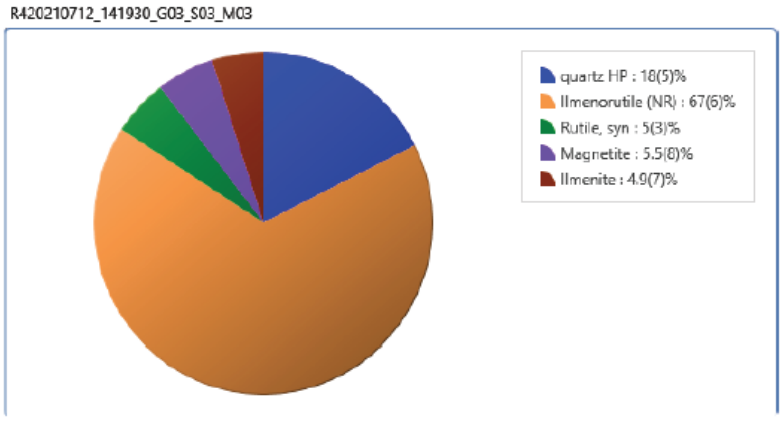


Table of results

Dataset / Weight Fraction, wt%	Value, Unit	quartz HP	Ilmenorutile (NR)	Rutile, syn	Magnetite	Ilmenite
R4_20210712_141930_G03_S03...	0	18(5)	67(6)	5(3)	5.5(8)	4.9(7)

Roasting XRD Results for 650^0C, 45 minutes

Path: C:\Users\Rigaku pc\Desktop\ANALYSIS\OGA\12-07-2021\THE 18 \R5 Solution.rmrsln

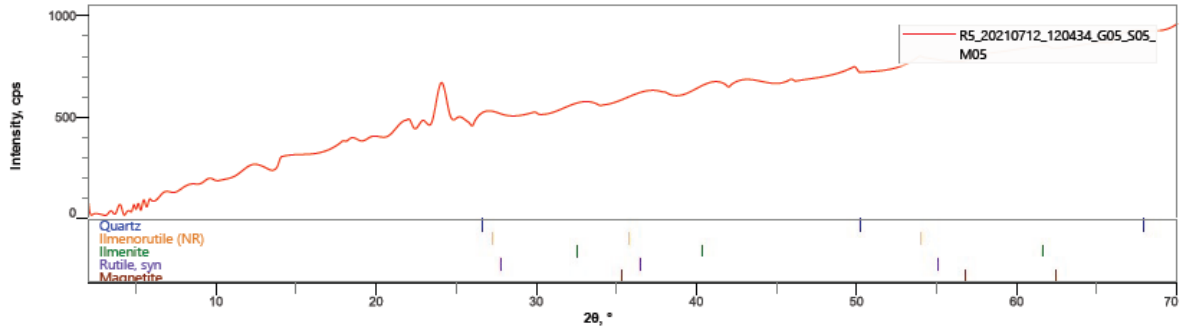
Solution

Quantitative analysis report

General information

Analysis date	2021-07-13 15:52:18	Measurement start time	2021-07-12 12:20:58
Analyst	Administrator	Operator	Administrator
Sample name	R5	Comment	
Measured data name	C:\Users\Rigaku pc\Desktop\ANALYSIS\OGA\12-07-2021\TH...	Memo	

Multiple Profile



Path: C:\Users\Rigaku pc\Desktop\ANALYSIS\OGA\12-07-2021\THE 18 \R5 Solution.rmrsln

Solution

Plot of results

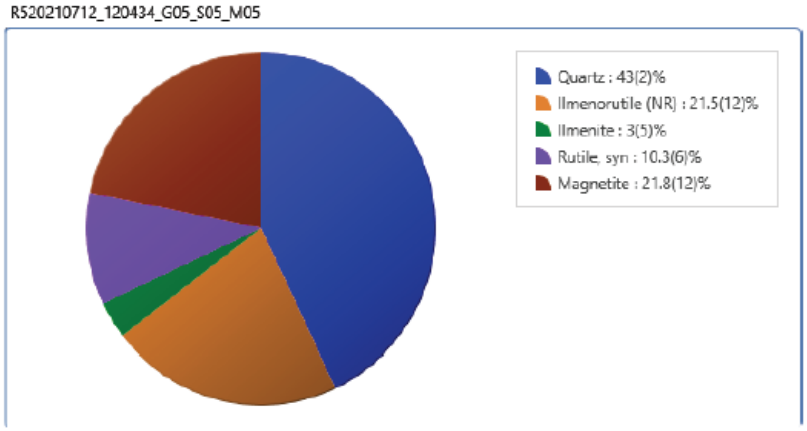


Table of results

Dataset / Weight Fraction, wt%	Value, Unit	Quartz	Ilmenorutile (NR)	Ilmenite	Rutile, syn	Magnetite
R5_20210712_120434_G05_S05...	0	43(2)	21.5(12)	3(5)	10.3(6)	21.8(12)

Roasting XRD Results for 650^0C, 60 minutes

Path: C:\Users\Rigaku pc\Desktop\ANALYSIS\OGA\12-07-2021\THE 18 \R6 Solution.rmrsln

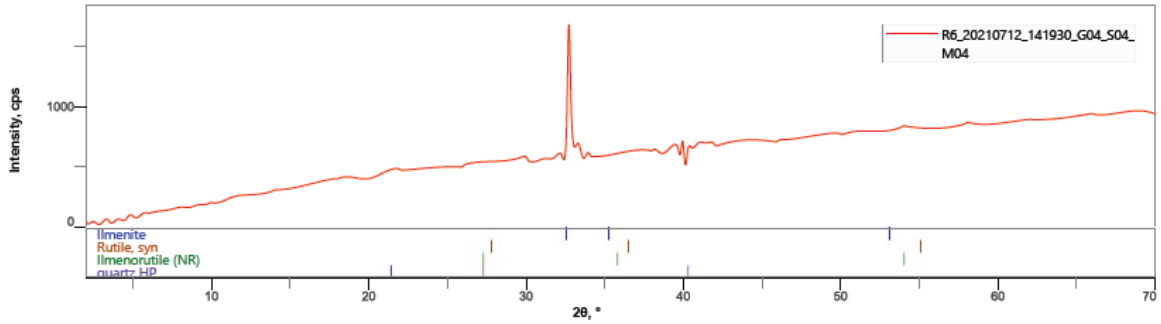
Solution

Quantitative analysis report

General information

Analysis date	2021-07-13 15:55:24	Measurement start time	2021-07-12 14:32:04
Analyst	Administrator	Operator	Administrator
Sample name	R6	Comment	
Measured data name	C:\Users\Rigaku pc\Desktop\ANALYSIS\OGA\12-07-2021\TH...	Memo	

Multiple Profile



Path: C:\Users\Rigaku pc\Desktop\ANALYSIS\OGA\12-07-2021\THE 18 \R6 Solution.rmrsln

Solution

Plot of results

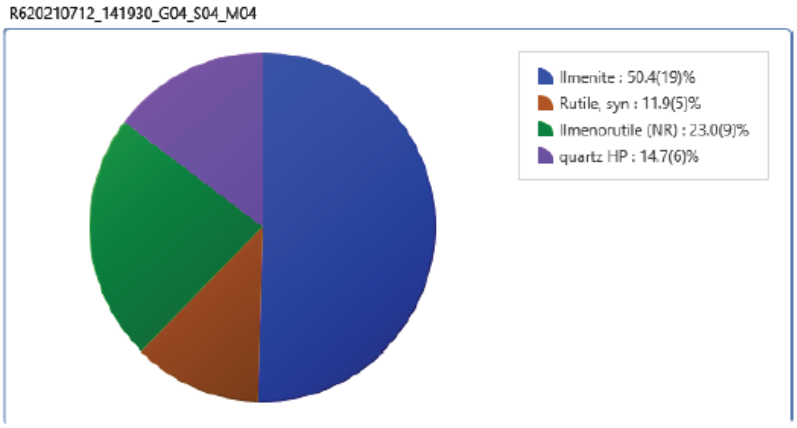


Table of results

Dataset / Weight Fraction, wt%	Value, Unit	Ilmenite	Rutile, syn	Ilmenorutile (NR)	quartz HP
R6_20210712_141930_G04_S04_M04	0	50.4(19)	11.9(5)	23.0(9)	14.7(6)

Roasting XRD Results for 1000^0C, 30 minutes

Path: C:\Users\Rigaku pc\Desktop\ANALYSIS\OGA\12-07-2021\THE 18 \R7 Solution.rmrsln

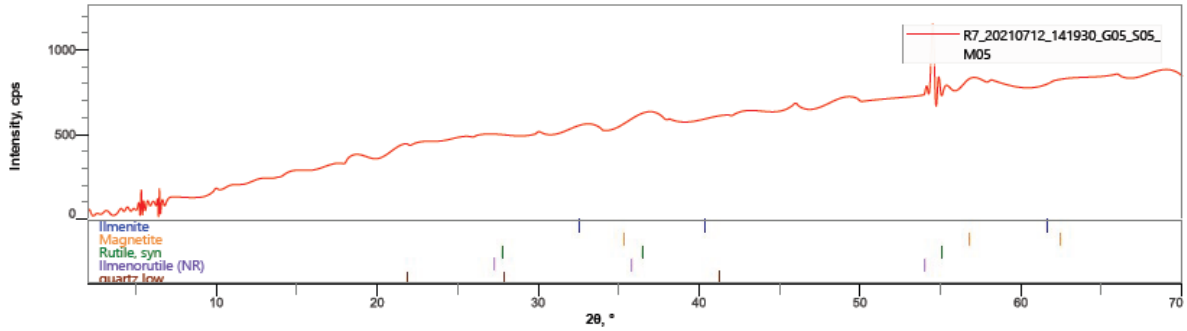
Solution

Quantitative analysis report

General information

Analysis date	2021-07-13 15:58:19	Measurement start time	2021-07-12 14:35:54
Analyst	Administrator	Operator	Administrator
Sample name	R7	Comment	
Measured data name	C:\Users\Rigaku pc\Desktop\ANALYSIS\OGA\12-07-2021\TH...	Memo	

Multiple Profile



Path: C:\Users\Rigaku pc\Desktop\ANALYSIS\OGA\12-07-2021\THE 18 \R7 Solution.rmrsln

Solution

Plot of results

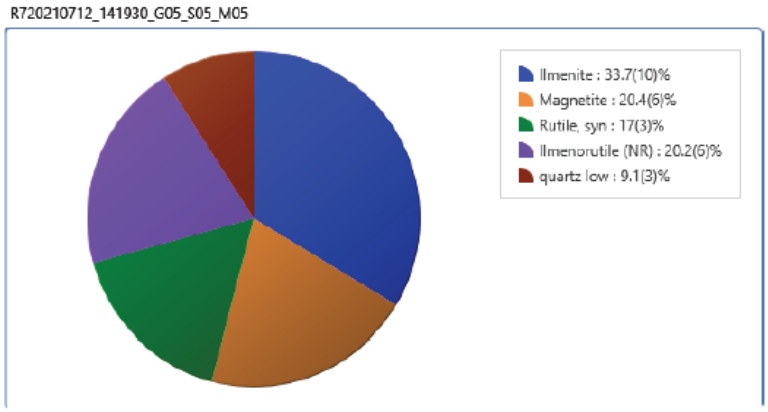


Table of results

Dataset / Weight Fraction, wt%	Value, Unit	Ilmenite	Magnetite	Rutile, syn	Ilmenorutile (NR)	quartz low
R7_20210712_141930_G05_S05...	0	33.7(10)	20.4(6)	17(3)	20.2(6)	9.1(3)

Roasting XRD Results for 1000^0C, 45 minutes

Path: C:\Users\Rigaku pc\Desktop\ANALYSIS\OGA\12-07-2021\THE 18 \R8 Solution.rmrsln

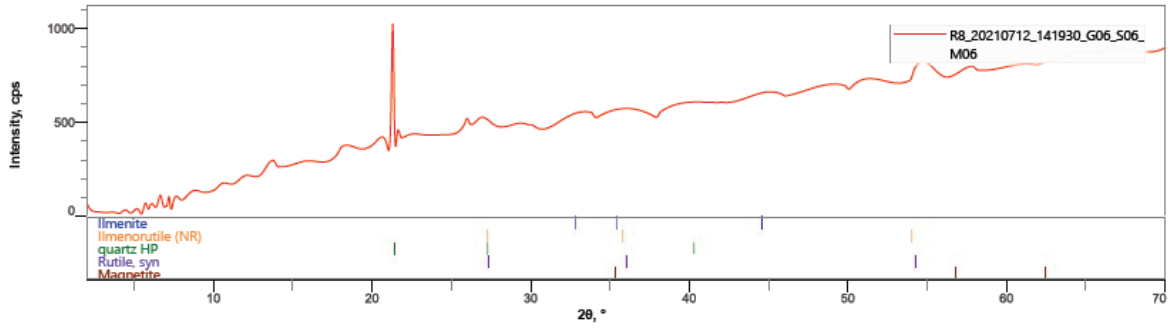
Solution

Quantitative analysis report

General information

Analysis date	2021-07-13 16:02:02	Measurement start time	2021-07-12 14:39:43
Analyst	Administrator	Operator	Administrator
Sample name	R8	Comment	
Measured data name	C:\Users\Rigaku pc\Desktop\ANALYSIS\OGA\12-07-2021\TH...	Memo	

Multiple Profile



Path: C:\Users\Rigaku pc\Desktop\ANALYSIS\OGA\12-07-2021\THE 18 \R8 Solution.rmrsln

Solution

Plot of results

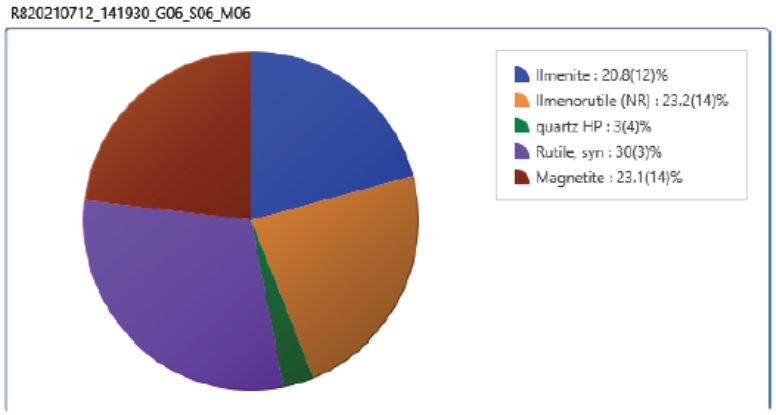


Table of results

Dataset / Weight Fraction, wt%	Value, Unit	Ilmenite	Ilmenorutile (NR)	quartz HP	Rutile, syn	Magnetite
R8_20210712_141930_G06_S06...	0	20.8(12)	23.2(14)	3(4)	30(3)	23.1(14)

Roasting XRD Results for 1000^0C, 60 minutes

Path: C:\Users\Rigaku pc\Desktop\ANALYSIS\OGA\12-07-2021\THE 18 \R9 Solution.rmrsln

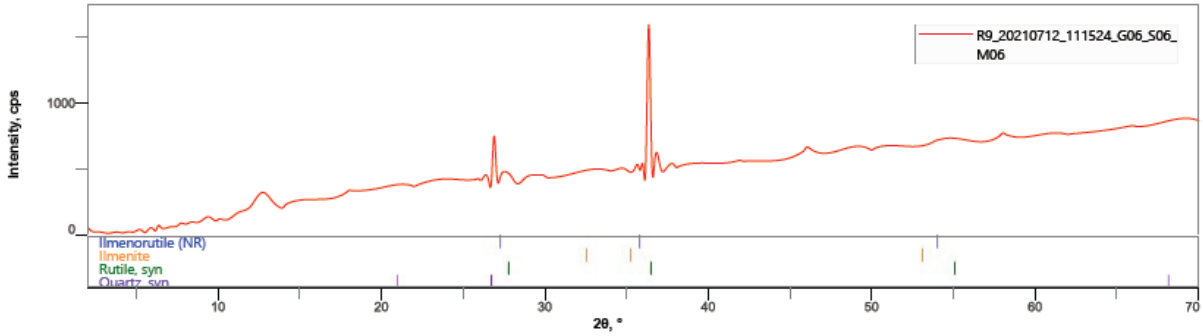
Solution

Quantitative analysis report

General information

Analysis date	2021-07-13 16:04:50	Measurement start time	2021-07-12 11:34:33
Analyst	Administrator	Operator	Administrator
Sample name	R9	Comment	
Measured data name	C:\Users\Rigaku pc\Desktop\ANALYSIS\OGA\12-07-2021\TH...	Memo	

Multiple Profile



Path: C:\Users\Rigaku pc\Desktop\ANALYSIS\OGA\12-07-2021\THE 18 \R9 Solution.rmrsln

Solution

Plot of results

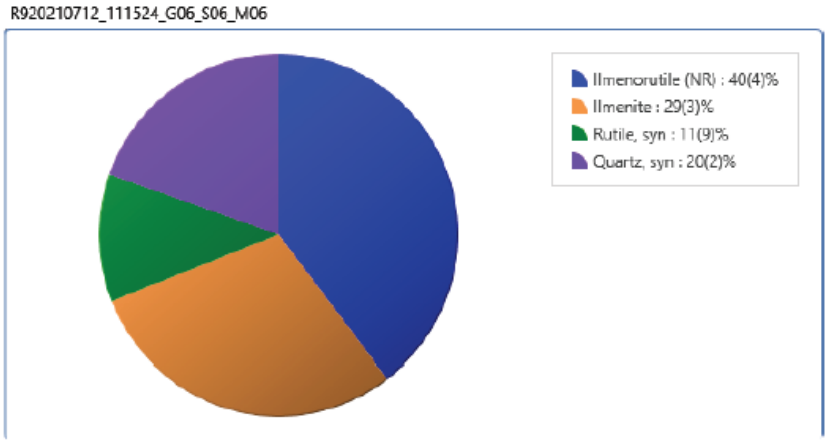


Table of results

Dataset / Weight Fraction, wt%	Value, Unit	Ilmenorutile (NR)	Ilmenite	Rutile, syn	Quartz, syn
R9_20210712_111524_G06_S06_M06	0	40(4)	29(3)	11(9)	20(2)

APPENDIX F
Calcination XRF Results for 300^0C, 30 minutes

CrossRoads Scientific XRS-FP Analysis Report

File: C:\Users\Xenemetrix\Music\New folder\New folder\C1.str

4:14:40 PM 12-Jul-21

Comment line

Layer Table ==========

#	Thick	Type	Error	Units	Density	Norm.	Total
1	0.00	Bulk	0.00	mg/cm2	0.00F	On	100.00

Sample Table ==========

Layer	Component	Type	Concn.	Error	Units	Mole%	Error
1	SiO2	Calc	3.475	0.458	wt.%	4.949	0.652
1	V2O5	Calc	0.812	0.085	wt.%	0.382	0.040
1	Cr2O3	Calc	0.000	0.000	wt.%	0.000	0.000
1	MnO	Calc	0.743	0.032	wt.%	0.896	0.039
1	Fe2O3	Calc	17.427	0.146	wt.%	9.337	0.078
1	Co3O4	Calc	0.085	0.045	wt.%	0.030	0.016
1	NiO	Calc	0.000	0.000	wt.%	0.000	0.000
1	CuO	Calc	0.035	0.011	wt.%	0.038	0.012
1	Nb2O3	Calc	0.015	0.362	wt.%	0.005	0.133
1	MoO3	Calc	0.000	0.000	wt.%	0.000	0.000
1	WO3	Calc	0.353	0.062	wt.%	0.130	0.023
1	P2O5	Calc	0.000	0.000	wt.%	0.000	0.000
1	SO3	Calc	0.000	0.000	wt.%	0.000	0.000
1	CaO	Calc	0.192	0.021	wt.%	0.292	0.033
1	MgO	Calc	2.411	6.395	wt.%	5.118	13.575
1	K2O	Calc	0.025	0.025	wt.%	0.022	0.022
1	BaO	Calc	0.581	0.714	wt.%	0.324	0.399
1	Al2O3	Calc	3.700	1.403	wt.%	3.105	1.177
1	Ta2O5	Calc	0.232	0.049	wt.%	0.045	0.009
1	TiO2	Calc	69.273	0.291	wt.%	74.212	0.312
1	ZnO	Calc	0.075	0.012	wt.%	0.079	0.012
1	Ag2O	Calc	0.000	0.000	wt.%	0.000	0.000
1	Cl	Calc	0.399	0.035	wt.%	0.962	0.084
1	ZrO2	Calc	0.027	0.093	wt.%	0.019	0.065
1	SnO2	Calc	0.000	0.000	wt.%	0.000	0.000
1	PbO	Calc	0.140	0.029	wt.%	0.054	0.011

Element Table ==========

Element Table ==========

Elmt	Line	Cond	Ratio	Intensity	Error	Intensity	Conc.	Conc	Calibration
	Code	Code	Method	(c/s)	(c/s)	Method		Method	Coefficient
O	Ka	0	None	0.000	0.0000	Gaussian	38.354	None	0.000
Mg	Ka	1	None	0.331	0.8793	Gaussian	1.454	FP	0.000
Al	Ka	1	None	5.264	1.9954	Gaussian	1.958	FP	0.000
Si	Ka	1	None	25.433	3.3500	Gaussian	1.625	FP	0.000
P	Ka	1	None	0.000	2.1082	Gaussian	0.000	FP	0.000
S	Ka	1	None	0.000	2.5051	Gaussian	0.000	FP	0.000
Cl	Ka	1	None	58.883	5.1685	Gaussian	0.399	FP	0.000
K	Ka	1	None	4.622	4.6114	Gaussian	0.020	FP	0.000
Ca	Ka	1	None	44.795	4.9986	Gaussian	0.137	FP	0.000
Ti	Ka	1	None	17517.530	73.6859	Gaussian	41.530	FP	0.000
V	Ka	1	None	248.599	26.0429	Gaussian	0.455	FP	0.000
Cr	Ka	1	None	0.000	4.2143	Gaussian	0.000	FP	0.000
Mn	Ka	1	None	179.154	7.8380	Gaussian	0.575	FP	0.000
Fe	Ka	1	None	4384.650	36.8405	Gaussian	12.189	FP	0.000
Co	Ka	1	None	24.998	13.0945	Gaussian	0.062	FP	0.000
Ni	Ka	1	None	0.000	4.6428	Gaussian	0.000	FP	0.000
Cu	Ka	1	None	10.429	3.1853	Gaussian	0.028	FP	0.000
Zn	Ka	1	None	24.216	3.8184	Gaussian	0.060	FP	0.000
Zr	Ka	1	None	0.578	1.9792	Gaussian	0.020	FP	0.000
Nb	Ka	1	None	0.069	1.7050	Gaussian	0.012	FP	0.000
Mo	Ka	1	None	0.000	1.3663	Gaussian	0.000	FP	0.000
Ag	Ka	1	None	0.000	0.0000	Gaussian	0.000	FP	0.000
Sn	Ka	1	None	0.000	0.0000	Gaussian	0.000	FP	0.000
Ba	La	1	None	55.612	68.3616	Gaussian	0.521	FP	0.000
Ta	La	1	None	17.759	3.7219	Gaussian	0.190	FP	0.000
W	La	1	None	26.641	4.6853	Gaussian	0.280	FP	0.000
Pb	La	1	None	12.028	2.4987	Gaussian	0.130	FP	0.000

Analysis Conditions ==========

#	Tar	Filter	Thick.	kV	uA	---Detector---		Thick.	Atm	Preset	Actual
	get		mg/cm2			Type	Filter	mg/cm2		Time(s)	Time(s)
1	Rh	None	0.00	20.0	20.0	SDD	None	0.00	Air	60.0	30.0

Processing Conditions ==========

#	No. Smths	Escape Peaks	Sum Peaks	Back Type	C/R Ratio	Blank Rem.	----Blank---- ----File-----
1	1	Yes	Yes	Auto	No	No	

Calcination XRF Results for 300^0C, 45 minutes

CrossRoads Scientific XRS-FP Analysis Report

File: C:\Users\Xenemetrix\Music\New folder\New folder\C2.str

4:15:59 PM 12-Jul-21

Comment line

Layer Table ==========

#	Thick	Type	Error	Units	Density	Norm.	Total
1	0.00	Bulk	0.00	mg/cm2	0.00F	On	100.00

Sample Table ==========

Layer	Component	Type	Concn.	Error	Units	Mole%	Error
1	SiO2	Calc	6.586	0.593	wt.%	9.488	0.855
1	V2O5	Calc	0.711	0.085	wt.%	0.338	0.041
1	Cr2O3	Calc	0.000	0.000	wt.%	0.000	0.000
1	MnO	Calc	0.734	0.032	wt.%	0.896	0.040
1	Fe2O3	Calc	16.856	0.144	wt.%	9.138	0.078
1	Co3O4	Calc	0.081	0.044	wt.%	0.029	0.016
1	NiO	Calc	0.000	0.000	wt.%	0.000	0.000
1	CuO	Calc	0.019	0.010	wt.%	0.021	0.011
1	Nb2O3	Calc	0.174	0.382	wt.%	0.064	0.141
1	MoO3	Calc	0.000	0.000	wt.%	0.000	0.000
1	WO3	Calc	0.263	0.060	wt.%	0.098	0.023
1	P2O5	Calc	0.000	0.000	wt.%	0.000	0.000
1	SO3	Calc	0.015	0.059	wt.%	0.016	0.063
1	CaO	Calc	0.315	0.026	wt.%	0.487	0.040
1	MgO	Calc	0.000	0.000	wt.%	0.000	0.000
1	K2O	Calc	0.027	0.024	wt.%	0.025	0.022
1	BaO	Calc	0.654	0.717	wt.%	0.369	0.405
1	Al2O3	Calc	3.720	1.548	wt.%	3.158	1.314
1	Ta2O5	Calc	0.177	0.045	wt.%	0.035	0.009
1	TiO2	Calc	69.066	0.292	wt.%	74.861	0.317
1	ZnO	Calc	0.110	0.012	wt.%	0.117	0.013
1	Ag2O	Calc	0.000	0.000	wt.%	0.000	0.000
1	Cl	Calc	0.321	0.032	wt.%	0.783	0.078
1	ZrO2	Calc	0.035	0.092	wt.%	0.024	0.064
1	SnO2	Calc	0.000	0.000	wt.%	0.000	0.000

Element Table ==========

Elmt	Line Code	Cond Code	Ratio Method	Intensity (c/s)	Error (c/s)	Intensity Method	Conc.	Conc Method	Calibration Coefficient
O	Ka	0	None	0.000	0.0000	Gaussian	38.823	None	0.000
Mg	Ka	1	None	0.000	0.8273	Gaussian	0.000	FP	0.000
Al	Ka	1	None	5.409	2.2512	Gaussian	1.969	FP	0.000
Si	Ka	1	None	49.099	4.4237	Gaussian	3.078	FP	0.000
P	Ka	1	None	0.000	2.5473	Gaussian	0.000	FP	0.000
S	Ka	1	None	0.632	2.4774	Gaussian	0.006	FP	0.000
Cl	Ka	1	None	46.743	4.6773	Gaussian	0.321	FP	0.000
K	Ka	1	None	5.088	4.5219	Gaussian	0.023	FP	0.000
Ca	Ka	1	None	72.848	5.9768	Gaussian	0.225	FP	0.000
Ti	Ka	1	None	17309.180	73.2350	Gaussian	41.406	FP	0.000
V	Ka	1	None	215.890	25.9494	Gaussian	0.398	FP	0.000
Cr	Ka	1	None	0.000	4.1462	Gaussian	0.000	FP	0.000
Mn	Ka	1	None	176.692	7.7999	Gaussian	0.568	FP	0.000
Fe	Ka	1	None	4237.749	36.2260	Gaussian	11.790	FP	0.000
Co	Ka	1	None	23.693	12.9149	Gaussian	0.059	FP	0.000
Ni	Ka	1	None	0.000	4.7263	Gaussian	0.000	FP	0.000
Cu	Ka	1	None	5.597	3.0036	Gaussian	0.015	FP	0.000
Zn	Ka	1	None	35.658	4.0452	Gaussian	0.088	FP	0.000
Zr	Ka	1	None	0.746	1.9623	Gaussian	0.026	FP	0.000
Nb	Ka	1	None	0.825	1.8096	Gaussian	0.138	FP	0.000
Mo	Ka	1	None	0.248	1.5570	Gaussian	0.000	FP	0.000
Ag	Ka	1	None	0.000	0.0000	Gaussian	0.000	FP	0.000
Sn	Ka	1	None	0.000	0.0000	Gaussian	0.000	FP	0.000
Ba	La	1	None	61.999	67.9493	Gaussian	0.586	FP	0.000
Ta	La	1	None	13.599	3.4435	Gaussian	0.145	FP	0.000
W	La	1	None	19.954	4.5863	Gaussian	0.208	FP	0.000
Pb	La	1	None	11.845	2.6511	Gaussian	0.127	FP	0.000

Analysis Conditions ==========

#	Tar get	Filter	Thick. mg/cm2	kV	uA	---Detector--- Type	Filter	Thick. mg/cm2	Atm	Preset Time(s)	Actual Time(s)
1	Rh	None	0.00	20.0	20.0	SDD	None	0.00	Air	60.0	30.0

Processing Conditions ==========

#	No. Smths	Escape Peaks	Sum Peaks	Back Type	C/R Ratio	Blank Rem	----Blank---- ----File----

Calcination XRF Results for 300^{0}C, 60 minutes

CrossRoads Scientific XRS-FP Analysis Report

File: C:\Users\Xenemetrix\Music\New folder\New folder (2)\C3.str

8:13:12 PM 12-Jul-21

Comment line

Layer Table ==========

#	Thick	Type	Error	Units	Density	Norm.	Total
1	0.00	Bulk	0.00	mg/cm2	0.00F	On	100.00

Sample Table ==========

Layer	Component	Type	Concn.	Error	Units	Mole%	Error
1	SiO2	Calc	7.653	0.638	wt.%	11.155	0.930
1	V2O5	Calc	1.106	0.082	wt.%	0.532	0.039
1	Cr2O3	Calc	0.000	0.000	wt.%	0.000	0.000
1	MnO	Calc	1.053	0.038	wt.%	1.300	0.047
1	Fe2O3	Calc	19.608	0.152	wt.%	10.754	0.083
1	Co3O4	Calc	0.080	0.047	wt.%	0.029	0.017
1	NiO	Calc	0.000	0.000	wt.%	0.000	0.000
1	CuO	Calc	0.036	0.011	wt.%	0.040	0.012
1	Nb2O3	Calc	0.279	0.380	wt.%	0.104	0.142
1	MoO3	Calc	0.000	0.000	wt.%	0.000	0.000
1	WO3	Calc	0.252	0.058	wt.%	0.095	0.022
1	P2O5	Calc	0.000	0.000	wt.%	0.000	0.000
1	SO3	Calc	0.044	0.056	wt.%	0.048	0.061
1	CaO	Calc	0.643	0.036	wt.%	1.005	0.056
1	MgO	Calc	0.000	0.000	wt.%	0.000	0.000
1	K2O	Calc	0.145	0.027	wt.%	0.135	0.026
1	BaO	Calc	0.688	0.688	wt.%	0.393	0.393
1	Al2O3	Calc	3.911	1.612	wt.%	3.360	1.385
1	Ta2O5	Calc	0.220	0.048	wt.%	0.044	0.009
1	TiO2	Calc	63.629	0.279	wt.%	69.778	0.306
1	ZnO	Calc	0.065	0.011	wt.%	0.070	0.012
1	Ag2O	Calc	0.000	0.000	wt.%	0.000	0.000
1	Cl	Calc	0.444	0.037	wt.%	1.098	0.093
1	ZrO2	Calc	0.008	0.086	wt.%	0.006	0.061
1	SnO2	Calc	0.000	0.000	wt.%	0.000	0.000

Element Table ==========

Elmt	Line Code	Cond Code	Ratio Method	Intensity (c/s)	Error (c/s)	Intensity Method	Conc.	Conc Method	Calibration Coefficient
O	Ka	0	None	0.000	0.0000	Gaussian	38.525	None	0.000
Mg	Ka	1	None	0.000	0.8055	Gaussian	0.000	FP	0.000
Al	Ka	1	None	5.712	2.3545	Gaussian	2.070	FP	0.000
Si	Ka	1	None	57.154	4.7631	Gaussian	3.577	FP	0.000
P	Ka	1	None	0.000	2.5508	Gaussian	0.000	FP	0.000
S	Ka	1	None	1.838	2.3277	Gaussian	0.018	FP	0.000
Cl	Ka	1	None	63.998	5.3954	Gaussian	0.444	FP	0.000
K	Ka	1	None	26.547	5.0246	Gaussian	0.121	FP	0.000
Ca	Ka	1	None	145.626	8.0699	Gaussian	0.460	FP	0.000
Ti	Ka	1	None	16096.720	70.6241	Gaussian	38.147	FP	0.000
V	Ka	1	None	338.466	24.9766	Gaussian	0.619	FP	0.000
Cr	Ka	1	None	0.000	4.8442	Gaussian	0.000	FP	0.000
Mn	Ka	1	None	265.661	9.5144	Gaussian	0.815	FP	0.000
Fe	Ka	1	None	5138.225	39.8763	Gaussian	13.715	FP	0.000
Co	Ka	1	None	24.329	14.2411	Gaussian	0.059	FP	0.000
Ni	Ka	1	None	0.000	5.1829	Gaussian	0.000	FP	0.000
Cu	Ka	1	None	10.763	3.2775	Gaussian	0.029	FP	0.000
Zn	Ka	1	None	21.354	3.5344	Gaussian	0.053	FP	0.000
Zr	Ka	1	None	0.180	1.8540	Gaussian	0.006	FP	0.000
Nb	Ka	1	None	1.323	1.8033	Gaussian	0.222	FP	0.000
Mo	Ka	1	None	0.233	1.4283	Gaussian	0.000	FP	0.000
Ag	Ka	1	None	0.000	0.0000	Gaussian	0.000	FP	0.000
Sn	Ka	1	None	0.000	0.0000	Gaussian	0.000	FP	0.000
Ba	La	1	None	65.526	65.5348	Gaussian	0.616	FP	0.000
Ta	La	1	None	16.921	3.6816	Gaussian	0.180	FP	0.000
W	La	1	None	19.192	4.4401	Gaussian	0.200	FP	0.000
Pb	La	1	None	11.828	2.7087	Gaussian	0.126	FP	0.000

Analysis Conditions ==========

#	Tar get	Filter	Thick. mg/cm2	kV	uA	---Detector--- Type	Filter	Thick. mg/cm2	Atm	Preset Time(s)	Actual Time(s)
1	Rh	None	0.00	20.0	20.0	SDD	None	0.00	Air	60.0	30.0

Processing Conditions ==========

#	No. Smths	Escape Peaks	Sum Peaks	Back Type	C/R Ratio	Blank Rem.	----Blank---- ----File-----

Calcination XRF Results for 650^{0}C, 30 minutes

CrossRoads Scientific XRS-FP Analysis Report

File: C:\Users\Xenemetrix\Music\New folder\New folder (2)\C4.str

8:14:31 PM 12-

Comment line

Layer Table ==========

#	Thick	Type	Error	Units	Density	Norm.	Total
1	0.00	Bulk	0.00	mg/cm2	0.00F	On	100.00

Sample Table ==========

Layer	Component	Type	Concn.	Error	Units	Mole%	Error
1	SiO2	Calc	6.135	0.590	wt.%	8.953	0.861
1	V2O5	Calc	0.899	0.081	wt.%	0.434	0.039
1	Cr2O3	Calc	0.000	0.000	wt.%	0.000	0.000
1	MnO	Calc	1.218	0.040	wt.%	1.505	0.050
1	Fe2O3	Calc	21.255	0.159	wt.%	11.671	0.087
1	Co3O4	Calc	0.108	0.049	wt.%	0.039	0.018
1	NiO	Calc	0.000	0.000	wt.%	0.000	0.000
1	CuO	Calc	0.016	0.010	wt.%	0.018	0.011
1	Nb2O3	Calc	0.167	0.354	wt.%	0.063	0.133
1	MoO3	Calc	0.000	0.000	wt.%	0.000	0.000
1	WO3	Calc	0.226	0.056	wt.%	0.085	0.021
1	P2O5	Calc	0.000	0.000	wt.%	0.000	0.000
1	SO3	Calc	0.252	0.067	wt.%	0.276	0.074
1	CaO	Calc	0.873	0.042	wt.%	1.365	0.065
1	MgO	Calc	1.191	6.745	wt.%	2.591	14.673
1	K2O	Calc	0.127	0.028	wt.%	0.118	0.026
1	BaO	Calc	0.645	0.681	wt.%	0.369	0.390
1	Al2O3	Calc	4.411	1.616	wt.%	3.793	1.390
1	Ta2O5	Calc	0.193	0.045	wt.%	0.038	0.009
1	TiO2	Calc	61.763	0.276	wt.%	67.808	0.303
1	ZnO	Calc	0.073	0.011	wt.%	0.078	0.012
1	Ag2O	Calc	0.000	0.000	wt.%	0.000	0.000
1	Cl	Calc	0.294	0.032	wt.%	0.727	0.079
1	ZrO2	Calc	0.025	0.088	wt.%	0.018	0.063
1	SnO2	Calc	0.000	0.000	wt.%	0.000	0.000

Element Table ==========

Elmt	Line Code	Cond Code	Ratio Method	Intensity (c/s)	Error (c/s)	Intensity Method	Conc.	Conc Method	Calibration Coefficient
O	Ka	0	None	0.000	0.0000	Gaussian	38.277	None	0.000
Mg	Ka	1	None	0.161	0.9112	Gaussian	0.718	FP	0.000
Al	Ka	1	None	6.227	2.2811	Gaussian	2.334	FP	0.000
Si	Ka	1	None	44.197	4.2520	Gaussian	2.868	FP	0.000
P	Ka	1	None	0.000	2.3113	Gaussian	0.000	FP	0.000
S	Ka	1	None	10.360	2.7623	Gaussian	0.101	FP	0.000
Cl	Ka	1	None	41.630	4.5387	Gaussian	0.294	FP	0.000
K	Ka	1	None	22.975	4.9930	Gaussian	0.106	FP	0.000
Ca	Ka	1	None	195.163	9.2801	Gaussian	0.624	FP	0.000
Ti	Ka	1	None	15489.760	69.2925	Gaussian	37.028	FP	0.000
V	Ka	1	None	272.892	24.5546	Gaussian	0.504	FP	0.000
Cr	Ka	1	None	0.000	4.5743	Gaussian	0.000	FP	0.000
Mn	Ka	1	None	307.617	10.1728	Gaussian	0.943	FP	0.000
Fe	Ka	1	None	5555.081	41.4396	Gaussian	14.867	FP	0.000
Co	Ka	1	None	32.722	14.7702	Gaussian	0.079	FP	0.000
Ni	Ka	1	None	0.000	5.2485	Gaussian	0.000	FP	0.000
Cu	Ka	1	None	4.717	2.9974	Gaussian	0.013	FP	0.000
Zn	Ka	1	None	23.154	3.5243	Gaussian	0.059	FP	0.000
Zr	Ka	1	None	0.527	1.8521	Gaussian	0.019	FP	0.000
Nb	Ka	1	None	0.775	1.6455	Gaussian	0.133	FP	0.000
Mo	Ka	1	None	0.000	1.2579	Gaussian	0.000	FP	0.000
Ag	Ka	1	None	0.000	0.0000	Gaussian	0.000	FP	0.000
Sn	Ka	1	None	0.000	0.0000	Gaussian	0.000	FP	0.000
Ba	La	1	None	60.823	64.2975	Gaussian	0.577	FP	0.000
Ta	La	1	None	14.513	3.4042	Gaussian	0.158	FP	0.000
W	La	1	None	16.758	4.1946	Gaussian	0.179	FP	0.000
Pb	La	1	None	10.904	2.4414	Gaussian	0.119	FP	0.000

Analysis Conditions ==========

#	Tar get	Filter	Thick. mg/cm2	kV	uA	---Detector--- Type	Filter	Thick. mg/cm2	Atm	Preset Time(s)	Actual Time(s)
1	Rh	None	0.00	20.0	15.0	SDD	None	0.00	Air	60.0	30.0

Processing Conditions ==========

# Smths	No. Peaks	Escape Peaks	Sum Peaks	Back Type	C/R Ratio	Blank Rem.	----Blank---- ----File-----

Calcination XRF Results for 650^0C, 45 minutes

CrossRoads Scientific XRS-FP Analysis Report

File: C:\Users\Xenemetrix\Music\New folder\New folder (2)\C5.str

8:15:47 PM 12-

Comment line

Layer Table ==========

#	Thick	Type	Error	Units	Density	Norm.	Total
1	0.00	Bulk	0.00	mg/cm2	0.00F	On	100.00

Sample Table ==========

Layer	Component	Type	Concn.	Error	Units	Mole%	Error
1	SiO2	Calc	5.368	0.537	wt.%	7.848	0.786
1	V2O5	Calc	0.868	0.079	wt.%	0.419	0.038
1	Cr2O3	Calc	0.000	0.000	wt.%	0.000	0.000
1	MnO	Calc	0.986	0.036	wt.%	1.221	0.044
1	Fe2O3	Calc	21.538	0.155	wt.%	11.849	0.085
1	Co3O4	Calc	0.127	0.047	wt.%	0.047	0.017
1	NiO	Calc	0.000	0.000	wt.%	0.000	0.000
1	CuO	Calc	0.032	0.010	wt.%	0.035	0.011
1	Nb2O3	Calc	0.136	0.360	wt.%	0.051	0.135
1	MoO3	Calc	0.000	0.000	wt.%	0.000	0.000
1	WO3	Calc	0.359	0.061	wt.%	0.136	0.023
1	P2O5	Calc	0.000	0.000	wt.%	0.000	0.000
1	SO3	Calc	0.173	0.059	wt.%	0.190	0.065
1	CaO	Calc	0.834	0.039	wt.%	1.306	0.061
1	MgO	Calc	1.399	6.598	wt.%	3.049	14.381
1	K2O	Calc	0.036	0.026	wt.%	0.034	0.024
1	BaO	Calc	0.513	0.665	wt.%	0.294	0.381
1	Al2O3	Calc	4.311	1.527	wt.%	3.714	1.316
1	Ta2O5	Calc	0.174	0.046	wt.%	0.035	0.009
1	TiO2	Calc	62.581	0.270	wt.%	68.838	0.297
1	ZnO	Calc	0.089	0.012	wt.%	0.096	0.013
1	Ag2O	Calc	0.000	0.000	wt.%	0.000	0.000
1	Cl	Calc	0.309	0.031	wt.%	0.766	0.077
1	ZrO2	Calc	0.023	0.086	wt.%	0.016	0.061
1	SnO2	Calc	0.000	0.000	wt.%	0.000	0.000

Element Table ==========

Elmt	Line Code	Cond Code	Ratio Method	Intensity (c/s)	Error (c/s)	Intensity Method	Conc.	Conc Method	Calibration Coefficient
O	Ka	0	None	0.000	0.0000	Gaussian	38.192	None	0.000
Mg	Ka	1	None	0.200	0.9428	Gaussian	0.844	FP	0.000
Al	Ka	1	None	6.428	2.2773	Gaussian	2.281	FP	0.000
Si	Ka	1	None	40.929	4.0976	Gaussian	2.509	FP	0.000
P	Ka	1	None	0.000	2.3190	Gaussian	0.000	FP	0.000
S	Ka	1	None	7.558	2.5740	Gaussian	0.069	FP	0.000
Cl	Ka	1	None	46.560	4.7003	Gaussian	0.309	FP	0.000
K	Ka	1	None	6.986	4.9277	Gaussian	0.030	FP	0.000
Ca	Ka	1	None	198.748	9.3396	Gaussian	0.596	FP	0.000
Ti	Ka	1	None	16662.900	71.8911	Gaussian	37.518	FP	0.000
V	Ka	1	None	279.568	25.4116	Gaussian	0.486	FP	0.000
Cr	Ka	1	None	0.000	4.5802	Gaussian	0.000	FP	0.000
Mn	Ka	1	None	263.007	9.4780	Gaussian	0.763	FP	0.000
Fe	Ka	1	None	5943.540	42.8810	Gaussian	15.064	FP	0.000
Co	Ka	1	None	40.967	15.2282	Gaussian	0.094	FP	0.000
Ni	Ka	1	None	0.000	5.3450	Gaussian	0.000	FP	0.000
Cu	Ka	1	None	9.784	3.1195	Gaussian	0.026	FP	0.000
Zn	Ka	1	None	29.982	4.0691	Gaussian	0.072	FP	0.000
Zr	Ka	1	None	0.500	1.8985	Gaussian	0.017	FP	0.000
Nb	Ka	1	None	0.663	1.7561	Gaussian	0.108	FP	0.000
Mo	Ka	1	None	0.000	1.3630	Gaussian	0.000	FP	0.000
Ag	Ka	1	None	0.000	0.0000	Gaussian	0.000	FP	0.000
Sn	Ka	1	None	0.000	0.0000	Gaussian	0.000	FP	0.000
Ba	La	1	None	51.471	66.6965	Gaussian	0.460	FP	0.000
Ta	La	1	None	13.801	3.6393	Gaussian	0.143	FP	0.000
W	La	1	None	28.135	4.7722	Gaussian	0.285	FP	0.000
Pb	La	1	None	12.962	2.6288	Gaussian	0.135	FP	0.000

Analysis Conditions ==========

#	Tar get	Filter	Thick. mg/cm2	kV	uA	---Detector--- Type	Filter	Thick. mg/cm2	Atm	Preset Time(s)	Actual Time(s)
1	Rh	None	0.00	20.0	20.0	SDD	None	0.00	Air	60.0	30.0

Processing Conditions ==========

#	No.	Escape	Sum	Back	C/R	Blank	----Blank----

Calcination XRF Results for 650^{0}C, 60 minutes

CrossRoads Scientific XRS-FP Analysis Report

File: C:\Users\Xenemetrix\Music\New folder\New folder (2)\C6.str

8:17:07 PM 12-

Comment line

Layer Table ==========

#	Thick	Type	Error	Units	Density	Norm.	Total
1	0.00	Bulk	0.00	mg/cm2	0.00F	On	100.00

Sample Table ==========

Layer	Component	Type	Concn.	Error	Units	Mole%	Error
1	SiO2	Calc	9.066	0.672	wt.%	12.828	0.951
1	V2O5	Calc	0.883	0.077	wt.%	0.413	0.036
1	Cr2O3	Calc	0.000	0.000	wt.%	0.000	0.000
1	MnO	Calc	0.932	0.034	wt.%	1.116	0.040
1	Fe2O3	Calc	18.059	0.139	wt.%	9.614	0.074
1	Co3O4	Calc	0.093	0.042	wt.%	0.033	0.015
1	NiO	Calc	0.000	0.000	wt.%	0.000	0.000
1	CuO	Calc	0.021	0.009	wt.%	0.023	0.010
1	Nb2O3	Calc	0.357	0.353	wt.%	0.130	0.128
1	MoO3	Calc	0.000	0.000	wt.%	0.000	0.000
1	WO3	Calc	0.211	0.051	wt.%	0.077	0.019
1	P2O5	Calc	0.000	0.000	wt.%	0.000	0.000
1	SO3	Calc	0.217	0.064	wt.%	0.231	0.068
1	CaO	Calc	1.255	0.047	wt.%	1.903	0.071
1	MgO	Calc	1.261	6.504	wt.%	2.659	13.720
1	K2O	Calc	0.087	0.026	wt.%	0.078	0.024
1	BaO	Calc	0.590	0.654	wt.%	0.327	0.363
1	Al2O3	Calc	4.626	1.672	wt.%	3.857	1.395
1	Ta2O5	Calc	0.186	0.041	wt.%	0.036	0.008
1	TiO2	Calc	61.507	0.265	wt.%	65.475	0.282
1	ZnO	Calc	0.059	0.010	wt.%	0.062	0.010
1	Ag2O	Calc	0.000	0.000	wt.%	0.000	0.000
1	Cl	Calc	0.444	0.036	wt.%	1.066	0.087
1	ZrO2	Calc	0.049	0.082	wt.%	0.034	0.057

Element Table ==========

Elmt	Line Code	Cond Code	Ratio Method	Intensity (c/s)	Error (c/s)	Intensity Method	Conc.	Conc Method	Calibration Coefficient
O	Ka	0	None	0.000	0.0000	Gaussian	38.940	None	0.000
Mg	Ka	1	None	0.192	0.9928	Gaussian	0.760	FP	0.000
Al	Ka	1	None	7.363	2.6624	Gaussian	2.448	FP	0.000
Si	Ka	1	None	73.244	5.4321	Gaussian	4.238	FP	0.000
P	Ka	1	None	0.000	2.7162	Gaussian	0.000	FP	0.000
S	Ka	1	None	9.726	2.8657	Gaussian	0.087	FP	0.000
Cl	Ka	1	None	68.166	5.5502	Gaussian	0.444	FP	0.000
K	Ka	1	None	16.904	5.1221	Gaussian	0.072	FP	0.000
Ca	Ka	1	None	302.999	11.3517	Gaussian	0.897	FP	0.000
Ti	Ka	1	None	16681.990	71.9188	Gaussian	36.874	FP	0.000
V	Ka	1	None	290.343	25.4529	Gaussian	0.494	FP	0.000
Cr	Ka	1	None	0.000	4.5908	Gaussian	0.000	FP	0.000
Mn	Ka	1	None	259.863	9.3865	Gaussian	0.721	FP	0.000
Fe	Ka	1	None	5242.792	40.2797	Gaussian	12.631	FP	0.000
Co	Ka	1	None	31.477	14.3806	Gaussian	0.068	FP	0.000
Ni	Ka	1	None	0.000	5.2273	Gaussian	0.000	FP	0.000
Cu	Ka	1	None	7.154	3.1683	Gaussian	0.017	FP	0.000
Zn	Ka	1	None	21.578	3.5197	Gaussian	0.047	FP	0.000
Zr	Ka	1	None	1.195	1.9932	Gaussian	0.037	FP	0.000
Nb	Ka	1	None	1.908	1.8894	Gaussian	0.284	FP	0.000
Mo	Ka	1	None	0.340	1.4114	Gaussian	0.000	FP	0.000
Ag	Ka	1	None	0.000	0.0000	Gaussian	0.000	FP	0.000
Sn	Ka	1	None	0.000	0.0000	Gaussian	0.000	FP	0.000
Ba	La	1	None	60.190	66.7296	Gaussian	0.528	FP	0.000
Ta	La	1	None	16.094	3.5844	Gaussian	0.152	FP	0.000
W	La	1	None	18.010	4.3217	Gaussian	0.167	FP	0.000
Pb	La	1	None	9.601	2.7048	Gaussian	0.091	FP	0.000

Analysis Conditions ==========

#	Tar Filter get		Thick. mg/cm2	kV	uA	---Detector--- Type	Filter	Thick. mg/cm2	Atm	Preset Time(s)	Actual Time(s)
1	Rh	None	0.00	20.0	20.0	SDD	None	0.00	Air	60.0	30.0

Processing Conditions ==========

#	No	Escape	Sum	Back	C/B	Blank	----Blank----

Calcination XRF Results for 1000^0C, 30 minutes

CrossRoads Scientific XRS-FP Analysis Report

File: C:\Users\Xenemetrix\Music\New folder\New folder (2)\C7.str

8:18:20 PM

Comment line

Layer Table ==========

#	Thick	Type	Error	Units	Density	Norm.	Total
1	0.00	Bulk	0.00	mg/cm2	0.00F	On	100.00

Sample Table ==========

Layer	Component	Type	Concn.	Error	Units	Mole%	Error
1	SiO2	Calc	8.908	0.681	wt.%	12.648	0.967
1	V2O5	Calc	0.961	0.082	wt.%	0.451	0.039
1	Cr2O3	Calc	0.000	0.000	wt.%	0.000	0.000
1	MnO	Calc	1.027	0.037	wt.%	1.235	0.044
1	Fe2O3	Calc	16.300	0.138	wt.%	8.708	0.074
1	Co3O4	Calc	0.066	0.042	wt.%	0.024	0.015
1	NiO	Calc	0.000	0.000	wt.%	0.000	0.000
1	CuO	Calc	0.013	0.010	wt.%	0.014	0.010
1	Nb2O3	Calc	0.271	0.380	wt.%	0.099	0.139
1	MoO3	Calc	0.000	0.000	wt.%	0.000	0.000
1	WO3	Calc	0.296	0.055	wt.%	0.109	0.020
1	P2O5	Calc	0.000	0.000	wt.%	0.000	0.000
1	SO3	Calc	0.000	0.000	wt.%	0.000	0.000
1	CaO	Calc	0.913	0.042	wt.%	1.388	0.063
1	MgO	Calc	0.400	6.049	wt.%	0.847	12.804
1	K2O	Calc	0.068	0.026	wt.%	0.061	0.023
1	BaO	Calc	0.612	0.693	wt.%	0.341	0.386
1	Al2O3	Calc	4.408	1.703	wt.%	3.689	1.425
1	Ta2O5	Calc	0.133	0.043	wt.%	0.026	0.008
1	TiO2	Calc	65.127	0.282	wt.%	69.569	0.301
1	ZnO	Calc	0.076	0.011	wt.%	0.079	0.012
1	Ag2O	Calc	0.000	0.000	wt.%	0.000	0.000
1	Cl	Calc	0.268	0.032	wt.%	0.645	0.078
1	ZrO2	Calc	0.029	0.088	wt.%	0.020	0.061
1	SnO2	Calc	0.000	0.000	wt.%	0.000	0.000

Element Table ==========

Elmt	Line Code	Cond Code	Ratio Method	Intensity (c/s)	Error (c/s)	Intensity Method	Conc.	Conc Method	Calibration Coefficient
O	Ka	0	None	0.000	0.0000	Gaussian	39.142	None	0.000
Mg	Ka	1	None	0.057	0.8634	Gaussian	0.241	FP	0.000
Al	Ka	1	None	6.624	2.5584	Gaussian	2.333	FP	0.000
Si	Ka	1	None	68.044	5.1997	Gaussian	4.164	FP	0.000
P	Ka	1	None	0.000	2.7309	Gaussian	0.000	FP	0.000
S	Ka	1	None	0.000	3.7166	Gaussian	0.000	FP	0.000
Cl	Ka	1	None	39.064	4.7394	Gaussian	0.268	FP	0.000
K	Ka	1	None	12.578	4.8043	Gaussian	0.056	FP	0.000
Ca	Ka	1	None	210.541	9.6269	Gaussian	0.652	FP	0.000
Ti	Ka	1	None	16562.770	71.6587	Gaussian	39.045	FP	0.000
V	Ka	1	None	296.339	25.3362	Gaussian	0.538	FP	0.000
Cr	Ka	1	None	0.000	4.5627	Gaussian	0.000	FP	0.000
Mn	Ka	1	None	260.273	9.3581	Gaussian	0.795	FP	0.000
Fe	Ka	1	None	4317.519	36.5382	Gaussian	11.401	FP	0.000
Co	Ka	1	None	20.477	13.0769	Gaussian	0.049	FP	0.000
Ni	Ka	1	None	0.000	4.8295	Gaussian	0.000	FP	0.000
Cu	Ka	1	None	4.119	3.0445	Gaussian	0.011	FP	0.000
Zn	Ka	1	None	25.941	3.8112	Gaussian	0.061	FP	0.000
Zr	Ka	1	None	0.660	1.9909	Gaussian	0.022	FP	0.000
Nb	Ka	1	None	1.353	1.8957	Gaussian	0.216	FP	0.000
Mo	Ka	1	None	1.036	1.5247	Gaussian	0.000	FP	0.000
Ag	Ka	1	None	0.000	0.0000	Gaussian	0.000	FP	0.000
Sn	Ka	1	None	0.000	0.0000	Gaussian	0.000	FP	0.000
Ba	La	1	None	58.721	66.4880	Gaussian	0.548	FP	0.000
Ta	La	1	None	10.756	3.5117	Gaussian	0.109	FP	0.000
W	La	1	None	23.658	4.4281	Gaussian	0.235	FP	0.000
Pb	La	1	None	11.289	2.6987	Gaussian	0.115	FP	0.000

Analysis Conditions ==========

#	Tar get	Filter	Thick. mg/cm2	kV	uA	---Detector--- Type	Filter	Thick. mg/cm2	Atm	Preset Time(s)	Actual Time(s)
1	Rh	None	0.00	20.0	20.0	SDD	None	0.00	Air	60.0	30.0

Processing Conditions ==========

#	No. Smths	Escape Peaks	Sum Peaks	Back Type	C/R Ratio	Blank Rem.	----Blank---- ----File-----

Calcination XRF Results for 1000^0C, 45 minutes

CrossRoads Scientific XRS-FP Analysis Report

File: C:\Users\Xenemetrix\Music\New folder\New folder (2)\C8.str

8:19:42 PM 12

Comment line

Layer Table ==========

#	Thick	Type	Error	Units	Density	Norm.	Total
1	0.00	Bulk	0.00	mg/cm2	0.00F	On	100.00

Sample Table ==========

Layer	Component	Type	Concn.	Error	Units	Mole%	Error
1	SiO2	Calc	9.452	0.736	wt.%	14.408	1.122
1	V2O5	Calc	0.854	0.070	wt.%	0.430	0.035
1	Cr2O3	Calc	0.000	0.000	wt.%	0.000	0.000
1	MnO	Calc	0.908	0.034	wt.%	1.173	0.044
1	Fe2O3	Calc	32.587	0.187	wt.%	18.691	0.107
1	Co3O4	Calc	0.119	0.057	wt.%	0.045	0.022
1	NiO	Calc	0.000	0.000	wt.%	0.000	0.000
1	CuO	Calc	0.012	0.011	wt.%	0.014	0.013
1	Nb2O3	Calc	0.092	0.366	wt.%	0.036	0.143
1	MoO3	Calc	0.000	0.000	wt.%	0.000	0.000
1	WO3	Calc	0.190	0.055	wt.%	0.075	0.022
1	P2O5	Calc	0.000	0.000	wt.%	0.000	0.000
1	SO3	Calc	0.094	0.066	wt.%	0.108	0.075
1	CaO	Calc	0.898	0.043	wt.%	1.467	0.071
1	MgO	Calc	1.637	7.079	wt.%	3.719	16.087
1	K2O	Calc	0.182	0.033	wt.%	0.177	0.032
1	BaO	Calc	0.641	0.589	wt.%	0.383	0.352
1	Al2O3	Calc	4.700	1.855	wt.%	4.222	1.666
1	Ta2O5	Calc	0.143	0.047	wt.%	0.030	0.010
1	TiO2	Calc	46.698	0.236	wt.%	53.554	0.271
1	ZnO	Calc	0.051	0.011	wt.%	0.057	0.012
1	Ag2O	Calc	0.000	0.000	wt.%	0.000	0.000
1	Cl	Calc	0.505	0.042	wt.%	1.304	0.108
1	ZrO2	Calc	0.033	0.095	wt.%	0.025	0.071

Element Table ==========

Elmt	Line Code	Cond Code	Ratio Method	Intensity (c/s)	Error (c/s)	Intensity Method	Conc.	Conc Method	Calibration Coefficient
O	Ka	0	None	0.000	0.0000	Gaussian	37.535	None	0.000
Mg	Ka	1	None	0.214	0.9248	Gaussian	0.987	FP	0.000
Al	Ka	1	None	6.373	2.5150	Gaussian	2.488	FP	0.000
Si	Ka	1	None	65.323	5.0875	Gaussian	4.418	FP	0.000
P	Ka	1	None	0.000	2.6717	Gaussian	0.000	FP	0.000
S	Ka	1	None	3.622	2.5216	Gaussian	0.038	FP	0.000
Cl	Ka	1	None	66.943	5.5627	Gaussian	0.505	FP	0.000
K	Ka	1	None	30.886	5.5907	Gaussian	0.151	FP	0.000
Ca	Ka	1	None	189.109	9.1528	Gaussian	0.642	FP	0.000
Ti	Ka	1	None	12110.130	61.2679	Gaussian	27.996	FP	0.000
V	Ka	1	None	267.877	21.8240	Gaussian	0.479	FP	0.000
Cr	Ka	1	None	0.000	4.9477	Gaussian	0.000	FP	0.000
Mn	Ka	1	None	260.962	9.6983	Gaussian	0.703	FP	0.000
Fe	Ka	1	None	9422.612	54.0523	Gaussian	22.793	FP	0.000
Co	Ka	1	None	40.179	19.1900	Gaussian	0.088	FP	0.000
Ni	Ka	1	None	0.000	6.7482	Gaussian	0.000	FP	0.000
Cu	Ka	1	None	3.321	3.0751	Gaussian	0.010	FP	0.000
Zn	Ka	1	None	15.470	3.2918	Gaussian	0.041	FP	0.000
Zr	Ka	1	None	0.669	1.9161	Gaussian	0.025	FP	0.000
Nb	Ka	1	None	0.409	1.6307	Gaussian	0.073	FP	0.000
Mo	Ka	1	None	0.526	1.3659	Gaussian	0.000	FP	0.000
Ag	Ka	1	None	0.000	0.1633	Gaussian	0.000	FP	0.000
Sn	Ka	1	None	0.000	0.0000	Gaussian	0.000	FP	0.000
Ba	La	1	None	61.926	56.8665	Gaussian	0.574	FP	0.000
Ta	La	1	None	10.317	3.4121	Gaussian	0.117	FP	0.000
W	La	1	None	13.536	3.9351	Gaussian	0.151	FP	0.000
Pb	La	1	None	16.420	2.8555	Gaussian	0.187	FP	0.000

Analysis Conditions ==========

#	Tar get	Filter	Thick. mg/cm2	kV	uA	---Detector--- Type	Filter	Thick. mg/cm2	Atm	Preset Time(s)	Actual Time(s)
1	Rh	None	0.00	20.0	30.0	SDD	None	0.00	Air	60.0	30.0

Processing Conditions ==========

#	No.	Escape	Sum	Back	C/R	Blank	----Blank----

Calcination XRF Results for 1000^0C, 60 minutes

CrossRoads Scientific XRS-FP Analysis Report

File: C:\Users\Xenemetrix\Music\New folder\New folder (2)\C9.str

8:20:59 PM 12-

Comment line

Layer Table ==

#	Thick	Type	Error	Units	Density	Norm.	Total
1	0.00	Bulk	0.00	mg/cm2	0.00F	On	100.00

Sample Table ==

Layer	Component	Type	Concn.	Error	Units	Mole%	Error
1	SiO2	Calc	7.863	0.635	wt.%	11.276	0.911
1	V2O5	Calc	1.133	0.077	wt.%	0.537	0.037
1	Cr2O3	Calc	0.000	0.000	wt.%	0.000	0.000
1	MnO	Calc	0.830	0.032	wt.%	1.009	0.039
1	Fe2O3	Calc	21.193	0.153	wt.%	11.434	0.082
1	Co3O4	Calc	0.093	0.047	wt.%	0.033	0.017
1	NiO	Calc	0.000	0.000	wt.%	0.000	0.000
1	CuO	Calc	0.019	0.010	wt.%	0.020	0.011
1	Nb2O3	Calc	0.423	0.374	wt.%	0.156	0.138
1	MoO3	Calc	0.000	0.000	wt.%	0.000	0.000
1	WO3	Calc	0.229	0.055	wt.%	0.085	0.020
1	P2O5	Calc	0.000	0.000	wt.%	0.000	0.000
1	SO3	Calc	0.108	0.055	wt.%	0.116	0.060
1	CaO	Calc	1.167	0.047	wt.%	1.793	0.072
1	MgO	Calc	2.246	6.611	wt.%	4.800	14.132
1	K2O	Calc	0.113	0.028	wt.%	0.103	0.025
1	BaO	Calc	0.625	0.652	wt.%	0.351	0.367
1	Al2O3	Calc	3.888	1.627	wt.%	3.285	1.375
1	Ta2O5	Calc	0.172	0.044	wt.%	0.034	0.009
1	TiO2	Calc	59.309	0.264	wt.%	63.981	0.285
1	ZnO	Calc	0.074	0.011	wt.%	0.079	0.012
1	Ag2O	Calc	0.000	0.000	wt.%	0.000	0.000
1	Cl	Calc	0.343	0.033	wt.%	0.834	0.081
1	ZrO2	Calc	0.025	0.086	wt.%	0.018	0.060

Element Table ==

Elmt	Line Code	Cond Code	Ratio Method	Intensity (c/s)	Error (c/s)	Intensity Method	Conc.	Conc Method	Calibration Coefficient
O	Ka	0	None	0.000	0.0000	Gaussian	38.425	None	0.000
Mg	Ka	1	None	0.325	0.9563	Gaussian	1.354	FP	0.000
Al	Ka	1	None	5.812	2.4316	Gaussian	2.058	FP	0.000
Si	Ka	1	None	60.225	4.8656	Gaussian	3.676	FP	0.000
P	Ka	1	None	0.000	2.5716	Gaussian	0.000	FP	0.000
S	Ka	1	None	4.643	2.3789	Gaussian	0.043	FP	0.000
Cl	Ka	1	None	50.522	4.8988	Gaussian	0.343	FP	0.000
K	Ka	1	None	21.150	5.1719	Gaussian	0.094	FP	0.000
Ca	Ka	1	None	270.701	10.8089	Gaussian	0.834	FP	0.000
Ti	Ka	1	None	15640.520	69.6311	Gaussian	35.557	FP	0.000
V	Ka	1	None	361.940	24.6061	Gaussian	0.635	FP	0.000
Cr	Ka	1	None	0.000	4.9459	Gaussian	0.000	FP	0.000
Mn	Ka	1	None	226.406	8.8549	Gaussian	0.643	FP	0.000
Fe	Ka	1	None	5975.268	43.0261	Gaussian	14.823	FP	0.000
Co	Ka	1	None	30.667	15.3307	Gaussian	0.068	FP	0.000
Ni	Ka	1	None	0.000	5.5136	Gaussian	0.000	FP	0.000
Cu	Ka	1	None	5.876	3.1442	Gaussian	0.015	FP	0.000
Zn	Ka	1	None	25.536	3.7381	Gaussian	0.060	FP	0.000
Zr	Ka	1	None	0.571	1.9404	Gaussian	0.019	FP	0.000
Nb	Ka	1	None	2.111	1.8706	Gaussian	0.336	FP	0.000
Mo	Ka	1	None	0.109	1.4193	Gaussian	0.000	FP	0.000
Ag	Ka	1	None	0.000	0.0000	Gaussian	0.000	FP	0.000
Sn	Ka	1	None	0.000	0.0000	Gaussian	0.000	FP	0.000
Ba	La	1	None	61.942	64.6121	Gaussian	0.560	FP	0.000
Ta	La	1	None	13.984	3.5724	Gaussian	0.141	FP	0.000
W	La	1	None	18.341	4.4173	Gaussian	0.181	FP	0.000
Pb	La	1	None	13.300	2.7415	Gaussian	0.135	FP	0.000

Analysis Conditions ==

#	Tar get	Filter	Thick. mg/cm2	kV	uA	---Detector--- Type	Filter	Thick. mg/cm2	Atm	Preset Time(s)	Actual Time(s)
1	Rh	None	0.00	20.0	20.0	SDD	None	0.00	Air	60.0	30.0

Processing Conditions ==============================

#	No.	Escape	Sum	Back	C/R	Blank	----Blank----

APPENDIX G
Roasting XRF Results for 300^{0}C, 30 minutes

CrossRoads Scientific XRS-FP Analysis Report

File: C:\Users\Xenemetrix\Music\New folder\R1.str

11:25:15 AM

Comment line

Layer Table ==========

#	Thick	Type	Error	Units	Density	Norm.	Total
1	0.00	Bulk	0.00	mg/cm2	0.00F	On	100.00

Sample Table ==========

Layer	Component	Type	Concn.	Error	Units	Mole%	Error
1	SiO2	Calc	5.788	0.555	wt.%	8.467	0.811
1	V2O5	Calc	0.873	0.080	wt.%	0.422	0.039
1	Cr2O3	Calc	0.000	0.000	wt.%	0.000	0.000
1	MnO	Calc	1.175	0.038	wt.%	1.456	0.047
1	Fe2O3	Calc	20.191	0.150	wt.%	11.113	0.083
1	Co3O4	Calc	0.135	0.046	wt.%	0.049	0.017
1	NiO	Calc	0.000	0.000	wt.%	0.000	0.000
1	CuO	Calc	0.039	0.010	wt.%	0.043	0.011
1	Nb2O3	Calc	0.135	0.361	wt.%	0.051	0.136
1	MoO3	Calc	0.000	0.000	wt.%	0.000	0.000
1	WO3	Calc	0.287	0.056	wt.%	0.109	0.021
1	P2O5	Calc	0.000	0.000	wt.%	0.000	0.000
1	SO3	Calc	0.081	0.054	wt.%	0.089	0.059
1	CaO	Calc	0.728	0.038	wt.%	1.142	0.059
1	MgO	Calc	0.937	6.465	wt.%	2.044	14.098
1	K2O	Calc	0.044	0.031	wt.%	0.041	0.029
1	BaO	Calc	0.688	0.674	wt.%	0.394	0.386
1	Al2O3	Calc	4.058	1.515	wt.%	3.498	1.306
1	Ta2O5	Calc	0.145	0.044	wt.%	0.029	0.009
1	TiO2	Calc	63.271	0.273	wt.%	69.631	0.301
1	ZnO	Calc	0.070	0.011	wt.%	0.075	0.012
1	Ag2O	Calc	0.000	0.000	wt.%	0.000	0.000
1	Cl	Calc	0.305	0.031	wt.%	0.757	0.077
1	ZrO2	Calc	0.011	0.085	wt.%	0.008	0.061
1	SnO2	Calc	0.916	0.145	wt.%	0.534	0.085

Element Table ==========

Elmt	Line Code	Cond Code	Ratio Method	Intensity (c/s)	Error (c/s)	Intensity Method	Conc.	Conc Method	Calibration Coefficient
O	Ka	0	None	0.000	0.0000	Gaussian	38.134	None	0.000
Mg	Ka	1	None	0.137	0.9430	Gaussian	0.565	FP	0.000
Al	Ka	1	None	6.199	2.3151	Gaussian	2.148	FP	0.000
Si	Ka	1	None	45.244	4.3355	Gaussian	2.706	FP	0.000
P	Ka	1	None	0.000	2.4386	Gaussian	0.000	FP	0.000
S	Ka	1	None	3.615	2.4041	Gaussian	0.032	FP	0.000
Cl	Ka	1	None	47.064	4.8046	Gaussian	0.305	FP	0.000
K	Ka	1	None	8.580	6.0858	Gaussian	0.037	FP	0.000
Ca	Ka	1	None	175.653	9.1291	Gaussian	0.521	FP	0.000
Ti	Ka	1	None	16621.300	71.7871	Gaussian	37.932	FP	0.000
V	Ka	1	None	277.608	25.5033	Gaussian	0.489	FP	0.000
Cr	Ka	1	None	0.000	4.7647	Gaussian	0.000	FP	0.000
Mn	Ka	1	None	314.086	10.2460	Gaussian	0.910	FP	0.000
Fe	Ka	1	None	5597.331	41.5901	Gaussian	14.122	FP	0.000
Co	Ka	1	None	43.401	14.8120	Gaussian	0.099	FP	0.000
Ni	Ka	1	None	0.000	5.2814	Gaussian	0.000	FP	0.000
Cu	Ka	1	None	12.156	3.1146	Gaussian	0.031	FP	0.000
Zn	Ka	1	None	23.892	3.7254	Gaussian	0.056	FP	0.000
Zr	Ka	1	None	0.259	1.9296	Gaussian	0.008	FP	0.000
Nb	Ka	1	None	0.677	1.8090	Gaussian	0.107	FP	0.000
Mo	Ka	1	None	1.014	1.4643	Gaussian	0.000	FP	0.000
Ag	Ka	1	None	0.000	0.0000	Gaussian	0.000	FP	0.000
Sn	La	1	None	50.821	8.0511	Gaussian	0.721	FP	0.000
Ba	La	1	None	67.973	66.6193	Gaussian	0.616	FP	0.000
Ta	La	1	None	11.718	3.5374	Gaussian	0.119	FP	0.000
W	La	1	None	22.968	4.4885	Gaussian	0.228	FP	0.000
Pb	La	1	None	11.285	2.6904	Gaussian	0.115	FP	0.000

Analysis Conditions ==========

#	Tar get	Filter	Thick. mg/cm2	kV	uA	---Detector--- Type	Filter	Thick. mg/cm2	Atm	Preset Time(s)	Actual Time(s)
1	Rh	None	0.00	20.0	20.0	SDD	None	0.00	Air	60.0	30.0

Processing Conditions ==========

#	No.	Escape	Sum	Back	C/R	Blank	----Blank----

Roasting XRF Results for 300^0C, 45 minutes

CrossRoads Scientific XRS-FP Analysis Report

File: C:\Users\Xenemetrix\Music\New folder\New folder\R2.str

4:36:09 PM 12-

Comment line

Layer Table ==

#	Thick	Type	Error	Units	Density	Norm.	Total
1	0.00	Bulk	0.00	mg/cm2	0.00F	On	100.00

Sample Table ==

Layer	Component	Type	Concn.	Error	Units	Mole%	Error
1	SiO2	Calc	7.289	0.613	wt.%	10.428	0.877
1	V2O5	Calc	0.739	0.081	wt.%	0.349	0.038
1	Cr2O3	Calc	0.000	0.000	wt.%	0.000	0.000
1	MnO	Calc	1.272	0.040	wt.%	1.541	0.049
1	Fe2O3	Calc	18.234	0.144	wt.%	9.815	0.077
1	Co3O4	Calc	0.107	0.044	wt.%	0.038	0.016
1	NiO	Calc	0.000	0.000	wt.%	0.000	0.000
1	CuO	Calc	0.010	0.009	wt.%	0.011	0.010
1	Nb2O3	Calc	0.423	0.360	wt.%	0.155	0.132
1	MoO3	Calc	0.000	0.000	wt.%	0.000	0.000
1	WO3	Calc	0.232	0.051	wt.%	0.086	0.019
1	P2O5	Calc	0.000	0.000	wt.%	0.000	0.000
1	SO3	Calc	0.061	0.053	wt.%	0.066	0.056
1	CaO	Calc	0.644	0.035	wt.%	0.988	0.054
1	MgO	Calc	1.192	6.278	wt.%	2.543	13.389
1	K2O	Calc	0.090	0.025	wt.%	0.082	0.023
1	BaO	Calc	0.606	0.680	wt.%	0.340	0.381
1	Al2O3	Calc	3.649	1.567	wt.%	3.076	1.321
1	Ta2O5	Calc	0.159	0.042	wt.%	0.031	0.008
1	TiO2	Calc	64.801	0.276	wt.%	69.744	0.298
1	ZnO	Calc	0.052	0.010	wt.%	0.055	0.010
1	Ag2O	Calc	0.000	0.000	wt.%	0.000	0.000
1	Cl	Calc	0.230	0.028	wt.%	0.558	0.068
1	ZrO2	Calc	0.041	0.086	wt.%	0.028	0.060

Element Table ==

Elmt	Line Code	Cond Code	Ratio Method	Intensity (c/s)	Error (c/s)	Intensity Method	Conc.	Conc Method	Calibration Coefficient
O	Ka	0	None	0.000	0.0000	Gaussian	38.643	None	0.000
Mg	Ka	1	None	0.172	0.9072	Gaussian	0.719	FP	0.000
Al	Ka	1	None	5.511	2.3658	Gaussian	1.931	FP	0.000
Si	Ka	1	None	56.495	4.7539	Gaussian	3.407	FP	0.000
P	Ka	1	None	0.000	2.6128	Gaussian	0.000	FP	0.000
S	Ka	1	None	2.681	2.2944	Gaussian	0.025	FP	0.000
Cl	Ka	1	None	34.450	4.1759	Gaussian	0.230	FP	0.000
K	Ka	1	None	17.249	4.8412	Gaussian	0.075	FP	0.000
Ca	Ka	1	None	152.620	8.2851	Gaussian	0.461	FP	0.000
Ti	Ka	1	None	17030.380	72.6655	Gaussian	38.849	FP	0.000
V	Ka	1	None	235.403	25.7698	Gaussian	0.414	FP	0.000
Cr	Ka	1	None	0.000	4.3696	Gaussian	0.000	FP	0.000
Mn	Ka	1	None	332.126	10.4609	Gaussian	0.985	FP	0.000
Fe	Ka	1	None	4955.679	39.1101	Gaussian	12.753	FP	0.000
Co	Ka	1	None	33.774	13.9506	Gaussian	0.079	FP	0.000
Ni	Ka	1	None	0.000	4.9737	Gaussian	0.000	FP	0.000
Cu	Ka	1	None	3.080	2.9638	Gaussian	0.008	FP	0.000
Zn	Ka	1	None	17.681	3.3694	Gaussian	0.041	FP	0.000
Zr	Ka	1	None	0.916	1.9408	Gaussian	0.030	FP	0.000
Nb	Ka	1	None	2.104	1.7902	Gaussian	0.336	FP	0.000
Mo	Ka	1	None	0.017	1.3929	Gaussian	0.000	FP	0.000
Ag	Ka	1	None	0.000	0.0000	Gaussian	0.000	FP	0.000
Sn	Ka	1	None	0.000	0.0000	Gaussian	0.000	FP	0.000
Ba	La	1	None	60.036	67.4206	Gaussian	0.543	FP	0.000
Ta	La	1	None	12.882	3.4088	Gaussian	0.130	FP	0.000
W	La	1	None	18.543	4.0564	Gaussian	0.184	FP	0.000
Pb	La	1	None	15.361	2.7863	Gaussian	0.156	FP	0.000

Analysis Conditions ==

#	Tar Filter get	Thick. mg/cm2	kV	uA	---Detector--- Type	Filter	Thick. mg/cm2	Atm	Preset Time(s)	Actual Time(s)
1	Rh None	0.00	20.0	20.0	SDD	None	0.00	Air	60.0	30.0

Processing Conditions ============================

#	No.	Escape	Sum	Back	C/R	Blank	----Blank----

Roasting XRF Results for 300^0C, 60 minutes

CrossRoads Scientific XRS-FP Analysis Report

File: C:\Users\Xenemetrix\Music\New folder\New folder\R3.str

4:37:38 PM 12·

Comment line

Layer Table ==========

#	Thick	Type	Error	Units	Density	Norm.	Total
1	0.00	Bulk	0.00	mg/cm2	0.00F	On	100.00

Sample Table ==========

Layer	Component	Type	Concn.	Error	Units	Mole%	Error
1	SiO2	Calc	9.312	0.688	wt.%	13.194	0.974
1	V2O5	Calc	0.837	0.083	wt.%	0.392	0.039
1	Cr2O3	Calc	0.000	0.000	wt.%	0.000	0.000
1	MnO	Calc	1.257	0.041	wt.%	1.508	0.049
1	Fe2O3	Calc	15.537	0.135	wt.%	8.283	0.072
1	Co3O4	Calc	0.068	0.042	wt.%	0.024	0.015
1	NiO	Calc	0.002	0.016	wt.%	0.003	0.018
1	CuO	Calc	0.059	0.011	wt.%	0.063	0.012
1	Nb2O3	Calc	0.298	0.387	wt.%	0.108	0.141
1	MoO3	Calc	0.000	0.000	wt.%	0.000	0.000
1	WO3	Calc	0.223	0.056	wt.%	0.082	0.021
1	P2O5	Calc	0.000	0.000	wt.%	0.000	0.000
1	SO3	Calc	0.051	0.054	wt.%	0.055	0.058
1	CaO	Calc	0.517	0.032	wt.%	0.785	0.049
1	MgO	Calc	0.000	0.000	wt.%	0.000	0.000
1	K2O	Calc	0.020	0.026	wt.%	0.018	0.023
1	BaO	Calc	0.664	0.700	wt.%	0.368	0.388
1	Al2O3	Calc	3.921	1.686	wt.%	3.273	1.408
1	Ta2O5	Calc	0.188	0.047	wt.%	0.036	0.009
1	TiO2	Calc	66.522	0.285	wt.%	70.906	0.303
1	ZnO	Calc	0.055	0.010	wt.%	0.057	0.011
1	Ag2O	Calc	0.000	0.000	wt.%	0.000	0.000
1	Cl	Calc	0.323	0.032	wt.%	0.776	0.078
1	ZrO2	Calc	0.037	0.091	wt.%	0.025	0.063

Element Table ==========

Elmt	Line Code	Cond Code	Ratio Method	Intensity (c/s)	Error (c/s)	Intensity Method	Conc.	Conc Method	Calibration Coefficient
O	Ka	0	None	0.000	0.0000	Gaussian	39.218	None	0.000
Mg	Ka	1	None	0.000	0.8743	Gaussian	0.000	FP	0.000
Al	Ka	1	None	5.892	2.5340	Gaussian	2.075	FP	0.000
Si	Ka	1	None	71.412	5.2723	Gaussian	4.353	FP	0.000
P	Ka	1	None	0.000	2.8674	Gaussian	0.000	FP	0.000
S	Ka	1	None	2.171	2.2950	Gaussian	0.021	FP	0.000
Cl	Ka	1	None	47.099	4.7192	Gaussian	0.323	FP	0.000
K	Ka	1	None	3.796	4.7674	Gaussian	0.017	FP	0.000
Ca	Ka	1	None	119.540	7.4786	Gaussian	0.370	FP	0.000
Ti	Ka	1	None	16935.630	72.4548	Gaussian	39.881	FP	0.000
V	Ka	1	None	258.430	25.7089	Gaussian	0.469	FP	0.000
Cr	Ka	1	None	0.000	4.7065	Gaussian	0.000	FP	0.000
Mn	Ka	1	None	314.618	10.2858	Gaussian	0.973	FP	0.000
Fe	Ka	1	None	4069.961	35.4559	Gaussian	10.867	FP	0.000
Co	Ka	1	None	20.681	12.7378	Gaussian	0.050	FP	0.000
Ni	Ka	1	None	0.694	4.7501	Gaussian	0.002	FP	0.000
Cu	Ka	1	None	18.414	3.4296	Gaussian	0.047	FP	0.000
Zn	Ka	1	None	18.576	3.4340	Gaussian	0.044	FP	0.000
Zr	Ka	1	None	0.826	2.0491	Gaussian	0.027	FP	0.000
Nb	Ka	1	None	1.480	1.9211	Gaussian	0.237	FP	0.000
Mo	Ka	1	None	0.610	1.5496	Gaussian	0.000	FP	0.000
Ag	Ka	1	None	0.000	0.0000	Gaussian	0.000	FP	0.000
Sn	Ka	1	None	0.000	0.0000	Gaussian	0.000	FP	0.000
Ba	La	1	None	63.775	67.2285	Gaussian	0.594	FP	0.000
Ta	La	1	None	15.151	3.7621	Gaussian	0.154	FP	0.000
W	La	1	None	17.737	4.4692	Gaussian	0.177	FP	0.000
Pb	La	1	None	9.958	2.8306	Gaussian	0.102	FP	0.000

Analysis Conditions ==========

#	Target	Filter	Thick. mg/cm2	kV	uA	---Detector--- Type	Filter	Thick. mg/cm2	Atm	Preset Time(s)	Actual Time(s)
1	Rh	None	0.00	20.0	20.0	SDD	None	0.00	Air	60.0	30.0

Processing Conditions ==========

#	No.	Escape	Sum	Back	C/R	Blank	----Blank----

Roasting XRF Results for 650^0C, 30 minutes

CrossRoads Scientific XRS-FP Analysis Report

File: C:\Users\Xenemetrix\Music\New folder\New folder\R4.str

4:38:43 PM

Comment line

Layer Table ==========

#	Thick	Type	Error	Units	Density	Norm.	Total
1	0.00	Bulk	0.00	mg/cm2	0.00F	On	100.00

Sample Table ==========

Layer	Component	Type	Concn.	Error	Units	Mole%	Error
1	SiO2	Calc	5.545	0.552	wt.%	8.086	0.805
1	V2O5	Calc	0.806	0.082	wt.%	0.388	0.039
1	Cr2O3	Calc	0.000	0.000	wt.%	0.000	0.000
1	MnO	Calc	1.008	0.036	wt.%	1.245	0.045
1	Fe2O3	Calc	18.374	0.146	wt.%	10.081	0.080
1	Co3O4	Calc	0.128	0.045	wt.%	0.047	0.016
1	NiO	Calc	0.000	0.000	wt.%	0.000	0.000
1	CuO	Calc	0.012	0.010	wt.%	0.013	0.011
1	Nb2O3	Calc	0.223	0.369	wt.%	0.084	0.138
1	MoO3	Calc	0.000	0.000	wt.%	0.000	0.000
1	WO3	Calc	0.235	0.081	wt.%	0.089	0.031
1	P2O5	Calc	0.000	0.000	wt.%	0.000	0.000
1	SO3	Calc	1.526	0.119	wt.%	1.670	0.131
1	CaO	Calc	0.628	0.035	wt.%	0.981	0.054
1	MgO	Calc	0.000	0.000	wt.%	0.000	0.000
1	K2O	Calc	0.000	0.000	wt.%	0.000	0.000
1	BaO	Calc	0.629	0.687	wt.%	0.359	0.393
1	Al2O3	Calc	4.171	1.503	wt.%	3.584	1.292
1	Ta2O5	Calc	0.191	0.046	wt.%	0.038	0.009
1	TiO2	Calc	65.756	0.280	wt.%	72.135	0.307
1	ZnO	Calc	0.343	0.019	wt.%	0.369	0.020
1	Ag2O	Calc	0.000	0.000	wt.%	0.000	0.000
1	Cl	Calc	0.319	0.034	wt.%	0.788	0.083
1	ZrO2	Calc	0.007	0.084	wt.%	0.005	0.060

Element Table ==========

Elmt	Line Code	Cond Code	Ratio Method	Intensity (c/s)	Error (c/s)	Intensity Method	Conc.	Conc Method	Calibration Coefficient
O	Ka	0	None	0.000	0.0000	Gaussian	38.756	None	0.000
Mg	Ka	1	None	0.000	0.8327	Gaussian	0.000	FP	0.000
Al	Ka	1	None	6.267	2.2588	Gaussian	2.207	FP	0.000
Si	Ka	1	None	42.565	4.2390	Gaussian	2.592	FP	0.000
P	Ka	1	None	0.000	2.6800	Gaussian	0.000	FP	0.000
S	Ka	1	None	66.951	5.2419	Gaussian	0.611	FP	0.000
Cl	Ka	1	None	47.552	5.0114	Gaussian	0.319	FP	0.000
K	Ka	1	None	0.000	5.5160	Gaussian	0.000	FP	0.000
Ca	Ka	1	None	148.525	8.1861	Gaussian	0.449	FP	0.000
Ti	Ka	1	None	17149.790	72.9074	Gaussian	39.422	FP	0.000
V	Ka	1	None	254.411	25.8241	Gaussian	0.451	FP	0.000
Cr	Ka	1	None	0.000	4.4000	Gaussian	0.000	FP	0.000
Mn	Ka	1	None	258.877	9.3162	Gaussian	0.781	FP	0.000
Fe	Ka	1	None	4911.485	38.9719	Gaussian	12.851	FP	0.000
Co	Ka	1	None	39.917	13.9200	Gaussian	0.094	FP	0.000
Ni	Ka	1	None	0.000	5.0623	Gaussian	0.000	FP	0.000
Cu	Ka	1	None	3.572	3.1192	Gaussian	0.009	FP	0.000
Zn	Ka	1	None	115.604	6.4014	Gaussian	0.276	FP	0.000
Zr	Ka	1	None	0.146	1.8695	Gaussian	0.005	FP	0.000
Nb	Ka	1	None	1.095	1.8121	Gaussian	0.177	FP	0.000
Mo	Ka	1	None	1.696	1.5985	Gaussian	0.000	FP	0.000
Ag	Ka	1	None	0.000	0.0000	Gaussian	0.000	FP	0.000
Sn	Ka	1	None	0.000	0.0000	Gaussian	0.000	FP	0.000
Ba	La	1	None	61.878	67.6462	Gaussian	0.563	FP	0.000
Ta	La	1	None	15.196	3.6307	Gaussian	0.156	FP	0.000
W	La	1	None	18.508	6.3712	Gaussian	0.186	FP	0.000
Pb	La	1	None	8.996	2.5367	Gaussian	0.093	FP	0.000

Analysis Conditions ==========

#	Target	Filter	Thick. mg/cm2	kV	uA	---Detector--- Type	Filter	Thick. mg/cm2	Atm	Preset Time(s)	Actual Time(s)
1	Rh	None	0.00	20.0	20.0	SDD	None	0.00	Air	60.0	30.0

Roasting XRF Results for 650^0C, 45 minutes

CrossRoads Scientific XRS-FP Analysis Report

File: C:\Users\Xenemetrix\Music\New folder\New folder\R5.str

4:39:55 PM 12

Comment line

Layer Table ==========

#	Thick	Type	Error	Units	Density	Norm.	Total
1	0.00	Bulk	0.00	mg/cm2	0.00F	On	100.00

Sample Table ==========

Layer	Component	Type	Concn.	Error	Units	Mole%	Error
1	SiO2	Calc	5.588	0.555	wt.%	8.153	0.809
1	V2O5	Calc	0.903	0.083	wt.%	0.435	0.040
1	Cr2O3	Calc	0.000	0.000	wt.%	0.000	0.000
1	MnO	Calc	0.970	0.036	wt.%	1.199	0.045
1	Fe2O3	Calc	18.945	0.151	wt.%	10.400	0.083
1	Co3O4	Calc	0.093	0.046	wt.%	0.034	0.017
1	NiO	Calc	0.000	0.000	wt.%	0.000	0.000
1	CuO	Calc	0.017	0.011	wt.%	0.019	0.012
1	Nb2O3	Calc	0.087	0.375	wt.%	0.032	0.140
1	MoO3	Calc	0.000	0.000	wt.%	0.000	0.000
1	WO3	Calc	0.355	0.062	wt.%	0.134	0.024
1	P2O5	Calc	0.000	0.000	wt.%	0.000	0.000
1	SO3	Calc	0.341	0.072	wt.%	0.373	0.079
1	CaO	Calc	0.831	0.040	wt.%	1.299	0.062
1	MgO	Calc	0.000	0.000	wt.%	0.000	0.000
1	K2O	Calc	0.149	0.027	wt.%	0.139	0.025
1	BaO	Calc	0.720	0.699	wt.%	0.411	0.400
1	Al2O3	Calc	4.425	1.557	wt.%	3.805	1.339
1	Ta2O5	Calc	0.203	0.049	wt.%	0.040	0.010
1	TiO2	Calc	65.625	0.284	wt.%	72.032	0.312
1	ZnO	Calc	0.086	0.012	wt.%	0.093	0.013
1	Ag2O	Calc	0.000	0.000	wt.%	0.000	0.000
1	Cl	Calc	0.544	0.041	wt.%	1.346	0.102
1	ZrO2	Calc	0.027	0.089	wt.%	0.019	0.063

Element Table ==========

Elmt	Line Code	Cond Code	Ratio Method	Intensity (c/s)	Error (c/s)	Intensity Method	Conc.	Conc Method	Calibration Coefficient
O	Ka	0	None	0.000	0.0000	Gaussian	38.379	None	0.000
Mg	Ka	1	None	0.000	0.8743	Gaussian	0.000	FP	0.000
Al	Ka	1	None	6.471	2.2766	Gaussian	2.342	FP	0.000
Si	Ka	1	None	41.632	4.1317	Gaussian	2.612	FP	0.000
P	Ka	1	None	0.000	2.4000	Gaussian	0.000	FP	0.000
S	Ka	1	None	14.499	3.0659	Gaussian	0.136	FP	0.000
Cl	Ka	1	None	79.670	6.0296	Gaussian	0.544	FP	0.000
K	Ka	1	None	27.632	5.0266	Gaussian	0.124	FP	0.000
Ca	Ka	1	None	190.040	9.0963	Gaussian	0.594	FP	0.000
Ti	Ka	1	None	16520.870	71.5442	Gaussian	39.343	FP	0.000
V	Ka	1	None	275.148	25.3602	Gaussian	0.506	FP	0.000
Cr	Ka	1	None	0.000	4.5314	Gaussian	0.000	FP	0.000
Mn	Ka	1	None	241.077	9.0618	Gaussian	0.751	FP	0.000
Fe	Ka	1	None	4896.713	38.9352	Gaussian	13.251	FP	0.000
Co	Ka	1	None	27.943	13.9233	Gaussian	0.068	FP	0.000
Ni	Ka	1	None	0.000	5.1225	Gaussian	0.000	FP	0.000
Cu	Ka	1	None	5.088	3.2637	Gaussian	0.014	FP	0.000
Zn	Ka	1	None	28.085	4.0180	Gaussian	0.069	FP	0.000
Zr	Ka	1	None	0.573	1.9058	Gaussian	0.020	FP	0.000
Nb	Ka	1	None	0.411	1.7768	Gaussian	0.069	FP	0.000
Mo	Ka	1	None	0.421	1.4767	Gaussian	0.000	FP	0.000
Ag	Ka	1	None	0.000	0.0000	Gaussian	0.000	FP	0.000
Sn	Ka	1	None	0.000	0.0000	Gaussian	0.000	FP	0.000
Ba	La	1	None	68.315	66.3893	Gaussian	0.645	FP	0.000
Ta	La	1	None	15.627	3.7893	Gaussian	0.167	FP	0.000
W	La	1	None	26.958	4.7379	Gaussian	0.282	FP	0.000
Pb	La	1	None	7.885	2.4554	Gaussian	0.085	FP	0.000

Analysis Conditions ==========

#	Tar get	Filter	Thick. mg/cm2	kV	uA	---Detector--- Type	Filter	Thick. mg/cm2	Atm	Preset Time(s)	Actual Time(s)
1	Rh	None	0.00	20.0	20.0	SDD	None	0.00	Air	60.0	30.0

Processing Conditions ==========

#	No.	Escape	Sum	Back	C/R	Blank	----Blank----

Roasting XRF Results for 650^0C, 60 minutes

CrossRoads Scientific XRS-FP Analysis Report

File: C:\Users\Xenemetrix\Music\New folder\New folder\R6.str

4:41:05 PM 12

Comment line

Layer Table ==========

#	Thick	Type	Error	Units	Density	Norm.	Total
1	0.00	Bulk	0.00	mg/cm2	0.00F	On	100.00

Sample Table ==========

Layer	Component	Type	Concn.	Error	Units	Mole%	Error
1	SiO2	Calc	5.287	0.535	wt.%	7.786	0.788
1	V2O5	Calc	0.756	0.083	wt.%	0.368	0.041
1	Cr2O3	Calc	0.000	0.000	wt.%	0.000	0.000
1	MnO	Calc	0.919	0.035	wt.%	1.146	0.044
1	Fe2O3	Calc	19.711	0.154	wt.%	10.921	0.085
1	Co3O4	Calc	0.108	0.047	wt.%	0.040	0.017
1	NiO	Calc	0.000	0.000	wt.%	0.000	0.000
1	CuO	Calc	0.033	0.010	wt.%	0.037	0.011
1	Nb2O3	Calc	0.541	0.390	wt.%	0.205	0.148
1	MoO3	Calc	0.000	0.000	wt.%	0.000	0.000
1	WO3	Calc	0.245	0.056	wt.%	0.094	0.021
1	P2O5	Calc	0.000	0.000	wt.%	0.000	0.000
1	SO3	Calc	0.105	0.057	wt.%	0.116	0.063
1	CaO	Calc	0.690	0.036	wt.%	1.088	0.057
1	MgO	Calc	0.000	0.000	wt.%	0.000	0.000
1	K2O	Calc	0.049	0.027	wt.%	0.046	0.025
1	BaO	Calc	0.721	0.699	wt.%	0.416	0.403
1	Al2O3	Calc	3.879	1.494	wt.%	3.366	1.297
1	Ta2O5	Calc	0.147	0.044	wt.%	0.029	0.009
1	TiO2	Calc	66.356	0.284	wt.%	73.511	0.315
1	ZnO	Calc	0.072	0.011	wt.%	0.078	0.012
1	Ag2O	Calc	0.000	0.000	wt.%	0.000	0.000
1	Cl	Calc	0.283	0.031	wt.%	0.707	0.077
1	ZrO2	Calc	0.023	0.088	wt.%	0.017	0.063

Element Table ==========

Elmt	Line Code	Cond Code	Ratio Method	Intensity (c/s)	Error (c/s)	Intensity Method	Conc.	Conc Method	Calibration Coefficient
O	Ka	0	None	0.000	0.0000	Gaussian	38.273	None	0.000
Mg	Ka	1	None	0.000	0.8273	Gaussian	0.000	FP	0.000
Al	Ka	1	None	5.659	2.1805	Gaussian	2.053	FP	0.000
Si	Ka	1	None	39.550	4.0014	Gaussian	2.472	FP	0.000
P	Ka	1	None	0.000	2.4019	Gaussian	0.000	FP	0.000
S	Ka	1	None	4.513	2.4652	Gaussian	0.042	FP	0.000
Cl	Ka	1	None	41.614	4.5286	Gaussian	0.283	FP	0.000
K	Ka	1	None	9.165	4.9616	Gaussian	0.041	FP	0.000
Ca	Ka	1	None	160.065	8.4496	Gaussian	0.493	FP	0.000
Ti	Ka	1	None	16892.350	72.3456	Gaussian	39.781	FP	0.000
V	Ka	1	None	232.857	25.6859	Gaussian	0.423	FP	0.000
Cr	Ka	1	None	0.000	4.3215	Gaussian	0.000	FP	0.000
Mn	Ka	1	None	228.821	8.7875	Gaussian	0.712	FP	0.000
Fe	Ka	1	None	5098.170	39.7154	Gaussian	13.786	FP	0.000
Co	Ka	1	None	32.630	14.1338	Gaussian	0.079	FP	0.000
Ni	Ka	1	None	0.000	5.0368	Gaussian	0.000	FP	0.000
Cu	Ka	1	None	9.754	2.9338	Gaussian	0.026	FP	0.000
Zn	Ka	1	None	23.183	3.5674	Gaussian	0.058	FP	0.000
Zr	Ka	1	None	0.499	1.8773	Gaussian	0.017	FP	0.000
Nb	Ka	1	None	2.549	1.8385	Gaussian	0.430	FP	0.000
Mo	Ka	1	None	0.484	1.4461	Gaussian	0.000	FP	0.000
Ag	Ka	1	None	0.000	0.0000	Gaussian	0.000	FP	0.000
Sn	Ka	1	None	0.000	0.0000	Gaussian	0.000	FP	0.000
Ba	La	1	None	69.250	67.1328	Gaussian	0.646	FP	0.000
Ta	La	1	None	11.255	3.3344	Gaussian	0.121	FP	0.000
W	La	1	None	18.541	4.2543	Gaussian	0.195	FP	0.000
Pb	La	1	None	6.369	2.5829	Gaussian	0.069	FP	0.000

Analysis Conditions ==========

#	Tar Filter get	Thick. mg/cm2	kV	uA	---Detector--- Type	Filter	Thick. mg/cm2	Atm	Preset Time(s)	Actual Time(s)
1	Rh None	0.00	20.0	20.0	SDD	None	0.00	Air	60.0	30.0

Processing Conditions ==========

#	No.	Escape	Sum	Back	C/R	Blank	----Blank----

Roasting XRF Results for 1000^0C, 30 minutes

CrossRoads Scientific XRS-FP Analysis Report

File: C:\Users\Xenemetrix\Music\New folder\New folder\R7.str

4:47:43 PM 1

Comment line

Layer Table ==========

#	Thick	Type	Error	Units	Density	Norm.	Total
1	0.00	Bulk	0.00	mg/cm2	0.00F	On	100.00

Sample Table ==========

Layer	Component	Type	Concn.	Error	Units	Mole%	Error
1	SiO2	Calc	5.149	0.536	wt.%	7.630	0.794
1	V2O5	Calc	0.969	0.081	wt.%	0.474	0.040
1	Cr2O3	Calc	0.000	0.000	wt.%	0.000	0.000
1	MnO	Calc	1.283	0.041	wt.%	1.611	0.052
1	Fe2O3	Calc	22.066	0.161	wt.%	12.302	0.090
1	Co3O4	Calc	0.090	0.050	wt.%	0.033	0.018
1	NiO	Calc	0.000	0.000	wt.%	0.000	0.000
1	CuO	Calc	0.012	0.011	wt.%	0.013	0.013
1	Nb2O3	Calc	0.250	0.392	wt.%	0.095	0.149
1	MoO3	Calc	0.000	0.000	wt.%	0.000	0.000
1	WO3	Calc	0.343	0.063	wt.%	0.132	0.024
1	P2O5	Calc	0.000	0.000	wt.%	0.000	0.000
1	SO3	Calc	0.124	0.057	wt.%	0.138	0.064
1	CaO	Calc	0.911	0.042	wt.%	1.447	0.066
1	MgO	Calc	0.445	5.942	wt.%	0.983	13.126
1	K2O	Calc	0.037	0.026	wt.%	0.035	0.024
1	BaO	Calc	0.685	0.684	wt.%	0.398	0.397
1	Al2O3	Calc	3.404	1.455	wt.%	2.972	1.270
1	Ta2O5	Calc	0.224	0.051	wt.%	0.045	0.010
1	TiO2	Calc	63.448	0.278	wt.%	70.729	0.309
1	ZnO	Calc	0.083	0.012	wt.%	0.091	0.013
1	Ag2O	Calc	0.000	0.000	wt.%	0.000	0.000
1	Cl	Calc	0.320	0.032	wt.%	0.803	0.081
1	ZrO2	Calc	0.017	0.093	wt.%	0.012	0.067

Element Table ==========

Elmt	Line Code	Cond Code	Ratio Method	Intensity (c/s)	Error (c/s)	Intensity Method	Conc.	Conc Method	Calibration Coefficient
O	Ka	0	None	0.000	0.0000	Gaussian	37.911	None	0.000
Mg	Ka	1	None	0.061	0.8105	Gaussian	0.268	FP	0.000
Al	Ka	1	None	4.890	2.0899	Gaussian	1.802	FP	0.000
Si	Ka	1	None	38.118	3.9674	Gaussian	2.407	FP	0.000
P	Ka	1	None	0.000	2.2764	Gaussian	0.000	FP	0.000
S	Ka	1	None	5.269	2.4386	Gaussian	0.050	FP	0.000
Cl	Ka	1	None	46.697	4.7314	Gaussian	0.320	FP	0.000
K	Ka	1	None	6.779	4.7746	Gaussian	0.030	FP	0.000
Ca	Ka	1	None	209.611	9.5727	Gaussian	0.651	FP	0.000
Ti	Ka	1	None	16187.520	70.8314	Gaussian	38.038	FP	0.000
V	Ka	1	None	298.784	25.1029	Gaussian	0.543	FP	0.000
Cr	Ka	1	None	0.000	4.6923	Gaussian	0.000	FP	0.000
Mn	Ka	1	None	325.389	10.4115	Gaussian	0.994	FP	0.000
Fe	Ka	1	None	5782.768	42.2761	Gaussian	15.434	FP	0.000
Co	Ka	1	None	27.264	15.0846	Gaussian	0.066	FP	0.000
Ni	Ka	1	None	0.000	5.4340	Gaussian	0.000	FP	0.000
Cu	Ka	1	None	3.465	3.2755	Gaussian	0.010	FP	0.000
Zn	Ka	1	None	26.354	3.8991	Gaussian	0.067	FP	0.000
Zr	Ka	1	None	0.354	1.9398	Gaussian	0.013	FP	0.000
Nb	Ka	1	None	1.152	1.8044	Gaussian	0.199	FP	0.000
Mo	Ka	1	None	0.000	1.3760	Gaussian	0.000	FP	0.000
Ag	Ka	1	None	0.000	0.0000	Gaussian	0.000	FP	0.000
Sn	Ka	1	None	0.000	0.0000	Gaussian	0.000	FP	0.000
Ba	La	1	None	65.757	65.7274	Gaussian	0.613	FP	0.000
Ta	La	1	None	16.773	3.8024	Gaussian	0.183	FP	0.000
W	La	1	None	25.445	4.6319	Gaussian	0.272	FP	0.000
Pb	La	1	None	11.818	2.6521	Gaussian	0.130	FP	0.000

Analysis Conditions ==========

#	Tar get	Filter	Thick. mg/cm2	kV	uA	---Detector--- Type	Filter	Thick. mg/cm2	Atm	Preset Time(s)	Actual Time(s)
1	Rh	None	0.00	20.0	20.0	SDD	None	0.00	Air	60.0	30.0

Processing Conditions ==========

#	No.	Escape	Sum	Back	C/R	Blank	----Blank----

Roasting XRF Results for 1000^0C, 45 minutes

CrossRoads Scientific XRS-FP Analysis Report

File: C:\Users\Xenemetrix\Music\New folder\New folder\R8.str

4:50:11 PM 1

Comment line

Layer Table ==========

#	Thick	Type	Error	Units	Density	Norm.	Total
1	0.00	Bulk	0.00	mg/cm2	0.00F	On	100.00

Sample Table ==========

Layer	Component	Type	Concn.	Error	Units	Mole%	Error
1	SiO2	Calc	9.988	0.725	wt.%	14.425	1.047
1	V2O5	Calc	1.048	0.080	wt.%	0.500	0.038
1	Cr2O3	Calc	0.000	0.000	wt.%	0.000	0.000
1	MnO	Calc	0.889	0.035	wt.%	1.088	0.043
1	Fe2O3	Calc	20.379	0.154	wt.%	11.073	0.084
1	Co3O4	Calc	0.082	0.047	wt.%	0.030	0.017
1	NiO	Calc	0.000	0.000	wt.%	0.000	0.000
1	CuO	Calc	0.029	0.011	wt.%	0.032	0.012
1	Nb2O3	Calc	0.138	0.388	wt.%	0.051	0.144
1	MoO3	Calc	0.000	0.000	wt.%	0.000	0.000
1	WO3	Calc	0.179	0.056	wt.%	0.067	0.021
1	P2O5	Calc	0.000	0.000	wt.%	0.000	0.000
1	SO3	Calc	0.365	0.078	wt.%	0.396	0.084
1	CaO	Calc	1.289	0.051	wt.%	1.995	0.079
1	MgO	Calc	0.000	0.000	wt.%	0.000	0.000
1	K2O	Calc	0.097	0.033	wt.%	0.090	0.030
1	BaO	Calc	0.495	0.678	wt.%	0.280	0.384
1	Al2O3	Calc	3.531	1.735	wt.%	3.005	1.477
1	Ta2O5	Calc	0.217	0.048	wt.%	0.043	0.009
1	TiO2	Calc	60.664	0.275	wt.%	65.909	0.299
1	ZnO	Calc	0.054	0.010	wt.%	0.057	0.011
1	Ag2O	Calc	0.000	0.000	wt.%	0.000	0.000
1	Cl	Calc	0.353	0.035	wt.%	0.865	0.086
1	ZrO2	Calc	0.052	0.095	wt.%	0.037	0.067

Element Table ==========

Elmt	Line Code	Cond Code	Ratio Method	Intensity (c/s)	Error (c/s)	Intensity Method	Conc.	Conc Method	Calibration Coefficient
O	Ka	0	None	0.000	0.0000	Gaussian	38.885	None	0.000
Mg	Ka	1	None	0.000	0.8844	Gaussian	0.000	FP	0.000
Al	Ka	1	None	5.122	2.5172	Gaussian	1.869	FP	0.000
Si	Ka	1	None	74.329	5.3954	Gaussian	4.669	FP	0.000
P	Ka	1	None	0.000	2.9120	Gaussian	0.000	FP	0.000
S	Ka	1	None	14.934	3.1819	Gaussian	0.146	FP	0.000
Cl	Ka	1	None	49.669	4.9567	Gaussian	0.353	FP	0.000
K	Ka	1	None	17.411	5.8698	Gaussian	0.081	FP	0.000
Ca	Ka	1	None	285.671	11.2566	Gaussian	0.922	FP	0.000
Ti	Ka	1	None	15124.920	68.5186	Gaussian	36.369	FP	0.000
V	Ka	1	None	316.498	24.1969	Gaussian	0.587	FP	0.000
Cr	Ka	1	None	0.000	4.7460	Gaussian	0.000	FP	0.000
Mn	Ka	1	None	227.857	8.9178	Gaussian	0.689	FP	0.000
Fe	Ka	1	None	5411.260	40.9510	Gaussian	14.254	FP	0.000
Co	Ka	1	None	25.507	14.6247	Gaussian	0.060	FP	0.000
Ni	Ka	1	None	0.000	5.3583	Gaussian	0.000	FP	0.000
Cu	Ka	1	None	8.698	3.3273	Gaussian	0.023	FP	0.000
Zn	Ka	1	None	17.517	3.3846	Gaussian	0.043	FP	0.000
Zr	Ka	1	None	1.118	2.0413	Gaussian	0.038	FP	0.000
Nb	Ka	1	None	0.660	1.8497	Gaussian	0.110	FP	0.000
Mo	Ka	1	None	0.889	1.5270	Gaussian	0.000	FP	0.000
Ag	Ka	1	None	0.000	0.0000	Gaussian	0.000	FP	0.000
Sn	Ka	1	None	0.000	0.0000	Gaussian	0.000	FP	0.000
Ba	La	1	None	46.434	63.5729	Gaussian	0.444	FP	0.000
Ta	La	1	None	16.744	3.6892	Gaussian	0.178	FP	0.000
W	La	1	None	13.646	4.2768	Gaussian	0.142	FP	0.000
Pb	La	1	None	12.898	2.8007	Gaussian	0.137	FP	0.000

Analysis Conditions ==========

#	Tar get	Filter	Thick. mg/cm2	kV	uA	Detector Type	Detector Filter	Thick. mg/cm2	Atm	Preset Time(s)	Actual Time(s)
1	Rh	None	0.00	20.0	20.0	SDD	None	0.00	Air	60.0	30.0

Processing Conditions ==========

#	No.	Escape	Sum	Back	C/R	Blank	----Blank----

Roasting XRF Results for 1000^{0}C, 60 minutes

CrossRoads Scientific XRS-FP Analysis Report

File: C:\Users\Xenemetrix\Music\New folder\New folder\R9.str

4:42:30 PM 12

Comment line

Layer Table ==========

#	Thick	Type	Error	Units	Density	Norm.	Total
1	0.00	Bulk	0.00	mg/cm2	0.00F	On	100.00

Sample Table ==========

Layer	Component	Type	Concn.	Error	Units	Mole%	Error
1	SiO2	Calc	8.445	0.673	wt.%	11.824	0.942
1	V2O5	Calc	1.165	0.075	wt.%	0.539	0.035
1	Cr2O3	Calc	0.000	0.000	wt.%	0.000	0.000
1	MnO	Calc	0.898	0.033	wt.%	1.065	0.040
1	Fe2O3	Calc	21.328	0.151	wt.%	11.237	0.080
1	Co3O4	Calc	0.086	0.046	wt.%	0.030	0.016
1	NiO	Calc	0.000	0.000	wt.%	0.000	0.000
1	CuO	Calc	0.003	0.010	wt.%	0.003	0.010
1	Nb2O3	Calc	0.350	0.346	wt.%	0.126	0.124
1	MoO3	Calc	0.000	0.000	wt.%	0.000	0.000
1	WO3	Calc	0.228	0.051	wt.%	0.083	0.019
1	P2O5	Calc	0.000	0.000	wt.%	0.000	0.000
1	SO3	Calc	0.220	0.068	wt.%	0.231	0.072
1	CaO	Calc	0.924	0.042	wt.%	1.386	0.063
1	MgO	Calc	4.391	6.798	wt.%	9.165	14.189
1	K2O	Calc	0.099	0.027	wt.%	0.089	0.024
1	BaO	Calc	0.585	0.635	wt.%	0.321	0.349
1	Al2O3	Calc	4.045	1.693	wt.%	3.338	1.397
1	Ta2O5	Calc	0.154	0.043	wt.%	0.029	0.008
1	TiO2	Calc	56.553	0.257	wt.%	59.573	0.271
1	ZnO	Calc	0.060	0.010	wt.%	0.062	0.010
1	Ag2O	Calc	0.000	0.000	wt.%	0.000	0.000
1	Cl	Calc	0.361	0.034	wt.%	0.856	0.081
1	ZrO2	Calc	0.008	0.083	wt.%	0.006	0.057
1	SnO2	Calc	0.000	0.000	wt.%	0.000	0.000

Element Table ==========

Elmt	Line Code	Cond Code	Ratio Method	Intensity (c/s)	Error (c/s)	Intensity Method	Conc.	Conc Method	Calibration Coefficient
O	Ka	0	None	0.000	0.0000	Gaussian	38.582	None	0.000
Mg	Ka	1	None	0.637	0.9869	Gaussian	2.648	FP	0.000
Al	Ka	1	None	5.941	2.4857	Gaussian	2.141	FP	0.000
Si	Ka	1	None	63.492	5.0591	Gaussian	3.947	FP	0.000
P	Ka	1	None	0.000	2.8906	Gaussian	0.000	FP	0.000
S	Ka	1	None	9.233	2.8759	Gaussian	0.088	FP	0.000
Cl	Ka	1	None	52.087	4.9444	Gaussian	0.361	FP	0.000
K	Ka	1	None	18.303	5.0125	Gaussian	0.082	FP	0.000
Ca	Ka	1	None	211.668	9.5861	Gaussian	0.660	FP	0.000
Ti	Ka	1	None	15029.000	68.2595	Gaussian	33.904	FP	0.000
V	Ka	1	None	375.033	24.0953	Gaussian	0.653	FP	0.000
Cr	Ka	1	None	0.000	4.9951	Gaussian	0.000	FP	0.000
Mn	Ka	1	None	250.470	9.2952	Gaussian	0.695	FP	0.000
Fe	Ka	1	None	6144.558	43.6275	Gaussian	14.918	FP	0.000
Co	Ka	1	None	28.918	15.5569	Gaussian	0.063	FP	0.000
Ni	Ka	1	None	0.000	5.6324	Gaussian	0.000	FP	0.000
Cu	Ka	1	None	0.951	3.0916	Gaussian	0.002	FP	0.000
Zn	Ka	1	None	20.941	3.5215	Gaussian	0.048	FP	0.000
Zr	Ka	1	None	0.194	1.9088	Gaussian	0.006	FP	0.000
Nb	Ka	1	None	1.782	1.7581	Gaussian	0.278	FP	0.000
Mo	Ka	1	None	0.000	1.3132	Gaussian	0.000	FP	0.000
Ag	Ka	1	None	0.000	0.0000	Gaussian	0.000	FP	0.000
Sn	Ka	1	None	0.000	0.0000	Gaussian	0.000	FP	0.000
Ba	La	1	None	58.286	63.3383	Gaussian	0.524	FP	0.000
Ta	La	1	None	12.630	3.5633	Gaussian	0.126	FP	0.000
W	La	1	None	18.525	4.1429	Gaussian	0.181	FP	0.000
Pb	La	1	None	9.097	2.6824	Gaussian	0.091	FP	0.000

Analysis Conditions ==========

#	Tar get	Filter	Thick. mg/cm2	kV	uA	---Detector--- Type	Filter	Thick. mg/cm2	Atm	Preset Time(s)	Actual Time(s)
1	Rh	None	0.00	20.0	20.0	SDD	None	0.00	Air	60.0	30.0

Processing Conditions ==========

#	No.	Escape	Sum	Back	C/R	Blank	----Blank----

APPENDIX H
XRF Results of Beneficiated Samples

XRF result of Calcined Sample MGS Tailings

CrossRoads Scientific XRS-FP Analysis Report

File: C:\Users\Xenemetrix\Desktop\TODAY\A-.str

12:28:54 PM 14-Oct-21

Comment line

Layer Table ==========

#	Thick	Type	Error	Units	Density	Norm.	Total
1	0.00	Bulk	0.00	mg/cm2	0.00F	On	100.00

Sample Table ==========

Layer	Component	Type	Concn.	Error	Units	Mole%	Error
1	SiO2	Calc	2.024	0.399	wt.%	3.309	0.653
1	V2O5	Calc	0.771	0.078	wt.%	0.416	0.042
1	Cr2O3	Calc	0.000	0.000	wt.%	0.000	0.000
1	MnO	Calc	1.775	0.050	wt.%	2.458	0.069
1	Fe2O3	Calc	36.469	0.218	wt.%	22.430	0.134
1	Co3O4	Calc	0.151	0.067	wt.%	0.062	0.027
1	NiO	Calc	0.000	0.000	wt.%	0.000	0.000
1	CuO	Calc	0.025	0.013	wt.%	0.031	0.016
1	Nb2O3	Calc	0.128	0.444	wt.%	0.054	0.186
1	MoO3	Calc	0.000	0.000	wt.%	0.000	0.000
1	WO3	Calc	0.257	0.072	wt.%	0.109	0.030
1	P2O5	Calc	0.000	0.000	wt.%	0.000	0.000
1	SO3	Calc	0.124	0.069	wt.%	0.152	0.084
1	CaO	Calc	0.100	0.021	wt.%	0.175	0.036
1	MgO	Calc	0.000	0.000	wt.%	0.000	0.000
1	K2O	Calc	0.095	0.030	wt.%	0.099	0.031
1	BaO	Calc	0.654	0.659	wt.%	0.419	0.422
1	Al2O3	Calc	4.132	1.501	wt.%	3.980	1.446
1	Ta2O5	Calc	0.236	0.058	wt.%	0.052	0.013
1	TiO2	Calc	52.096	0.265	wt.%	64.064	0.326
1	ZnO	Calc	0.093	0.014	wt.%	0.113	0.017
1	Ag2O	Calc	0.000	0.000	wt.%	0.000	0.000
1	Cl	Calc	0.714	0.051	wt.%	1.977	0.141
1	ZrO2	Calc	0.000	0.000	wt.%	0.000	0.000
1	SnO2	Calc	0.157	0.105	wt.%	0.102	0.068

Element Table ==========

Element Table ==========

Elmt	Line Code	Cond Code	Ratio Method	Intensity (c/s)	Error (c/s)	Intensity Method	Conc.	Conc Method	Calibration Coefficient
O	Ka	0	None	0.000	0.0000	Gaussian	35.993	None	0.000
Mg	Ka	1	None	0.000	0.7424	Gaussian	0.000	FP	0.000
Al	Ka	1	None	4.743	1.7234	Gaussian	2.187	FP	0.000
Si	Ka	1	None	11.964	2.3598	Gaussian	0.946	FP	0.000
P	Ka	1	None	0.000	1.7839	Gaussian	0.000	FP	0.000
S	Ka	1	None	4.343	2.4150	Gaussian	0.050	FP	0.000
Cl	Ka	1	None	86.425	6.1437	Gaussian	0.714	FP	0.000
K	Ka	1	None	14.534	4.6121	Gaussian	0.079	FP	0.000
Ca	Ka	1	None	19.152	3.9724	Gaussian	0.071	FP	0.000
Ti	Ka	1	None	11942.440	60.8327	Gaussian	31.232	FP	0.000
V	Ka	1	None	212.711	21.6293	Gaussian	0.432	FP	0.000
Cr	Ka	1	None	0.000	4.2269	Gaussian	0.000	FP	0.000
Mn	Ka	1	None	421.235	11.8072	Gaussian	1.375	FP	0.000
Fe	Ka	1	None	8671.527	51.7638	Gaussian	25.508	FP	0.000
Co	Ka	1	None	41.196	18.3782	Gaussian	0.111	FP	0.000
Ni	Ka	1	None	0.000	6.4208	Gaussian	0.000	FP	0.000
Cu	Ka	1	None	5.600	2.9560	Gaussian	0.020	FP	0.000
Zn	Ka	1	None	22.755	3.4426	Gaussian	0.075	FP	0.000
Zr	Ka	1	None	0.000	1.6330	Gaussian	0.000	FP	0.000
Nb	Ka	1	None	0.458	1.5913	Gaussian	0.101	FP	0.000
Mo	Ka	1	None	0.246	1.1688	Gaussian	0.000	FP	0.000
Ag	Ka	1	None	0.000	0.0000	Gaussian	0.000	FP	0.000
Sn	La	1	None	6.899	4.6019	Gaussian	0.124	FP	0.000
Ba	La	1	None	56.059	56.4578	Gaussian	0.586	FP	0.000
Ta	La	1	None	13.598	3.3159	Gaussian	0.193	FP	0.000
W	La	1	None	14.655	4.0975	Gaussian	0.204	FP	0.000

Analysis Conditions ==========

#	Target	Filter	Thick. mg/cm2	kV	uA	Detector Type	Detector Filter	Thick. mg/cm2	Atm	Preset Time(s)	Actual Time(s)
1	Rh	None	0.00	20.0	15.0	SDD	None	0.00	Air	60.0	30.0

Processing Conditions ==========

#	No. Smths	Escape Peaks	Sum Peaks	Back Type	C/R Ratio	Blank Rem.	Blank File
1	1	Yes	Yes	Auto	No	No	

XRF result of Roasted Sample MGS Tailings

CrossRoads Scientific XRS-FP Analysis Report

File: C:\Users\Xenemetrix\Desktop\TODAY\B-.str

12:29:58 PM

Comment line

Layer Table ==========

#	Thick	Type	Error	Units	Density	Norm.	Total
1	0.00	Bulk	0.00	mg/cm2	0.00F	On	100.00

Sample Table ==========

Layer	Component	Type	Concn.	Error	Units	Mole%	Error
1	SiO2	Calc	2.313	0.422	wt.%	3.779	0.690
1	V2O5	Calc	0.744	0.077	wt.%	0.401	0.042
1	Cr2O3	Calc	0.000	0.000	wt.%	0.000	0.000
1	MnO	Calc	1.866	0.051	wt.%	2.582	0.070
1	Fe2O3	Calc	36.914	0.218	wt.%	22.692	0.134
1	Co3O4	Calc	0.203	0.067	wt.%	0.083	0.027
1	NiO	Calc	0.001	0.031	wt.%	0.001	0.040
1	CuO	Calc	0.021	0.012	wt.%	0.026	0.015
1	Nb2O3	Calc	0.043	0.398	wt.%	0.018	0.167
1	MoO3	Calc	0.000	0.000	wt.%	0.000	0.000
1	WO3	Calc	0.256	0.071	wt.%	0.108	0.030
1	P2O5	Calc	0.000	0.000	wt.%	0.000	0.000
1	SO3	Calc	0.026	0.064	wt.%	0.031	0.079
1	CaO	Calc	0.136	0.021	wt.%	0.238	0.037
1	MgO	Calc	0.000	0.000	wt.%	0.000	0.000
1	K2O	Calc	0.015	0.028	wt.%	0.015	0.029
1	BaO	Calc	0.525	0.651	wt.%	0.336	0.417
1	Al2O3	Calc	4.273	1.544	wt.%	4.114	1.486
1	Ta2O5	Calc	0.172	0.054	wt.%	0.038	0.012
1	TiO2	Calc	51.663	0.262	wt.%	63.500	0.322
1	ZnO	Calc	0.104	0.014	wt.%	0.126	0.017
1	Ag2O	Calc	0.000	0.000	wt.%	0.000	0.000
1	Cl	Calc	0.676	0.049	wt.%	1.871	0.136
1	ZrO2	Calc	0.049	0.100	wt.%	0.039	0.079

Element Table ==========

Elmt	Line Code	Cond Code	Ratio Method	Intensity (c/s)	Error (c/s)	Intensity Method	Conc.	Conc Method	Calibration Coefficient
O	Ka	0	None	0.000	0.0000	Gaussian	36.073	None	0.000
Mg	Ka	1	None	0.000	0.7944	Gaussian	0.000	FP	0.000
Al	Ka	1	None	4.915	1.7757	Gaussian	2.262	FP	0.000
Si	Ka	1	None	13.693	2.4987	Gaussian	1.081	FP	0.000
P	Ka	1	None	0.000	1.8762	Gaussian	0.000	FP	0.000
S	Ka	1	None	0.900	2.2637	Gaussian	0.010	FP	0.000
Cl	Ka	1	None	82.101	5.9520	Gaussian	0.676	FP	0.000
K	Ka	1	None	2.255	4.3674	Gaussian	0.012	FP	0.000
Ca	Ka	1	None	26.362	4.0873	Gaussian	0.097	FP	0.000
Ti	Ka	1	None	12028.050	61.0597	Gaussian	30.972	FP	0.000
V	Ka	1	None	208.437	21.6351	Gaussian	0.417	FP	0.000
Cr	Ka	1	None	0.000	4.1020	Gaussian	0.000	FP	0.000
Mn	Ka	1	None	448.351	12.1455	Gaussian	1.445	FP	0.000
Fe	Ka	1	None	8875.834	52.3571	Gaussian	25.819	FP	0.000
Co	Ka	1	None	56.088	18.5777	Gaussian	0.149	FP	0.000
Ni	Ka	1	None	0.150	6.4871	Gaussian	0.001	FP	0.000
Cu	Ka	1	None	4.722	2.7790	Gaussian	0.017	FP	0.000
Zn	Ka	1	None	25.468	3.5365	Gaussian	0.084	FP	0.000
Zr	Ka	1	None	0.798	1.6193	Gaussian	0.036	FP	0.000
Nb	Ka	1	None	0.157	1.4340	Gaussian	0.035	FP	0.000
Mo	Ka	1	None	1.637	1.4096	Gaussian	0.000	FP	0.000
Ag	Ka	1	None	0.000	0.0000	Gaussian	0.000	FP	0.000
Sn	La	1	None	0.000	4.1355	Gaussian	0.000	FP	0.000
Ba	La	1	None	45.666	56.6558	Gaussian	0.470	FP	0.000
Ta	La	1	None	9.944	3.1229	Gaussian	0.141	FP	0.000
W	La	1	None	14.616	4.0268	Gaussian	0.203	FP	0.000

Analysis Conditions ==========

#	Target	Filter	Thick. mg/cm2	kV	uA	Detector Type	Detector Filter	Thick. mg/cm2	Atm	Preset Time(s)	Actual Time(s)
1	Rh	None	0.00	20.0	15.0	SDD	None	0.00	Air	60.0	30.0

Processing Conditions ==========

#	No. Escape	Sum	Back	C/R	Blank	----Blank----

XRF result of Roasted Sample GVS Tailings

CrossRoads Scientific XRS-FP Analysis Report

File: C:\Users\Xenemetrix\Desktop\TODAY\D-.str

12:32:04 PM

Comment line

Layer Table ==========

#	Thick	Type	Error	Units	Density	Norm.	Total
1	0.00	Bulk	0.00	mg/cm2	0.00F	On	100.00

Sample Table ==========

Layer	Component	Type	Concn.	Error	Units	Mole%	Error
1	SiO2	Calc	13.235	0.759	wt.%	17.459	1.002
1	V2O5	Calc	0.905	0.082	wt.%	0.394	0.036
1	Cr2O3	Calc	0.000	0.000	wt.%	0.000	0.000
1	MnO	Calc	0.165	0.016	wt.%	0.184	0.018
1	Fe2O3	Calc	5.670	0.078	wt.%	2.815	0.039
1	Co3O4	Calc	0.055	0.024	wt.%	0.018	0.008
1	NiO	Calc	0.000	0.000	wt.%	0.000	0.000
1	CuO	Calc	0.064	0.010	wt.%	0.064	0.010
1	Nb2O3	Calc	0.356	0.371	wt.%	0.121	0.126
1	MoO3	Calc	0.000	0.000	wt.%	0.000	0.000
1	WO3	Calc	0.340	0.054	wt.%	0.116	0.019
1	P2O5	Calc	0.040	0.167	wt.%	0.022	0.093
1	SO3	Calc	0.356	0.084	wt.%	0.352	0.083
1	CaO	Calc	1.109	0.044	wt.%	1.568	0.062
1	MgO	Calc	1.042	5.468	wt.%	2.050	10.753
1	K2O	Calc	0.186	0.028	wt.%	0.157	0.024
1	BaO	Calc	0.641	0.693	wt.%	0.331	0.358
1	Al2O3	Calc	3.379	1.671	wt.%	2.627	1.299
1	Ta2O5	Calc	0.201	0.045	wt.%	0.036	0.008
1	TiO2	Calc	70.997	0.283	wt.%	70.460	0.280
1	ZnO	Calc	0.049	0.010	wt.%	0.048	0.010
1	Ag2O	Calc	0.000	0.000	wt.%	0.000	0.000
1	Cl	Calc	0.252	0.029	wt.%	0.563	0.064
1	ZrO2	Calc	0.953	0.133	wt.%	0.613	0.085

Element Table ==========

Elmt	Line Code	Cond Code	Ratio Method	Intensity (c/s)	Error (c/s)	Intensity Method	Conc.	Conc Method	Calibration Coefficient
O	Ka	0	None	0.000	0.0000	Gaussian	40.742	None	0.000
Mg	Ka	1	None	0.180	0.9461	Gaussian	0.629	FP	0.000
Al	Ka	1	None	6.105	3.0193	Gaussian	1.789	FP	0.000
Si	Ka	1	None	121.710	6.9817	Gaussian	6.187	FP	0.000
P	Ka	1	None	1.087	4.5571	Gaussian	0.017	FP	0.000
S	Ka	1	None	16.853	3.9573	Gaussian	0.142	FP	0.000
Cl	Ka	1	None	40.703	4.6615	Gaussian	0.252	FP	0.000
K	Ka	1	None	38.372	5.8671	Gaussian	0.154	FP	0.000
Ca	Ka	1	None	282.993	11.1099	Gaussian	0.793	FP	0.000
Ti	Ka	1	None	19575.750	77.9158	Gaussian	42.564	FP	0.000
V	Ka	1	None	304.355	27.6078	Gaussian	0.507	FP	0.000
Cr	Ka	1	None	0.000	4.7944	Gaussian	0.000	FP	0.000
Mn	Ka	1	None	45.331	4.4572	Gaussian	0.128	FP	0.000
Fe	Ka	1	None	1662.112	22.8011	Gaussian	3.966	FP	0.000
Co	Ka	1	None	18.855	8.3660	Gaussian	0.040	FP	0.000
Ni	Ka	1	None	0.000	3.6576	Gaussian	0.000	FP	0.000
Cu	Ka	1	None	25.357	4.1176	Gaussian	0.051	FP	0.000
Zn	Ka	1	None	21.300	4.2641	Gaussian	0.039	FP	0.000
Zr	Ka	1	None	27.004	3.7560	Gaussian	0.705	FP	0.000
Nb	Ka	1	None	2.227	2.3198	Gaussian	0.283	FP	0.000
Mo	Ka	1	None	0.257	2.1455	Gaussian	0.000	FP	0.000
Ag	Ka	1	None	0.000	0.0000	Gaussian	0.000	FP	0.000
Sn	La	1	None	0.352	8.5730	Gaussian	0.005	FP	0.000
Ba	La	1	None	66.881	72.2905	Gaussian	0.574	FP	0.000
Ta	La	1	None	20.673	4.6467	Gaussian	0.164	FP	0.000
W	La	1	None	34.627	5.5300	Gaussian	0.270	FP	0.000

Analysis Conditions ==========

#	Tar get	Filter	Thick. mg/cm2	kV	uA	---Detector--- Type	Filter	Thick. mg/cm2	Atm	Preset Time(s)	Actual Time(s)
1	Rh	None	0.00	20.0	25.0	SDD	None	0.00	Air	60.0	30.0

Processing Conditions ==========

#	No. Peaks	Escape Peaks	Sum Peaks	Back Type	C/R Ratio	Blank Rem	----Blank---- File

XRF result of Roasted Sample GVS Concentrate

CrossRoads Scientific XRS-FP Analysis Report

File: C:\Users\Xenemetrix\Desktop\TODAY\E-.str

12:33:21 PM 14

Comment line

Layer Table ==========

#	Thick	Type	Error	Units	Density	Norm.	Total
1	0.00	Bulk	0.00	mg/cm2	0.00F	On	100.00

Sample Table ==========

Layer	Component	Type	Concn.	Error	Units	Mole%	Error
1	SiO2	Calc	3.699	0.442	wt.%	4.872	0.582
1	V2O5	Calc	1.001	0.094	wt.%	0.436	0.041
1	Cr2O3	Calc	0.000	0.000	wt.%	0.000	0.000
1	MnO	Calc	0.053	0.012	wt.%	0.059	0.013
1	Fe2O3	Calc	2.101	0.053	wt.%	1.041	0.026
1	Co3O4	Calc	0.023	0.017	wt.%	0.008	0.005
1	NiO	Calc	0.000	0.000	wt.%	0.000	0.000
1	CuO	Calc	0.033	0.009	wt.%	0.033	0.009
1	Nb2O3	Calc	0.154	0.339	wt.%	0.052	0.115
1	MoO3	Calc	0.000	0.000	wt.%	0.000	0.000
1	WO3	Calc	0.298	0.054	wt.%	0.102	0.018
1	P2O5	Calc	0.000	0.000	wt.%	0.000	0.000
1	SO3	Calc	0.182	0.056	wt.%	0.180	0.055
1	CaO	Calc	0.160	0.019	wt.%	0.225	0.027
1	MgO	Calc	2.499	5.872	wt.%	4.906	11.529
1	K2O	Calc	0.048	0.022	wt.%	0.041	0.019
1	BaO	Calc	0.572	0.785	wt.%	0.295	0.405
1	Al2O3	Calc	2.895	1.277	wt.%	2.247	0.991
1	Ta2O5	Calc	0.223	0.043	wt.%	0.040	0.008
1	TiO2	Calc	85.641	0.324	wt.%	84.851	0.321
1	ZnO	Calc	0.057	0.010	wt.%	0.056	0.010
1	Ag2O	Calc	0.000	0.000	wt.%	0.000	0.000
1	Cl	Calc	0.206	0.025	wt.%	0.459	0.057
1	ZrO2	Calc	0.153	0.095	wt.%	0.098	0.061

Element Table ==========

Elmt	Line Code	Cond Code	Ratio Method	Intensity (c/s)	Error (c/s)	Intensity Method	Conc.	Conc Method	Calibration Coefficient
O	Ka	0	None	0.000	0.0000	Gaussian	40.127	None	0.000
Mg	Ka	1	None	0.380	0.8929	Gaussian	1.507	FP	0.000
Al	Ka	1	None	4.558	2.0097	Gaussian	1.532	FP	0.000
Si	Ka	1	None	30.072	3.5914	Gaussian	1.729	FP	0.000
P	Ka	1	None	0.000	2.3907	Gaussian	0.000	FP	0.000
S	Ka	1	None	8.584	2.6310	Gaussian	0.073	FP	0.000
Cl	Ka	1	None	33.425	4.1316	Gaussian	0.206	FP	0.000
K	Ka	1	None	10.073	4.6734	Gaussian	0.040	FP	0.000
Ca	Ka	1	None	41.294	4.9526	Gaussian	0.114	FP	0.000
Ti	Ka	1	None	21697.180	82.0206	Gaussian	51.343	FP	0.000
V	Ka	1	None	309.049	28.9190	Gaussian	0.561	FP	0.000
Cr	Ka	1	None	0.000	4.4352	Gaussian	0.000	FP	0.000
Mn	Ka	1	None	11.765	2.6221	Gaussian	0.041	FP	0.000
Fe	Ka	1	None	499.206	12.5436	Gaussian	1.469	FP	0.000
Co	Ka	1	None	6.601	4.7008	Gaussian	0.017	FP	0.000
Ni	Ka	1	None	0.000	2.1929	Gaussian	0.000	FP	0.000
Cu	Ka	1	None	11.155	3.2046	Gaussian	0.026	FP	0.000
Zn	Ka	1	None	21.351	3.6966	Gaussian	0.046	FP	0.000
Zr	Ka	1	None	3.746	2.3385	Gaussian	0.113	FP	0.000
Nb	Ka	1	None	0.836	1.8392	Gaussian	0.123	FP	0.000
Mo	Ka	1	None	0.177	1.5511	Gaussian	0.000	FP	0.000
Ag	Ka	1	None	0.000	0.0000	Gaussian	0.000	FP	0.000
Sn	La	1	None	0.000	4.9719	Gaussian	0.000	FP	0.000
Ba	La	1	None	55.487	76.0836	Gaussian	0.513	FP	0.000
Ta	La	1	None	19.570	3.7471	Gaussian	0.183	FP	0.000
W	La	1	None	25.896	4.6499	Gaussian	0.237	FP	0.000

Analysis Conditions ==========

#	Tar get	Filter	Thick. mg/cm2	kV	uA	---Detector--- Type	Filter	Thick. mg/cm2	Atm	Preset Time(s)	Actual Time(s)
1	Rh	None	0.00	20.0	20.0	SDD	None	0.00	Air	60.0	30.0

Processing Conditions ==========

XRF result of Calcined Sample GVS Concentrate

CrossRoads Scientific XRS-FP Analysis Report

File: C:\Users\Xenemetrix\Desktop\TODAY\F-.str

12:35:35 P

Comment line

Layer Table ==========

#	Thick	Type	Error	Units	Density	Norm.	Total
1	0.00	Bulk	0.00	mg/cm2	0.00F	On	100.00

Sample Table ==========

Layer	Component	Type	Concn.	Error	Units	Mole%	Error
1	SiO2	Calc	2.263	0.353	wt.%	2.993	0.467
1	V2O5	Calc	1.202	0.092	wt.%	0.525	0.040
1	Cr2O3	Calc	0.000	0.000	wt.%	0.000	0.000
1	MnO	Calc	0.083	0.014	wt.%	0.093	0.016
1	Fe2O3	Calc	2.918	0.061	wt.%	1.452	0.030
1	Co3O4	Calc	0.071	0.019	wt.%	0.023	0.006
1	NiO	Calc	0.005	0.008	wt.%	0.006	0.008
1	CuO	Calc	0.025	0.008	wt.%	0.025	0.008
1	Nb2O3	Calc	0.440	0.366	wt.%	0.149	0.125
1	MoO3	Calc	0.000	0.000	wt.%	0.000	0.000
1	WO3	Calc	0.266	0.051	wt.%	0.091	0.018
1	P2O5	Calc	0.000	0.000	wt.%	0.000	0.000
1	SO3	Calc	0.158	0.072	wt.%	0.156	0.072
1	CaO	Calc	0.433	0.028	wt.%	0.614	0.039
1	MgO	Calc	3.543	6.302	wt.%	6.988	12.429
1	K2O	Calc	0.000	0.000	wt.%	0.000	0.000
1	BaO	Calc	1.329	0.763	wt.%	0.689	0.396
1	Al2O3	Calc	3.921	1.267	wt.%	3.057	0.988
1	Ta2O5	Calc	0.141	0.038	wt.%	0.025	0.007
1	TiO2	Calc	82.867	0.314	wt.%	82.476	0.312
1	ZnO	Calc	0.078	0.010	wt.%	0.076	0.010
1	Ag2O	Calc	0.000	0.000	wt.%	0.000	0.000
1	Cl	Calc	0.246	0.027	wt.%	0.552	0.061
1	ZrO2	Calc	0.011	0.079	wt.%	0.007	0.051
1	SnO2	Calc	0.000	0.000	wt.%	0.000	0.000

Element Table ==========

Elmt	Line Code	Cond Code	Ratio Method	Intensity (c/s)	Error (c/s)	Intensity Method	Conc.	Conc Method	Calibration Coefficient
O	Ka	0	None	0.000	0.0000	Gaussian	39.639	None	0.000
Mg	Ka	1	None	0.557	0.9904	Gaussian	2.137	FP	0.000
Al	Ka	1	None	6.288	2.0316	Gaussian	2.075	FP	0.000
Si	Ka	1	None	18.537	2.8937	Gaussian	1.058	FP	0.000
P	Ka	1	None	0.000	2.2998	Gaussian	0.000	FP	0.000
S	Ka	1	None	7.612	3.4988	Gaussian	0.063	FP	0.000
Cl	Ka	1	None	40.822	4.5130	Gaussian	0.246	FP	0.000
K	Ka	1	None	0.000	5.5498	Gaussian	0.000	FP	0.000
Ca	Ka	1	None	113.767	7.2960	Gaussian	0.310	FP	0.000
Ti	Ka	1	None	21581.220	81.6904	Gaussian	49.680	FP	0.000
V	Ka	1	None	380.684	29.1170	Gaussian	0.673	FP	0.000
Cr	Ka	1	None	0.000	5.3141	Gaussian	0.000	FP	0.000
Mn	Ka	1	None	19.285	3.3042	Gaussian	0.065	FP	0.000
Fe	Ka	1	None	721.623	15.0706	Gaussian	2.041	FP	0.000
Co	Ka	1	None	20.789	5.6881	Gaussian	0.052	FP	0.000
Ni	Ka	1	None	1.767	2.5095	Gaussian	0.004	FP	0.000
Cu	Ka	1	None	8.882	2.9367	Gaussian	0.020	FP	0.000
Zn	Ka	1	None	29.667	3.9542	Gaussian	0.062	FP	0.000
Zr	Ka	1	None	0.275	1.9869	Gaussian	0.008	FP	0.000
Nb	Ka	1	None	2.452	2.0435	Gaussian	0.349	FP	0.000
Mo	Ka	1	None	0.364	1.5476	Gaussian	0.000	FP	0.000
Ag	Ka	1	None	0.000	0.0000	Gaussian	0.000	FP	0.000
Sn	La	1	None	0.000	5.9457	Gaussian	0.000	FP	0.000
Ba	La	1	None	132.058	75.8375	Gaussian	1.190	FP	0.000
Ta	La	1	None	12.780	3.4198	Gaussian	0.116	FP	0.000
W	La	1	None	23.776	4.5769	Gaussian	0.211	FP	0.000

Analysis Conditions ==========

#	Tar get	Filter	Thick. mg/cm2	kV	uA	---Detector--- Type	Filter	Thick. mg/cm2	Atm	Preset Time(s)	Actual Time(s)
1	Rh	None	0.00	20.0	20.0	SDD	None	0.00	Air	60.0	30.0

Processing Conditions ==========

#	No.	Escape	Sum	Back	C/R	Blank	----Blank----

XRF result of Calcined Sample GVS Tailings

CrossRoads Scientific XRS-FP Analysis Report

File: C:\Users\Xenemetrix\Desktop\TODAY\G-.str

12:37:05

Comment line

Layer Table ==========

#	Thick	Type	Error	Units	Density	Norm.	Total
1	0.00	Bulk	0.00	mg/cm2	0.00F	On	100.00

Sample Table ==========

Layer	Component	Type	Concn.	Error	Units	Mole%	Error
1	SiO2	Calc	14.747	0.810	wt.%	19.247	1.057
1	V2O5	Calc	1.111	0.085	wt.%	0.479	0.037
1	Cr2O3	Calc	0.000	0.000	wt.%	0.000	0.000
1	MnO	Calc	0.079	0.013	wt.%	0.087	0.015
1	Fe2O3	Calc	3.136	0.060	wt.%	1.540	0.030
1	Co3O4	Calc	0.036	0.019	wt.%	0.012	0.006
1	NiO	Calc	0.000	0.000	wt.%	0.000	0.000
1	CuO	Calc	0.040	0.009	wt.%	0.040	0.009
1	Nb2O3	Calc	0.238	0.331	wt.%	0.080	0.111
1	MoO3	Calc	0.000	0.000	wt.%	0.000	0.000
1	WO3	Calc	0.290	0.050	wt.%	0.098	0.017
1	P2O5	Calc	0.000	0.000	wt.%	0.000	0.000
1	SO3	Calc	0.318	0.071	wt.%	0.311	0.070
1	CaO	Calc	1.256	0.046	wt.%	1.756	0.065
1	MgO	Calc	0.000	0.000	wt.%	0.000	0.000
1	K2O	Calc	0.139	0.026	wt.%	0.116	0.021
1	BaO	Calc	0.451	0.722	wt.%	0.230	0.369
1	Al2O3	Calc	4.106	1.807	wt.%	3.158	1.390
1	Ta2O5	Calc	0.161	0.040	wt.%	0.029	0.007
1	TiO2	Calc	73.525	0.295	wt.%	72.194	0.290
1	ZnO	Calc	0.059	0.009	wt.%	0.057	0.009
1	Ag2O	Calc	0.000	0.000	wt.%	0.000	0.000
1	Cl	Calc	0.235	0.028	wt.%	0.519	0.062
1	ZrO2	Calc	0.073	0.086	wt.%	0.047	0.055

Element Table ==========

Elmt	Line Code	Cond Code	Ratio Method	Intensity (c/s)	Error (c/s)	Intensity Method	Conc.	Conc Method	Calibration Coefficient
O	Ka	0	None	0.000	0.0000	Gaussian	41.487	None	0.000
Mg	Ka	1	None	0.000	0.9933	Gaussian	0.000	FP	0.000
Al	Ka	1	None	7.170	3.1560	Gaussian	2.173	FP	0.000
Si	Ka	1	None	130.069	7.1442	Gaussian	6.893	FP	0.000
P	Ka	1	None	0.000	3.6123	Gaussian	0.000	FP	0.000
S	Ka	1	None	14.535	3.2442	Gaussian	0.127	FP	0.000
Cl	Ka	1	None	36.957	4.3913	Gaussian	0.235	FP	0.000
K	Ka	1	None	28.098	5.1506	Gaussian	0.116	FP	0.000
Ca	Ka	1	None	312.754	11.5471	Gaussian	0.897	FP	0.000
Ti	Ka	1	None	19254.720	77.2925	Gaussian	44.079	FP	0.000
V	Ka	1	None	355.331	27.1926	Gaussian	0.622	FP	0.000
Cr	Ka	1	None	0.000	4.6800	Gaussian	0.000	FP	0.000
Mn	Ka	1	None	20.085	3.3827	Gaussian	0.061	FP	0.000
Fe	Ka	1	None	857.523	16.4387	Gaussian	2.194	FP	0.000
Co	Ka	1	None	11.571	6.1648	Gaussian	0.026	FP	0.000
Ni	Ka	1	None	0.000	2.9740	Gaussian	0.000	FP	0.000
Cu	Ka	1	None	15.535	3.5037	Gaussian	0.032	FP	0.000
Zn	Ka	1	None	24.992	4.0021	Gaussian	0.048	FP	0.000
Zr	Ka	1	None	2.040	2.3993	Gaussian	0.054	FP	0.000
Nb	Ka	1	None	1.471	2.0397	Gaussian	0.190	FP	0.000
Mo	Ka	1	None	0.474	1.6816	Gaussian	0.000	FP	0.000
Ag	Ka	1	None	0.000	0.0000	Gaussian	0.000	FP	0.000
Sn	La	1	None	0.000	8.4211	Gaussian	0.000	FP	0.000
Ba	La	1	None	44.757	71.6952	Gaussian	0.404	FP	0.000
Ta	La	1	None	16.042	4.0074	Gaussian	0.132	FP	0.000
W	La	1	None	28.549	4.9623	Gaussian	0.230	FP	0.000

Analysis Conditions ==========

#	Tar get	Filter	Thick. mg/cm2	kV	uA	---Detector--- Type	Filter	Thick. mg/cm2	Atm	Preset Time(s)	Actual Time(s)
1	Rh	None	0.00	20.0	20.0	SDD	None	0.00	Air	60.0	30.0

Processing Conditions ==========

#	No. Smths	Escape Peaks	Sum Peaks	Back Type	C/R Ratio	Blank Rem.	----Blank---- ----File-----